UNIVERSITA' DEGLI STUDI DI VERONA

DEPARTMENT OF

Neuroscience, Biomedicine and Movement Science

GRADUATE SCHOOL OF

Life and Health Sciences

DOCTORAL PROGRAM IN

Neuroscience, Psychological and Psychiatric Sciences, and Movement Sciences

Cycle: XXV°

TITLE OF THE DOCTORAL THESIS

The effects of neuromuscular fatigue on motor control and learning processes

S.S.D. M-EDF/01

Coordinator: Prof.ssa Michela Rimondini

Tutor: Prof. Matteo Bertucco

Doctoral Student: Dott. Mauro Nardon

The effects of neuromuscular fatigue on motor control and learning processes – Mauro Nardon

Ph.D. Thesis

Verona, December 11th 2023

ISBN

Author's address

Mauro Nardon
Department of Neuroscience, Biomedicine and Movement Sciences
University of Verona, Italy
mauro.nardon@univr.it

Supervisor

Prof. Matteo Bertucco, Ph.D.
Department of Neuroscience, Biomedicine and Movement Sciences
University of Verona, Italy
matteo.bertucco@univr.it

Reviewers

Prof. Gennaro Boccia, Ph.D
Department of Clinical and Biological Sciences
University of Turin, Italy
gennaro.boccia@unito.it

Prof. Giuseppe Marcolin, Ph.D.
Department of Biomedical Sciences
University of Padua, Italy
giuseppe.marcolin@unipd.it

SOMMARIO

Il controllo posturale è un processo complesso che coinvolge molteplici meccanismi all'interno del sistema nervoso centrale (CNS) e si fonda sull'integrazione senso-motoria di segnali di feedback di diversa natura per poter identificare e processare le informazioni relative ai singoli segmenti corporei ed all'ambiente circostante rispetto ad essi. I principali meccanismi che permettono il controllo della postura sono distinguibili in meccanismi ad input aperto, o *feedforward* e meccanismi a controllo retrogrado, o *feedback*. I primi permettono una risposta rapida e stereotipata ad una perturbazione posturale, attraverso la trasmissione di un input neurale che avviene in anticipo rispetto alla perturbazione stessa. Essi si basano su di una rappresentazione motoria – una sorta di previsione e relativa aspettativa degli effetti di instabilità generati – del compito motorio. La presenza stessa, l'intensità e la qualità dei meccanismi a *feedforward* dipendono da svariati fattori, tra cui l'esperienza pregressa, l'intensità e la prevedibilità della perturbazione posturale, la direzione ed il rischio correlato all'errore.

Il secondo meccanismo, più lento e preciso, prevede l'elaborazione e comparazione degli stimoli sensomotori provenienti dai recettori del corpo (visivi, uditivi, tattili, propriocettivi) con lo schema motorio desiderato, permettendo di correggerne i parametri (e.g. velocità, angoli articolari), in caso questi non corrispondano a quelli desiderati. I processi a feedback implicano la trasmissione sovra-spinale ed elaborazione degli stimoli sensomotori a livello di più aree del sistema nervoso centrale (CNS), perciò risentono di ritardi nella trasmissione del segnale e risultano più lenti.

Come accennato, l'esperienza pregressa – e quindi la pratica – permettono al CNS di ottimizzare l'esecuzione di un compito motorio in condizioni perturbate e/o di instabilità. Ciò avviene sia per gesti relativamente semplici come la prensione, sia per i più complessi come il lancio ed il puntamento di oggetti. Questo processo prende il nome di adattamento motorio. Differisce dall'apprendimento motorio *de-novo* in quanto non si tratta di apprendimento "da zero" di un'abilità o di un gesto motorio prima sconosciuto, ma consiste invece in una rimodulazione degli input motori in modo da ottimizzare la performance e ridurre gli errori causati da una

modifica nei parametri di tipo ambientale (e.g. perturbazione meccanica, modifica della superficie di appoggio) o del gesto stesso.

In questo contesto, la fatica neuromuscolare costituisce un chiaro caso di perturbazione di tipo fisiologico che modifica in modo transitorio le proprietà e la risposta dei muscoli. Effettuare un gesto in condizioni di affaticamento muscolare richiede quindi l'adattamento del comando motorio relativo. La fatica neuromuscolare – qui intesa come riduzione estemporanea della forza e/o potenza muscolare – è stata largamente studiata in relazione ai relativi effetti acuti sulla performance, sull'equilibrio posturale e più recentemente anche dal punto di vista preventivo relativamente al rischio di infortunio, sia nella popolazione sportiva che in soggetti sani e patologici.

Sorprendentemente, pochi studi al momento hanno esaminato gli effetti della fatica neuromuscolare sui processi di apprendimento (a breve termine) e di ritenzione del gesto appreso (a medio-lungo termine).

Per questo, gli obiettivi che si pone questa tesi sono di colmare queste lacune e nello specifico: *i)* valutare gli effetti di diverse modalità di esercizio fisico sulla modulazione dei meccanismi a *feedforward* e *feedback*; *ii)* investigare gli effetti della fatica neuromuscolare localizzata a livello dei muscoli posturali durante un paradigma di adattamento motorio in un *reaching task*; *iii)* valutare gli effetti a lungo termine (ritenzione/*savings*) determinati dallo stato di affaticamento durante il processo di adattamento motorio all'interno un innovativo paradigma posturale per valutare l'adattamento motorio.

Nel primo capitolo viene fornita una panoramica generale sui meccanismi responsabili del controllo posturale, di come essi vengano influenzati dalla fatica e viene introdotto il concetto di apprendimento motorio e adattamento. Il secondo capitolo presenta gli effetti di diverse modalità di esercizio sui meccanismi a *feedforward* e *feedback* nel controllo posturale. Il terzo capitolo si concentra sugli effetti dell'affaticamento localizzato a livello di un singolo distretto muscolare sulla performance e la stabilità posturale durante un paradigma di adattamento motorio (*reaching task*). Qui sono anche analizzati gli effetti a breve termine a livello di modifiche nell'attivazione dei singoli muscoli e di coppie di muscoli (agonista-antagonista). Nel quarto capitolo viene illustrato il razionale per lo sviluppo di un

paradigma innovativo per la misura dell'adattamento motorio e vengono riportati gli effetti della fatica neuromuscolare all'interno della stessa sessione (breve termine) e gli effetti a medio-lungo termine dell'affaticamento durante il processo di apprendimento, valutati attraverso la ritenzione (*savings*) in una seconda sessione. Infine, il capitolo finale delinea i principali risultati di ciascuno studio, seguito da una conclusione generale che sottolinea le possibili applicazioni dei risultati e suggerisce indicazioni future riguardo l'argomento di ricerca.

ABSTRACT

Human postural control is a complex, multifactorial mechanism that involves several structures within the central nervous system (CNS). It is based on sensory-motor integration of a variety of feedback signals in order to identify and process information about the individual body segments and their state relative to the environment. Fundamental mechanisms regulating postural control can be divided into feedforward and feedback mechanisms. The formers are based on anticipatory neural inputs which allow for rapid responses to postural perturbations. They are based on internal models – an internal representation of the action, based on motor planning and expected effects of the action on postural stability. The presence, intensity and characteristics of feedforward mechanisms depend on several factors, among which: preceding experience with the task/perturbation, intensity, direction and predictability of the perturbation.

The second mechanism, slower, but more sophisticated, requires the elaboration of sensory-motor stimuli (visual, auditory, tactile, proprioceptive) coming from different body regions and receptors and the comparation of the information with the desired motor output. It allows for corrections of task parameters (e.g., velocity, joint angles, muscle activation) differing from desired. Feedback processes require sensory-motor stimuli to be transmitted to, integrated and elaborated by several supraspinal regions of the CNS, and thus they are affected by signal-transmission delays and are slower.

As already mentioned, prior experience with the task and practice allow the CNS to optimize these processes and to master the execution of a motor action even in cases of perturbation and instability. This is true for both relatively simple motor actions such as grasping, and also for more complex actions like throwing and pointing objects. This process is named motor adaptation. It differs from *de-novo* learning since it does not imply learning a brand-new action or motor scheme, whereas it consists in the remodulation of neural inputs to the effectors (i.e., muscles) to optimize performance and reduce errors due to environmental (e.g., mechanical perturbations, changes in walking surface) or task parameters changes. In this context, neuromuscular fatigue represents a physiological perturbation that transiently influences muscle properties and their response. Performing a task in a

fatigued state requires an update of the relative motor command. Neuromuscular fatigue – here defined as a transient reduction in muscle force and/or power – acute effects on performance, postural stability and more recently in the context of injury risk, have been extensively studied, both in healthy and pathological populations. Surprisingly, to date just a few studies evaluated the effects of neuromuscular fatigue on motor learning (short-term) and motor retention (medium-long term) processes.

For this reason, the aim of the present thesis is to bridge these gaps in literature. In details: *i)* evaluate the effects of different exercise modalities on the modulation of feedforward and feedback mechanisms of postural control; *ii)* investigate the effects of localized neuromuscular fatigue at the level of postural muscles during a motor adaptation paradigm using a reaching task; *iii)* evaluate the long-term effects (retention/*savings*) of experiencing muscle fatigue while exposed to a motor adaptation process using a novel postural paradigm.

In the first chapter, a general overview on mechanisms responsible for human postural control and on the relative influence of neuromuscular fatigue is provided. Furthermore, concepts of motor learning and adaptation are discussed. The second chapter presents the effects of distinct exercise modalities on feedforward and feedback mechanisms of postural control. The third chapter focuses on the effects of localized muscle fatigue of a single muscle district on performance and postural stability during a motor adaptation paradigm (force-field reaching task). Furthermore, short-term effects on muscle activation at the level of single muscles and agonist-antagonist muscle pairs are investigated.

In the fourth chapter, the rationale for the development of a novel paradigm to test motor adaptation is illustrated. In such paradigm, the effects of neuromuscular fatigue within the same experimental session (short-term) and the effects of experiencing muscle fatigue during the adaptation process itself on motor retention (savings) during a second exposure (mid-long term) are described.

Finally, the last chapter summarizes the primary results of each study, followed by a general conclusion that highlights potential applications of the resulting evidence and possible future directions on this topic.

ACKNOWLEDGMENTS

This PhD program has definitely been a challenging experience, encompassing Covid-19 pandemic, with the related travel limitations and also due to some medical issues. Nonetheless, these years will always have a special place in my memory, and I can finally say I made it to the finish line!

This result would not have been possible alone, and one of the joys of having completed the thesis is looking back at everyone who has helped over the past years. Here, I will try my best at expressing my deepest gratitude to all the people who supported and guided me throughout this great, challenging journey, despite the many unforeseen obstacles that arose.

First and foremost, I would like to thank my PhD supervisor, Prof. Matteo Bertucco, for providing invaluable intellectual and personal support throughout the entire process. Your constant guidance and encouragement have been invaluable for nourishing and motivate my work as a researcher and I am deeply grateful for your contribution to my scientific development.

Secondly, much of the knowledge, scientific curiosity, passion for research and the "masochistic" pleasure to spend hours struggling with Matlab codes I developed during these years, would not have been possible without the long time I shared in the lab and in the office with my colleagues and friends from the University of Verona (and some now abroad): Fabio, Gaia, Camilla, Samuel, Francesco, Anna and Riccardo. The long chats and funny jokes during lunches and countless coffee breaks surely added fun to the daily lab routine. Thanks to Francesca for the professional help, attention and willingness to accommodate the overlapping lab requests, and also for the personal kindness and support.

I want to thank Prof. Enrico Tam and Dr. Francesco Piscitelli for their valuable collaboration in the setup definition, data collection and analysis of a relevant part of this research project (Study 1).

I want to express my gratitude to Prof. Tarkeshwar Singh, for the great opportunity and the formative experience at the Sensorimotor Neuroscience and Learning

Laboratory at the Pennsylvania State University. I really appreciated the inclusive environment in your lab and your scientific commitment and rigor. The weekly lab meetings and the *Action Club*'s invited speakers really created a scientifically rich environment which nourished my interest in research and the scientific curiosity. I would also like to acknowledge your time and efforts spent in regular video-calls getting the project ready before my arrival, and also your valuable and thoughtful guidance there. I would also like to thank Prof. Mark Latash for involving me in some ongoing projects in his lab during my stay at PennState.
The six months I spent in the US will always have a special place in my memory, and that would not have been possible without the warm welcome, company and both professional and personal support of many colleagues and friends. Oindrila and Sayan, your help and friendship made my stay at State College great. Your presence made the hours spent in the lab way less stressful and your company in the free time almost made me forget I was far from home. I wish you success in your PhD studies and hope to see you both very soon! I want to thank my colleague Joe, as a researcher I really appreciated your competence and ability to share your knowledge during our chats in the lab. I really can say I left PennState with far more knowledge and skills than I had when I arrived. Besides work, sharing dinner with other graduate & undergraduate students at your place was really fun, and your and Erika's hospitality and kindness is remarkable. I want to thank the undergraduate students in the lab, Eliza and John, for their precious help in the recruitment of participants and in data collection.

I would also like to thank Prof. Gennaro Boccia and Prof. Giuseppe Marcolin for the valuable comments and suggestions expressed while reviewing the thesis, which helped in the substantial improvement of this work.

Furthermore, I would like to express my gratitude to all the bachelor's and master's students from the University of Verona who invested their time helping me in the setup preparation and data collection, and also thank all the subjects who participated in this research. A special thanks to Luca, who was always available for helping us during pilot tests.

Finally, I want to thank my parents, my sister, and I am forever grateful for my whole family for the enduring support. And last but not least, I am grateful to my loving wife, Erika for being my inspiration, motivation and strength. Thank you especially for the patience, the support and the love even in “bad moments” or when several time-zones physically separated us.

To all of you, THANK YOU again!

Mauro Nardon

Table of Contents

Figure Captions

Table Captions

CHAPTER 1 – GENERAL INTRODUCTION

Summary

In this chapter, a general overview of the mechanism responsible for the control of posture and the inherent theories in motor control field is provided. The concept of motor adaptation is then reviewed relative to the broader concept of motor learning. The concept of motor learning is introduced and then narrowed down to the specific subspace of motor adaptation. Finally, the concept of neuromuscular fatigue is defined in relation to the current literature and its effects on human posture and movement execution are discussed.

Background

The most evident behavioral tract that differentiate humans from other animals and other humanoid primates is our ability and consistency in maintaining a standing posture on the lower limbs. This characteristic is not trivial and has guided both our cognitive and our physiological development across evolution. Standing posture, from a pure biomechanical point of view – although it favors the independent use of the upper limbs and allows a wider range of daily-life activities – poses a substantial threat in the physical stability of the body in the unpredictability of the environment. In this framework, controlling mechanism are required to ensure stability and rapid responses both expected and unexpected events and perturbations which affect the system. One of the most common, transient physiological perturbation for the human body during daily life is neuromuscular fatigue.

Despite the vast literature covering the physiological effects of neuromuscular fatigue on postural control, results are quite heterogeneous compared to that of the effects of fatigue on exercise physiology. That is partially due to the wide abundance of exercise modalities, fatiguing protocols and their characteristics (e.g., intensity, duration), which limit the generalization of results.

When it comes to movement and skill learning, only few studies have considered the possible influence of neuromuscular fatigue on ongoing learning processes and its potential long-term effects.

In this view, local muscle fatigue (i.e., limited to a single muscle or district) is an interesting model which poses a physiological perturbation to the integration of sensorimotor signals and motor commands and could therefore provide valuable insights about the underpinning mechanisms within the central nervous system (CNS) that are responsible for (1) the control of posture and (2) the learning or adaptation of a task to novel perturbations. For this reason, this thesis focuses on the effects of local muscle fatigue on processes of postural control, motor adaptation and retention of learning.

POSTURAL CONTROL

Human standing posture is a non-trivial task that requires continuous active control, due to the inherently unstable nature of human posture (high center of mass on a reduced support area). Standing balance is additionally challenged when the person performs rapid motor actions or interacts with the environment (Ivanenko and Gurfinkel, 2018), which result in changes of external forces acting on the body segments. Human body is scattered with receptors and equipped with specific structures within the CNS which are able to process and integrate sensorimotor information. As we know from engineering, however, great amount of information comes with a cost: delays. In contrast to electronic devices and computational models, biological systems incur in transmission delays which are inherently related to the nature of physiological signals (Jiang et al., 2016) Figure 1.1. Furthermore, these delays might vary depending on the relative distance and biological nature of the structures (e.g., myelinated vs de-myelinated nerves).

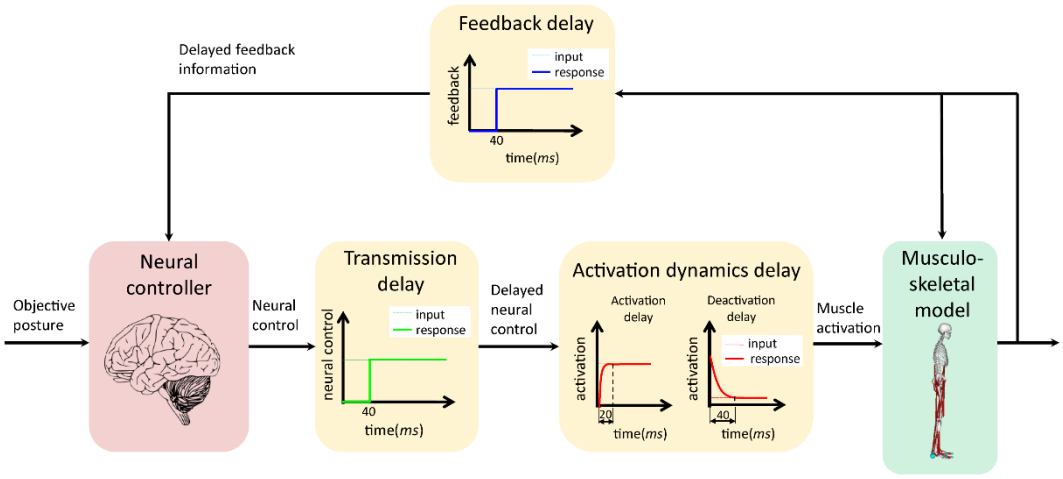

Figure 1.1 Diagram showing physiological signal transmissions delays in human postural control. (Taken from Jiang P, Chiba R et al, 2016)

To account for these problems, there are a number of mechanisms that the central nervous system (CNS) employes to maintain posture during self-induced perturbations, such as voluntary rapid movements, or when counteracting external perturbing forces. When postural perturbations can be predicted, anticipatory changes in the activation levels of postural muscles – defined as anticipatory postural adjustments (APA) – are evident. The role of APAs is to anticipate mechanical effects of the disturbance and counteract it by generating forces and joint torques (Belen'kiĭ et al., 1967; Massion, 1992). By their nature, APA are based on predictive feedforward control and quite stereotyped, therefore there will always be residual errors in these predictions that should be accounted for. That is achieved by slower corrective mechanism, based on feedback loops, named compensatory postural adjustments (CPAs). CPA appear after the onset of movement or external postural perturbation (Santos et al., 2010a, 2010b; Krishnan et al., 2012; Chen et al., 2015). It is worthwhile to mention that APAs and CPAs are mutually related: in the case of an unexpected perturbation, APAs are not applied, thus CPAs are the only mechanism used by the CNS for restoring balance, on the other hand when APAs are strongly involved, CPAs are less present (Santos et al., 2010b, 2010a), as shown in Figure 1.2.

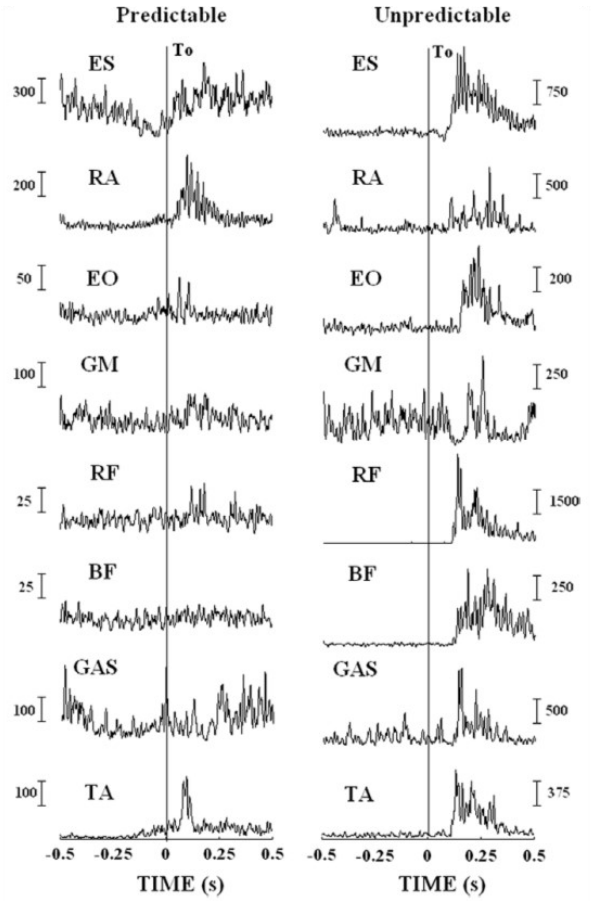

Figure 1.2 Typical EMG patterns for ventral (TA, RF, and RA), dorsal (GAS, BF, and ES), and lateral (EO and GM) muscles in conditions with predictable and unpredictable perturbations. The vertical lines represent the postural perturbation (T0). Muscle abbreviations: TA – tibialis anterior, GAS – gastrocnemius, BF – biceps femoris, RF – rectus femoris, GM – gluteus medius, EO – external obliques, RA – rectus abdominis, and ES – erector spine. (Taken and adapted from Santos MJ, Kanekar N, and Aruin AS, 2010)

Neuromuscular fatigue

Fatigue is a multifactorial psycho-physiological condition which encompasses several areas of human life sciences: from pure exercise physiology to cognition and psychology. As we know from literature, people suffering from several pathological conditions experience higher levels of fatigue (Brunton and Rice, 2012; Nardon et al., 2021; Brownstein et al., 2022), which can be considered as a subjective perception and is usually detected though specific scales and questionnaires (Kluger et al., 2013; Brunton and Bartlett, 2017).

In the present thesis, we specifically focus on neuromuscular fatigue (NMF), identified by the objective decrease in performance over time, – also defined as an exercise-induced reduction in the ability of muscle to produce force or power

(Bigland-Ritchie et al., 1986; Enoka and Duchateau, 2008) – a transient and reversible state that induces physiological changes at several levels in the neuromuscular system (Enoka et al., 2011; Finsterer, 2012; Amann et al., 2013; Taylor et al., 2016) and limits exercise performance. Our NMF definition is similar to what in clinics and rehabilitation setting is named "performance fatigability" (Finsterer, 2012; Kluger et al., 2013; Kim et al., 2018). In humans, NMF manifests as the inability to perform a motor task at the required intensity, finally leading to exhaustion (Theofilidis et al., 2018). NMF phenomenon encompasses factors related to muscles, nerves, cortical and subcortical areas in the CNS, and properties of biological signals travelling from-, to- and within the CNS system (Enoka and Duchateau, 2008; Enoka et al., 2011). Additionally, NMF is further differentiated into its peripheral and central components (Bigland-Ritchie et al., 1986; Gandevia, 2001), based on anatomical localization of the main biochemical and physical alterations (Figure 1.3). Briefly, central fatigue implies alterations of the neural drive to the muscle, whereas peripheral fatigue comprises biochemical alterations at the level of- or distal to the neuromuscular junction (Gandevia, 2001).

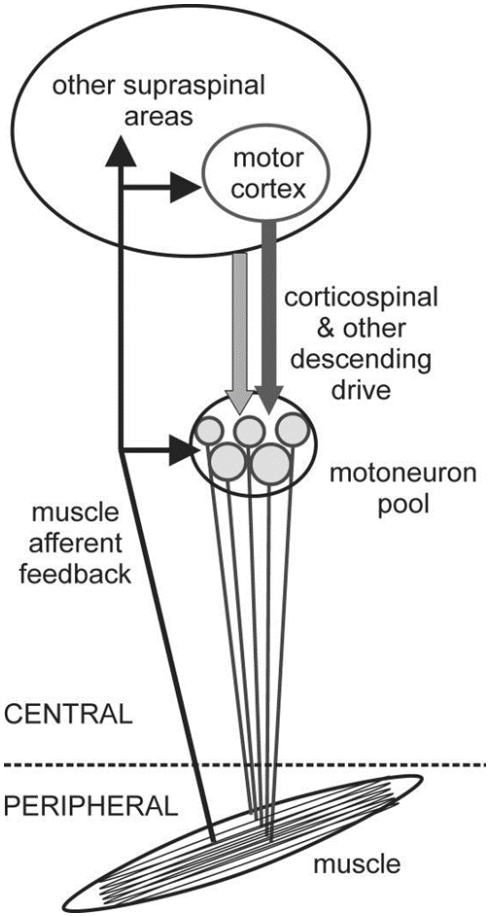

Figure 1.3 Schematic illustration of central and peripheral components and their neural contributions to muscle fatigue. (Taken from Taylor JL, Amann M, et al., 2016)

Several studies in the field of muscle and exercise physiology focused on unravelling the nature and relative role of central and peripheral components in the development of muscle fatigue during exercise, both in healthy (Amann et al., 2013; Weavil and Amann, 2019; Laginestra et al., 2021) and in pathological conditions (Brownstein et al., 2022; Martignon et al., 2022). These approaches offer valuable insight for the understanding of the basic mechanisms by which central and peripheral components are linked and influence each other. However, during most of human activities, a mixture of both components is present (Taylor et al., 2016; Carroll et al., 2017) and it is hard to set clear boundaries and separate these components. Thus, in daily-life activities, sports and leisure activities we usually see an activity-dependent interplay of both central and peripheral components, which together contribute to the phenomenon of neuromuscular fatigue (Theofilidis et al., 2018).

As a transient, acute physiological state, muscle fatigue follows a physiological recovery which is highly dependent on several parameters: exercise modality, intensity and duration, presence/absence of metabolite accumulation and/or muscle tissues damage – just to mention some of the main factors (Gandevia, 2001; Carroll et al., 2017). Generally – at least in short-to-medium duration submaximal exercise – central component is only partially involved and its recovery follows a timing closely related to the exercise duration that induced NMF, starting immediately after the exercise termination (Carroll et al., 2017). On the contrary, recovery of peripheral component tends to be slower because of metabolites accumulation and muscle damage (Carroll et al., 2017).

When considering exercise modality, we can first separate between localized/single muscle or joint exercises and whole-body/general exercises (Paillard, 2012; Carroll et al., 2017). The main difference between the two is the larger amount of muscle mass involved in the latter exercise modality, which implies a larger involvement of the cardiopulmonary system (Paillard, 2012). From an ecological point of view, it is more representative of daily life situations. Considering general exercise it is difficult, however, to disentangle the relative contribution of the single muscle groups from the limitations at each level of the cardiopulmonary system which eventually lead to exercise termination. For this reason, and because it allows to better control for confounders, much more literature focused on single-joint isometric exercises (Paillard, 2012; Carroll et al., 2017).

Effects of neuromuscular fatigue on postural control

Effects of NMF on postural control and balance during a variety of actions have been extensively investigated see (Paillard, 2012) for a review. In details, general muscle exercises – involving large muscle masses – during repeated, cyclical tasks such as running or cycling, have been demonstrated to deteriorate balance and postural control performance while increasing measures of postural instability (Nardone et al., 1997; Nagy et al., 2004; Coco et al., 2021). Effects of localized (i.e, single muscle or joint) NMF on postural control has been extensively studied (Kanekar et al., 2008; Singh and Latash, 2011; Lyu et al., 2021, 2022), however, the lack of an agreement on how muscle fatigue was defined and differences in the

fatiguing protocols used limits the generalization of the results. A series of earlier studies have reported an increase in the variance of activation of both fatigued and non-fatigued muscles following localized fatiguing exercise (Singh et al., 2010; Singh and Latash, 2011). In particular, fatigue of tibialis anterior muscle led to higher inter-trial variance in electromyographic (EMG) indexes for both the same and other, non-fatigued muscles of the legs and trunk participating in a whole-body task (Singh and Latash, 2011). These results have been interpreted as adaptive mechanisms within the neural circuits involved in the synergic control of muscles, in order to contrast NMF within a redundant multi-muscle system as the human body (Singh and Latash, 2011). Increasing and changing the recruitment of other, non-fatigued muscles potentially represents an adaptive strategy to compensate for the detrimental effects of NMF on the EMG activity within the fatigued muscle. Recently, we demonstrated that NMF of a single, non-compartmentalized muscle (tibialis anterior), negatively affected intra-muscle force-stabilizing synergy estimated in the space of motor unit groups (MU-modes) (Ricotta et al., 2023).

Motor learning and adaptation

Humans acquire and develop several skills in the course of their lives. Some of those are apparently simple (e.g., walking or reaching for an object), while some require a finer degree of precision and coordination and much more practice (e.g., riding a bike, skiing, dancing). The process of skill acquisition is complex and requires the integration of several sensorimotor inputs from the body in several brain regions, requiring various amounts of cognitive contribution (Krakauer et al., 2019). Motor learning processes have a relatively long time-scale and require the continuous refinement and update of encoded task-specific parameters (alternatively referred to as *motor schema* (Schmidt, 1975; Wulf, 2012), *efferent copy* (Bridgeman, 1995), or *internal models* (Kawato, 1999), according to different motor control theories) at the level of the CNS. Even in the case where a skill or movement is already acquired and the performance is stable in time, if environmental of task parameters are unexpectedly changed, performance takes several trials of practice to adapt to the new conditions (Ahmed and Wolpert, 2009; Pienciak-Siewert et al., 2016; Krakauer et al., 2019). This process in literature is

defined as motor adaptation and differs from *de-novo learning* (the acquisition of a new skill or movement "from scratch") since it requires to adapt and update the already internalized motor command to correct for the change in task and environment parameters (Krakauer et al., 2019). Paradigms used to evaluate motor adaptation consist in the execution of a simple task (e.g., reaching with a robotic handle) and after the performance stabilizes, changing the task parameters by either introducing a visual distortion (e.g., visuomotor rotation (Tanaka et al., 2009)) or a mechanical perturbation (e.g., force-fields (Ahmed and Wolpert, 2009)). These paradigms generally produce an exponential-shaped curve in performance errors (Figure 1.4), suggesting that adaptation processes are error-driven (Krakauer et al., 2019).

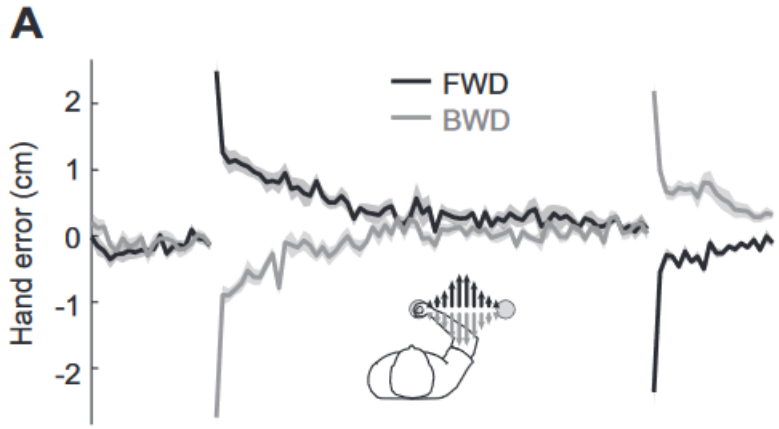

Figure 1.4 Performance error across trials during a force-field adaptation paradigm. Ligh- and dark-shaded traces represent backward (BWD and forward perturbation (FWD) trials, respectively. (Taken and adapted from Pienciak-Siewert A, Horan DP, Ahmed AA, 2019)

State-space models focused on the time-decays of motor adaptation curves and differentiated it into multiple distinct processes, each with its own rate in time (Smith et al., 2006; Huberdeau et al., 2015): a fast adaptation phase (explicit learning), presumably driven by sensorimotor integration coming from the error perception (vision, tactile and proprioceptive), and a slower, more implicit component (implicit learning). However, the distinction of the two components do not necessarily implicate separate neural systems (Smith et al., 2006).

Another characteristic of motor adaptation paradigms is the decay over time in the persistence of the observed improvement in performance, after the conclusion of

the paradigm. Interestingly, when people are re-exposed to the learned task, the adaptation process tends to be faster than the first time. This phenomenon is commonly known as *savings* (Huang et al., 2011; Herzfeld et al., 2014; Cassady et al., 2017) and encompasses a variety of learning domains and paradigms. It has been extensively studied in motor adaptation, where it consists in a faster learning process (fewer trials required) during a second exposure to a perturbation Figure 1.5. Savings are usually evaluated with multiple exposures to the same task that are spaced quite closely in time, usually on the same day or consecutive days. However, savings has been observed even several days after first exposure (Krakauer et al., 2005).

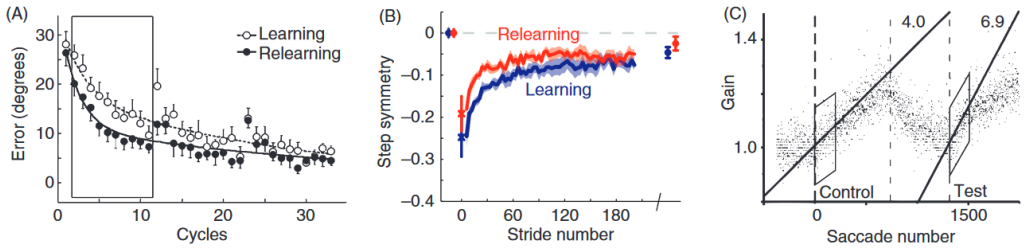

Figure 1.5 Savings in studies with different paradigms of motor adaptation. A) Savings in visuomotor rotation adaptation [Krakauer JW, Ghez C, Ghilardi MF, 2005]. B) Savings in locomotor adaptation [Malone LA, Vasudevan EVL, Bastian AJ, 2011]. Participants walked on a split-belt treadmill which imposed different speeds on each leg. This leg speed discrepancy reduces gait symmetry (y-axis, with 0 indicating perfect symmetry). C) Savings in saccadic adaptation in monkeys [Kojima Y, Iwamoto Y, Yoshida K, 2004]. The rate of relearning was faster, as indicated by the steeper slope in the learning curve for Test group – the one re-exposed to the task. (Taken from Krakauer, 2019)

Effects of neuromuscular fatigue on motor adaptation

The nature of the adaptation processes, together with its differences related to handedness (Wang and Sainburg, 2006), age-group (Takahashi et al., 2003; King et al., 2013) or pathological conditions (McGibbon and Krebs, 2004; Sadnicka et al., 2014) and its possible implications in rehabilitation (Bastian, 2008) have been extensively studied. Based on evidence of NMF effects on motor control, and its impact on muscle physiological characteristics (Gandevia, 2001; Carroll et al., 2017), it is worthwhile to inquire on possible long-term effects of NMF on motor adaptation and retention of learned skills. To date, only few studies have tried to answer this question. Takahashi et al. investigated how muscle fatigue affects internal model formation of arm movement in viscous force field paradigm

(Takahashi et al., 2006). While the findings support the hypothesis that muscle fatigue influences internal model formation of the reaching task, the characteristics of the fatiguing exercise potentially act as a confounder, since they fatigued the same muscles involved in the reaching task (effectors). In this context, it is difficult to differentiate direct effects of NMF on the processes within the CNS from the secondary effects of it, caused by the inherent transient changes in biochemical and functional characteristics of the fatigued muscle during motor adaptation. In a recent study, Branscheidt et al., investigated the effects of NMF beyond the short-term differences in task execution (Branscheidt et al., 2019). In their study they report that NMF negatively impacts task acquisition, resulting in reduced performance in a subsequent exposure to the task in the absence of NMF. Taken together, these results support our hypothesis that NMF not only has short-term, acute effects on performance and postural control, but also influences and negatively impacts on the processes of motor adaptation to a novel perturbation.

SUMMARY AND RESEARCH AIMS OF THIS PHD THESIS

In the previous chapter, it was provided an overview of the current state of the literature on the effects of neuromuscular fatigue on postural control and on motor adaptation. Gaps in literature have been addressed and therefore the purpose of this thesis is to analyze the effects of NMF on postural control and motor adaptation processes. In further details, the current thesis developed across these points:

1. Given the inconsistency of results concerning the effect of NMF on postural control, due to the heterogeneity in the fatiguing exercise protocols administered, the primary goal is to assess the effects of different exercise modalities (localized vs general/whole-body) on postural control. It is hypothesized that general fatigue would have a larger impact on the mechanisms of postural control and that these effects would persist for a longer time after exercise termination.
2. Humans can perform several tasks while standing on their feet without voluntary attention to the control of posture – at least in non-pathological conditions. Motor adaptation processes allow to efficiently perform motor tasks even when perturbations are introduced, or the environment conditions change. However, effects of NMF on motor adaptation processes are still debated. We hypothesized NMF during the exposure to a motor adaptation paradigm would negatively affect performance and postural control.
3. Frequently, in contexts of sport skills learning, and also in clinical and rehabilitation settings, humans are – voluntarily or involuntarily – exposed to NMF while learning (or re-learning) skills and movements. Despite the physiological nature of NMF and the ordinary presence of this phenomenon, only a few studies tried to assess the effects of NMF on the resulting learning processes and on retention of the learned task. It is hypothesized that the presence of NMF while adapting a motor task would a) negatively affect performance in the short-term period and b) impact the effective recall on a second exposure to the task.

CHAPTER 2 – EXPERIMENTAL RESEARCH: STUDY 1

The effects of generalized and local muscle fatigue on anticipatory and compensatory postural adjustments under an external perturbation

Mauro Nardon[1], Francesco Piscitelli[1], Enrico Tam[1], Matteo Bertucco[1*]

[1]Department of Neurosciences, Biomedicine and Movement Sciences, University of Verona

ABSTRACT

Vertical standing posture requires active control, and it is achieved through the interplay between anticipatory and compensatory mechanisms regulated by the central nervous system (CNS). In this context, general or localized neuromuscular fatigue (NMF) constitutes a transient physiological perturbation to the CNS. The goal of the present study was to evaluate and compare the effects of different fatiguing exercise modalities – with different cardio-metabolic responses – on the anticipatory and compensatory mechanisms of postural control. Fourteen young, healthy male participants (age: 25.3 ± 4.2 years; height: 1.78 ± 0.06 m; weight: 77.1 ± 6.8 kg) were exposed to a pendulum-like perturbation paradigm before- and after two different exercise protocols on separate sessions, in a crossover design.

Joint kinematics, postural stability – estimated from the root mean square of the Center of Pressure displacement (RMSCoP) and its mean velocity (VelCoP) – and muscle activation of postural muscle was measured during the postural task. Indexes of co-activation (C-index) and reciprocal activation (R-index) at the level of each joint were also computed. Contrary to our hypothesis, changes in postural stability were similar between protocols and rapidly compensated. We observed that apparently the CNS deployed opposite strategies after the distinct fatiguing protocols to maintain postural control. Namely, after the generalized fatiguing exercise participants tended to increase the co-activation of postural muscles both in preparation (anticipatory) and in response (compensatory phase) to the mechanical perturbation. On the contrary, after localized fatigue participants seemed to adopt a higher variability in the muscle activation, with a general decrease in the anticipatory and compensatory activity, reflected also by the increased displacement of their shoulders following the postural perturbation.

Surprisingly, no difference between the protocols were seen considering the measures of postural stability. Taken together these results confirm the ability of the CNS to efficiently compensate postural perturbations in suboptimal conditions and suggest the two fatiguing modalities elicit opposite strategies at the CNS level in terms of activation of the postural muscles.

INTRODUCTION

Upright standing posture can be viewed as a multi-segmented physical pendulum equipped with multiple muscles with their inherent viscoelastic properties. This makes ensuring the stability of a person's vertical posture in the field of gravity a challenging task that requires active control, especially when a standing person performs rapid motor actions or interacts with the environment (Ivanenko and Gurfinkel, 2018). Strategically, there are a number of mechanisms that the central nervous system (CNS) performs to maintain posture during self-induced perturbations, such as voluntary rapid movements, or when counteracting external perturbing forces. If these changes are predictable, there are anticipatory changes in the activation levels of postural muscles addressed as anticipatory postural adjustments (APA), starting 0-250 ms prior the movement or perturbation occurrence. The function of APAs is to generate forces and torques that counteract the direct mechanical effects of the foreseeable disturbance (Belen'kiĭ et al., 1967; Massion, 1992). By their nature, APA are based on predictive feedforward control and therefore there will always be residual disturbances affecting the body. They lead to compensatory postural adjustments (CPA) after the onset of movement or disturbance, which serve to maintain balance under the action of those actual disturbances (Santos et al., 2010a, 2010b; Krishnan et al., 2012; Chen et al., 2015). It is important to notice that APAs and CPAs are interconnected, when APAs are not applied CPAs are the mechanism used by the CNS for restoring balance, on the other hand when APAs are strongly involved, CPAs are less present (Santos et al., 2010b, 2010a).

Many task contexts and internal physiological factors affect the generation of APA, such as magnitude and direction of perturbation (Aruin and Latash, 1995), movement accuracy demands (Bertucco and Cesari, 2010), motor actions under

uncertainty (Piscitelli et al., 2017; Bertucco et al., 2021), body instability (Aruin et al., 1998), fear of falling (Adkin et al., 2002), mood state (Kitaoka et al., 2004), and hypoxia (Šarabon et al., 2018). Likewise, muscle fatigue represents a common transient physiological phenomenon that contributes to deteriorating the effectiveness of sensory and motor output (Enoka and Duchateau, 2008), which has a detrimental effect on the sensorimotor control of movement, and consequently the ability to maintain postural stability (Paillard, 2012; Monjo et al., 2015).

Muscle fatigue is defined as the exercise-induced reduction in the ability of the muscle to produce force or power (Enoka and Duchateau, 2008). In the fields of sport and rehabilitation, exercise-induced muscle fatigue can be classified as general and local fatigue. Exercise-induced general fatigue involves multiple joints and large muscle masses that vigorously solicit high cardiometabolic effort. While local fatigue often involves a single joint and a single muscle or small muscle masses that strongly stimulate the neuromuscular system (Paillard, 2012).

Several studies have investigated the effects of exercise-induced muscle fatigue on APA. Specifically, it has been reported that localized neuromuscular fatigue induces adaptations of APA in the form of earlier onset and alterations of EMGs activity in either fatigued or non-fatigued postural muscles, proving support for a centrally mediated adaptation of the CNS aimed at preserving postural stability (Vuillerme et al., 2002; Morris and Allison, 2006; Strang and Berg, 2007; Kanekar et al., 2008; Strang et al., 2009; Mezaour et al., 2010). Similarly, previous results showed that early onset of APA is not limited to cases of localized neuromuscular fatigue but can also occur as a result of strenuous aerobic exercise (Strang et al., 2008). The authors speculated that early APA may represent a functional modulation of the CNS to maximize stability. As far as it is concerned the CPA, a study investigated the effects of localized neuromuscular fatigue on balance recovery following a postural perturbation (Davidson et al., 2009). The authors showed changes in the center of mass trajectory consistent with a fatigue-induced decline in the ability to recover from the perturbations.

While the effects of fatigue on postural adjustments have been studied extensively, only a recent study has compared how the CNS reorganizes postural adjustments in response to local and central fatigue during a self-initiated rapid arm-raising

movement (Lyu et al., 2021). Local neuromuscular fatigue was induced by sub-maximal intermittent isometric knee extensions, while general fatigue was implemented with rowing ergometer at constant speed for 20 min such that non-postural muscles were involved. The results showed that APA coactivations in the trunk and thigh muscles were greater after local fatigue exercise than after general fatigue exercise, suggesting a general compensation by the CNS in response to the neuromuscular deficits in the locally fatigued muscle. The greater CPA coactivation of trunk and thigh muscles after both fatiguing exercises suggested the directional nature of muscle activation even under fatiguing conditions (Lyu et al., 2021). However, only muscles at the hip and knee joints were recorded in this study, so it remains to be clarified whether exercise-induced local and general fatigue regimes lead to different neuromuscular synergistic reorganization of muscle activations at the lower extremity joints during anticipatory and compensatory postural strategy phases. Indeed, a previous study has demonstrated that the biomechanical constraints and threat conditions influence the coupling between APA and CPA by differently controlling the coactivation of agonist-antagonist muscles at distal and proximal joints of lower extremities (Cesari et al., 2022).

Furthermore, it was shown that the changes in APA onset latencies persisted beyond the restoration of force production after ankle muscles were locally fatigued during externally initiated perturbations (Kennedy et al., 2012). This suggests a centrally mediating protective response, as opposed to a peripherally indicating limitation in performance. Nevertheless, no study has examined how different fatiguing regimes, i.e. intense cardiometabolic general exercise and localized neuromuscular fatigue, influence the adaptation and changes of neuromuscular strategies of APA and CPA throughout the recovery phase.

Therefore, the primary aim of the study was to investigate the effect of condition (pre and post) and type of fatiguing exercise (general and local fatigue) on the reorganization of muscles activity at the lower extremity joints during the anticipatory and compensatory phases of postural adjustments. In the current experiment participants were exposed to a predictable external perturbation to eliminate any confounding factors for changes of APA and CPA activity resulting from limitations in motor performance of self-initiated voluntary actions due to the

fatigue state. Indeed, any detectable changes of the APA and CPA would merely underlie the effect of fatigue on the feedforward and feedback postural control due to the unchanged mechanical characteristic of the triggered perturbation (Santos et al., 2010a; Chen et al., 2017; Cesari et al., 2022). As a second aim, we examined the differences in the adaptation of anticipatory and compensatory postural mechanisms during the recovery period after exhaustive exercise with high cardiometabolic effort and localized neuromuscular fatigue.

We hypothesized that 1) general fatigue would have a larger, detrimental effect on postural stability, requiring participants to increase postural correction – by increasing CPAs, 2) participants would explore alternative anticipatory strategies to compensate for the perturbation following the localized muscle fatigue, due to the imbalance in muscle proprioceptive feedback at the lower limbs.

MATERIALS AND METHODS

Participants

Fourteen healthy male subjects without history of cardiovascular disease and musculoskeletal injuries to the limbs were recruited for this study (age: 25.3 ± 4.2 years; height: 1.78 ± 0.06 m; weight: 77.1 ± 6.8 kg). Participants had normal or corrected to normal vision. The study protocol conformed to the principles of the Declaration of Helsinki and was approved by the local Ethical Committee (Prot. N°13/2019). Participants provided written informed consent before taking part in the study.

Study Design

Participants were exposed to two different exercise protocols in a crossover design: localized isometric exercise to induce localized neuromuscular fatigue (LocF) and generalized muscular exercise with upper extremities at high cardiometabolic effort (GenF). Exercise protocols are detailed later in the Exercise Protocols section. Participants were asked to come to the laboratory for assessments at two different visits with at least 72 hours interval between each visit, and exercise protocols order were randomized across participants. Each visit differed in the fatigue exercise tests (LocF or GenF), while the postural task (see later in section) – which was

administered prior to- and after the exercise – was identical. Participants were granted 10 trials at the beginning of each session to familiarize with the task and then performed 12 trials prior to exercise (Pre). Distance between the postural task setup and the exercise protocol instrumentation was minimized to allow participant to perform the subsequent trials post-exercise (Post) immediately after the termination of the protocol (≤5 s). Participants performed 14 trials during the following 10 minutes of recovery (One trial every 30 s for the first 3 minutes, 1 every 60 s for the following minutes). The time intervals between trials were based on pilot tests, where few participants experienced light-headed state after switching from the GenF protocol to a standing static position.

Postural task

Participants were asked to stand upright barefoot in front of a pendulum with knees slightly bent and their hands crossed behind their back. They were instructed to receive a series of pendulum perturbations directing frontally on their chest, and to maintain their balance after the perturbation for at least 5 seconds. A weighted pad (total mass: 0.75 kg), connected to the fulcrum by a 1-meter aluminum bar was kept horizontal (90° respect to the impact position) and released by an experimenter randomly within 5 seconds after an auditory cue. Fulcrum's height was adjusted to have the pad impacting at participant's sternum level and with the pendulum perpendicular to the ground. The magnitude of the pendulum impact on participants' chest was about 140 N (Figure 2.1, Panel A). A tri-axial accelerometer (CZL635, Robot Italy srl, Rome, Italy, sampling rate: 2000 Hz) was secured to the pendulum to detect its motion. Participant's feet position was marked on the ground and kept constant across trials. The experimental procedure was specifically designed to avoid the involvement of the upper limbs in the postural task.

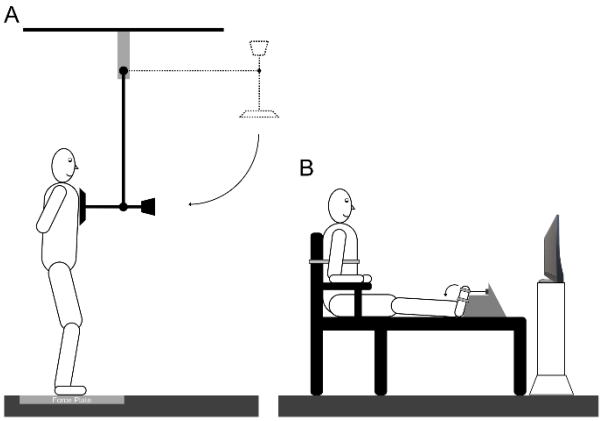

Figure 2.1 - A) Schematic diagram of the experimental set-up. Participants were asked to stand upright barefoot on a force plate in front of a pendulum with their hands crossed behind their back. They were instructed to receive a series of perturbations coming from the front, and to maintain their balance after the perturbation. B) Set-up for the localized neuromuscular fatigue exercise (LocF).

Exercise Protocols

When performing the LocF exercise protocol, participants were seated comfortably on a chair with their backs rested, the knees flexed at 90º, ankles in plantar flexion at 10º and the feet fastened together with nylon straps to a custom-made setup (Fig. 1B). The custom-made setup was connected through an inextensible cable to a load cell (System Pese, Milan, Italy; linear response: 1500N, sampling frequency: 1000 Hz). They performed 3 maximal voluntary contractions (MVC) in dorsiflexion of the two ankles and then started the submaximal intermittent isometric exercise with the dorsiflexors group muscles (60 ±5% MVC; 45s, duty cycle: 0.67; contraction/relaxation: 30s/15s). The sounds of a timer set the pace of the exercise and visual feedback of force production relative to the target force (marked as a green shaded area) was provided on a screen in front of participants. Participants were constantly motivated throughout the exercise. Task failure was determined when participants did not reach and hold for more than 1 sec. the target force for two consecutive cycles. The ankle dorsiflexors were chosen as the target muscles for the LocF exercise because their primary contribution to maintaining balance when receiving the pendulum perturbation (Santos et al., 2010a; Kaewmanee et al., 2020; Cesari et al., 2022).

The GenF exercise consisted in a step-incremental test on an electromagnetically braked arm ergometer (ergoselect 400, arm ergometer, ergoline GmbH, Bitz, Germany). The ergometer was connected to and operated by a PC running the

metabolimeter. The software (OmniaTM, Cosmed, Rome, Italy) allows to impose workloads according to predefined protocols. Participants were at rest for 2 min (rest), warmed up at 50 Watts (W) for 3 minutes, then workload increased by 10 W per minute until participants could no longer sustain the exercise. Participants were constantly motivated and reminded to maintain cadence within 70-80 RPM throughout the exercise. Task failure was determined when participants' cadence fell below 55 RPM despite verbal encouragement.

Kinematics and posturography

Kinematic data were collected at 250 Hz using an 8-camera Vicon motion capture system (MX 13, VICON, Oxfordshire, UK). Sixteen reflective markers (14 mm in diameter) were placed on the following anatomical landmarks of both sides of the body: heel (calcaneus), tip toe (distal phalanx), ankle joint (lateral malleolus), knee joint (lateral epicondyle of femur), hip joint (great trochanter), shoulder (acromion) and two additional markers on the mid-point between ankle-knee and knee-hip joints, respectively to improve the reconstruction of the 3-D model. Before starting the session, a static trial was performed to reconstruct the model and label each marker for the automatic software detection during the trials. The center of pressure (CoP) displacement while standing in front of the pendulum was recorded by means of a force platform (model OR-5, AMTI, USA: 90 x 90 cm, sample rate: 2000 Hz).

Surface EMG

Surface electromyogram (EMG) signals were recorded from 8 muscles on participants' dominant side using a wireless system (Zerowire, Aurion, Italy). After proper shaving and cleaning of the skin with alcohol swabs, Ag/AgCl electrodes (PG10C; Fiab, Vicchio, Italy) were attached to the skin with a 20-mm interelectrode distance. Electrodes were positioned over the bellies of the following muscles, following recommendations (Hermens et al., 2000): rectus femoris (RF; halfway on the line from the anterior superior iliac spine to the superior part of the patella), biceps femoris (BF; halfway between the ischial tuberosity and the lateral epicondyle of the tibia), tibialis anterior (TA; at one-third on the line between the tip of the fibula and the tip of the medial malleolus), gastrocnemius medialis (GM; on the most prominent bulge of the muscle, aligned to muscle fibers orientation),

rectus abdominis (RA; 3 cm lateral to the umbilicus) and erector spinae (ES; 3 cm lateral to L1). Electrode placement was confirmed by asking the participants to perform a set of isometric contractions and related free movements while observing the resulting EMG patterns (Kendall, 2005). EMG signal was sampled at 2000 Hz. Motion capture, force plate and EMG systems were synchronized with a hardware device (MX Control, VICON, Oxfordshire, UK) that matched the data acquisition across systems.

Cardio-metabolic parameters

Cardio-ventilatory parameters were collected for 2 minutes prior exercise (Rest), throughout the exercise phase (exercise) and for 10 min after the end of the exercise (Post) using a portable breath-by-breath indirect calorimeter system (K5, Cosmed, Rome, Italy), calibrated following manufacturer's instructions. The analyzers were calibrated before each test, with a gas mixture of known composition (FO_2 = 0.16; FCO_2= 0.04; N2 in equilibrium) and ambient air. The turbine was calibrated using a 3 L syringe (Hans Rudolph Inc., USA). Subjects wore a mask and breathed through a turbine flowmeter. The gases were sampled continuously through a capillary line inserted externally to the flowmeter and analyzed by fast-response O_2 (chemical) and CO_2 (infrared) sensors in the portable metabolimeter. Capillary-blood lactate concentration $[La]_b$ was sampled at rest (Rest) and in-between trials at three time points after the fatigue exercise at the 3rd,5th and 10th minute from participants' ear lobe and assessed using an electro-enzymatic method (Biosen C_line, EKF Diagnostics, Barleben, Germany).

Data processing

Cardio-metabolic data analysis

Breath-by-breath absolute values (litre/min) of oxygen consumption ($\dot{V}O_2$), carbon dioxide production ($\dot{V}CO_2$) and pulmonary ventilation ($\dot{V}_E$) were obtained by means of manufacture software (Omnia^{TM} , Cosmed, Rome, Italy) together with heart rate (HR) collected by telemetry Polar® wireless band (beats/min). Also, respiratory rate (RR) (l/min) has been obtained. $\dot{V}O_2$ has been reported normalized per Kg body mass ($\dot{V}O_2$/kg). The mechanical load (watt) of the arm ergometer was recorded

continuously by software running the metabolimeter. Resting data (Rest) was calculated as the mean values of the latter 30 s before warm-up phase begins; $\dot{V}O_2$ max and all maximal variables were calculated as the mean of the latter 30 s before the end of the exercise. All the metabolic variables were exported as spreadsheet files with an average time of 5 sec to get all metabolic data aligned with the starting of the recovery phase. Each $\dot{V}O_2$ five sec data was further averaged every 15 (data discrete binning) and then aligned to synchronous by time to the strokes provided by the pendulum. The same procedure was done for: $\dot{V}CO_2$,$\dot{V}_E$, HR, and RR. Data series of each participant were then ensemble average during the following three time points after fatigue exercise: Post1 (including data at time 0 – i.e., immediately after the end of the exercise, 30, and 60 sec.), Post2 (including data at time 1.5, 2, 2.5, and 3 min.), Post3 (including data at time 4, 5, 6, 7, 8, 9, and 10 min.).

Kinematics and posturography data analysis

Kinematic data were reconstructed using Vicon Nexus software, then offline processed together with all the other data using customized scripts in MATLAB software (R2021b, version 9.11.0, MathWorks, Natick, MA, USA). Load cell, force plate and kinematics data were low pass filtered (4th order Butterworth with cut-off frequencies of 10 Hz). The signal obtained from the accelerometer attached to the pendulum was used to identify the moment of the impact (t_0) and time of release (t_R). The instant of the impact t_0 of the pendulum on the participant's chest was defined as the time of the negative peak of the first derivative of the acceleration signal in the antero-posterior direction. The time of the release t_R of the pendulum was calculated as the instant when magnitude of the accelerometer signal in the antero-posterior direction crossed 5% of its maximal value before t_0 (Cesari et al., 2022). The maximum shoulder displacement in the sagittal plane after t_0 (S_{Back}) was measured to assess the compensatory effect on kinematics of the upper body following the perturbation. It was calculated as the distance covered by the marker attached to the acromion of the dominant side between t_0 and the instant when its tangential velocity crossed the zero value after t_0 (t_{SBack}) (Cesari et al., 2022) (Figure 2.2).

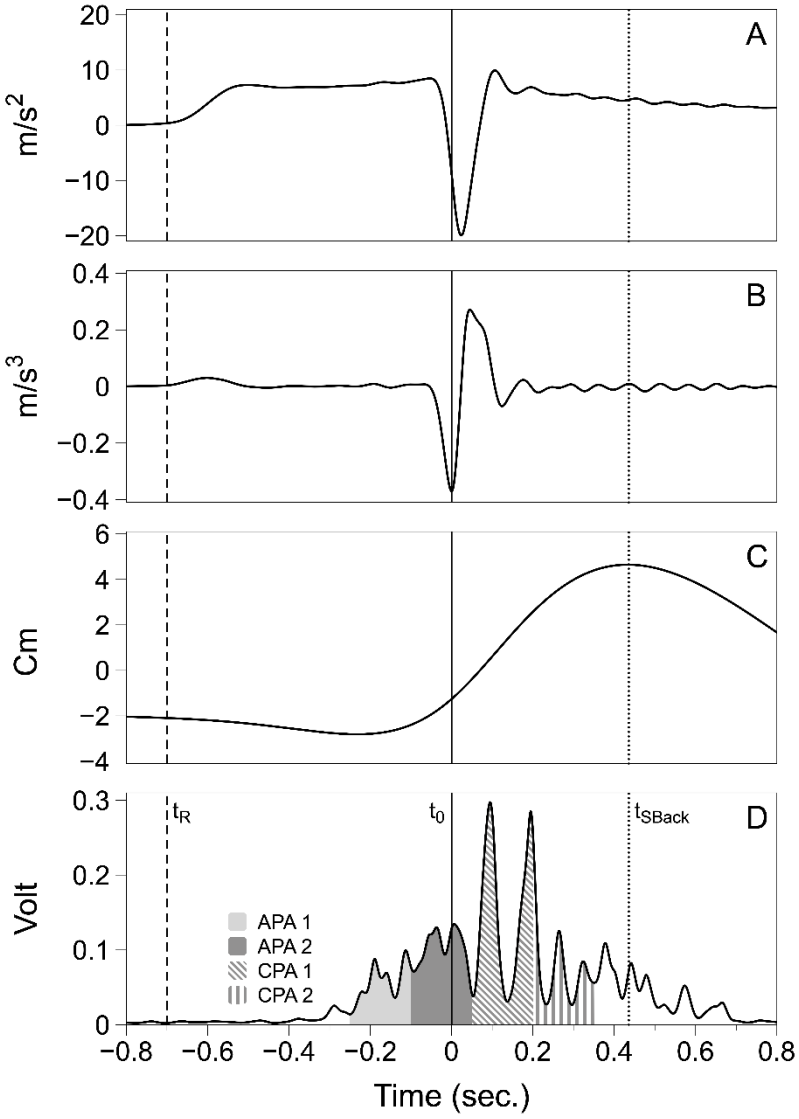

Figure 2.2 - A representative trial showing: A) the acceleration of the pendulum in antero-posterior direction; B) the 1st derivative of the acceleration of the pendulum; C) the displacement of the shoulder of the dominant side in antero-posterior direction; D) filtered EMG trace of the tibialis anterior (TA) of the dominant lower limb. APA1, APA2, CPA1, CPA2 are highlighted in light gray, dark gray, oblique and vertical lines pattern respectively. The solid, dashed, and dotted lines represent the t_0, t_R and t_{Sback} respectively.

The kinematics of relative joint angles of the dominant side in the sagittal plane were computed for the ankle (θ_{Ankle}), knee (θ_{Knee}) and hip (θ_{Hip}) joints at t_R, t_0 and t_{SBack}. The magnitude and polarity of each joint angle were described according to Perry and Burnfield (Perry and Burnfield, 2010). Specifically, for the ankle joint 90˚ between the shank and the foot was the boundary between plantarflexion ($\theta_{Ankle} < 0$) and dorsiflexion ($\theta_{Ankle} > 0$). When the knee was fully extended, it was described as 0˚ flexion, and when the shank moved to a posterior direction relative

to the thigh, the knee joint angle was said to be in flexion ($\theta_{Knee} > 0$). The θ_{Hip} was defined by the path of thigh displacement from the vertical with positive angles for hip flexion and negative angles for hip extension.

To assess the effect of the fatiguing protocols on the upright standing posture, we examined the CoP displacement before the impact during a time window of 2 seconds before t_R. Specifically, we computed the root mean square (RMS_{CoP}) and total mean velocity (Vel_{CoP}) of the total CoP in both antero-posterior and medio-lateral directions (Raymakers et al., 2005; Duarte and Freitas, 2010) as following:

$$RMS_{CoP} = \sqrt{\frac{(CoPx_1^2 + CoPx_2^2 + \cdots + CoPx_n^2) + (CoPy_1^2 + CoPy_2^2 + \cdots + CoPy_n^2)}{n}}$$

$$Vel_{CoP} = \frac{\sum \frac{\sqrt{(CoPx_i - CoPx_{i-1})^2 + (CoPy_i - CoPy_{i-1})^2}}{t_i - t_{i-1}}}{n}$$

where CoPx and CoPy are the de-meaned signals of CoP in medio-lateral and antero-posterior directions respectively, n is the number of samples. Note that for CoPx and CoPy with zero mean, RMS_{CoP} equals the planar standard deviation (i.e considering both medio-lateral and antero-posterior directions) (Raymakers et al., 2005; Duarte and Freitas, 2010).

EMG data analysis

EMG data were firstly detrended, band-pass filtered (5 – 450 Hz; 4th order Butterworth) and a notch filter (47 – 53 Hz, 4th order Butterworth) was applied to remove power-line noise. Signals were then high-pass filtered (20 Hz, 6th order Butterworth) to remove movement artifacts (Solnik et al., 2008, 2010). Resulting EMG signals were then separately processed for the determination of the timing of activation (onset) and the magnitude of the activity. The former was computed using Teager–Kaiser Energy Operator (Solnik et al., 2008, 2010) to determine bursts onset of EMG signal from ventral muscles. The latter was computed by full-wave rectifying, and low-pass filtering (20 Hz, 2nd order Butterworth)(Kaewmanee et al., 2020) to obtain EMG linear envelopes. EMG activity of all studied muscles

(∫EMG) was than calculated using a trapezoidal numerical integration (function trapz in Matlab) during the four epochs (relative to t0): (1) from -250 to -100 ms (anticipatory postural adjustment – window 1; APA1), (2) from -100 to +50 (anticipatory postural adjustment – window 2; APA2), (3) from +50 to +200 ms (compensatory postural adjustment – window 1; CPA1), (4) from +200 to +350 ms (compensatory postural adjustment – window 2; CPA2). Background EMG activity (EMGbackground) was computed from a 50 ms window at the beginning of each trial – EMG signal was visually inspected to confirm absence of abnormal activity – and subtracted to correct each epoch integral:

$$\int APA1_i = \int_{-250}^{-100} EMG(i) - 3 \int EMGbackgroundi(i)$$

$$\int APA2_i = \int_{-100}^{+50} EMG(i) - 3 \int EMGbackgroundi(i)$$

$$\int CPA1_i = \int_{+50}^{+200} EMG(i) - 3 \int EMGbackgroundi(i)$$

$$\int CPA2_i = \int_{+200}^{+350} EMG(i) - 3 \int EMGbackgroundi(i)$$

For comparison across subjects, EMG values were normalized by the highest positive value (∫EMGmax) within conditions, for each muscle and each subject separately (Slijper and Latash, 2000, 2004). Note that after this normalization, integrated EMG values were comprised within the range from + 1 to – 1, where negative values corresponded to a decrease in the EMG activity respect to the background window.

Furthermore, we computed indexes of co-activation (C-index) and reciprocal activation (R-index) within agonist–antagonist muscle pairs (TA/GM, RF/BF and RA/ES) acting at joint level within the framework of the equilibrium-point hypothesis (Feldman, 1986). Indexes were computed using EMG integrals of ventral and dorsal muscles for each time-epoch (Slijper and Latash, 2000, 2004; Bertucco et al., 2021; Cesari et al., 2022). Specifically, R-Index = ($\int EMG_{ventral}$ - $\int EMG_{dorsal}$) and C-Index = 0 if $\int EMG_{ventral}$ and $\int EMG_{dorsal}$ had different signs; C-

Index = min $\{|\int EMG_{ventral}|;|\int EMG_{dorsal}|\}$ if $\int EMG_{ventral}$ and $\int EMG_{dorsal}$ had the same signs (Piscitelli et al., 2017; Cesari et al., 2022).

Equally to cardio-metabolic variables, all the outcome variables considered for the kinematic, posturography and EMG analysis were averaged during the three time points after the fatigue exercise: Post1 (including data at time 0, 30, and 60 sec.), Post2 (including data at time 1.5, 2, 2.5, and 3 min.), Post3 (including data at time 4, 5, 6, 7, 8, 9, and 10 min.).

Statistical analysis

Data are presented in the figures as box plots depicting the median and the 25th and 75th quartiles and the whisker showing the min and max values. Skewness and kurtosis were used to assess the normality of the data. Two-way repeated-measures ANOVAs were performed to compare the fatiguing protocols to the Pre and Post conditions. As fixed effects, we used factors Condition [2 levels: GenF and LocF] and Time [4 levels: Pre or Rest, Post1, Post2 and Post3] for relative joint angles, RMS_{CoP}, Vel_{CoP} and the cardiometabolic variables. The fixed effect Time for the capillary-blood lactate concentration $[La]_b$ was considered at 4 levels [Rest, 3rd, 5th and 10th min.]. Two-way repeated-measures ANOVAs were used to compare the cardiometabolic responses of the two fatiguing exercise protocols at rest and at task failure. Thus, as fixed effects we considered Condition [2 levels: GenF and LocF] and Time [2 levels: Rest and Max (task failure)]. Since the EMGs were recorded and normalized for each of the two fatigue sessions, one-way repeated-measures ANOVAs were performed to compare the Pre and Post fixed effect conditions, Time [4 levels: Pre, Post1, Post2 and Post3], within each ∫EMG epoch (∫APA1, ∫APA2, ∫CPA1, ∫CPA2) separately, R-Index and C-Index for each muscle pairs (TA/GM, RF/BF and RA/ES). As random effects, we had intercepts for participants, as well as by-participant slopes for the effect of Condition and Time. To assess the effect of the submaximal intermittent isometric exercise on LocF, a paired-sample t-test was performed for the mean force produced (mF) between the first and last isometric sustained contraction (30 s).

Pairwise comparisons with Tukey's HSD corrections were used to explore significant effects. A Friedman non-parametric test was performed in case the normality of the data was not verified, and Durbin-Conover test was used for

multiple comparisons. A significance level of $p < 0.05$ was set for all statistical tests. Statistical analysis was performed using Jamovi (Version 2.3.21, Sydney, Australia).

RESULTS

Metabolic responses to the fatiguing protocols

The average maximum force exerted by the ankle dorsiflexors during MVC prior to the LocF fatigue exercise was 485.2 ± 81.9 N, with an average time to task failure of 592 ± 170 sec. The paired t-test revealed a significant decreased in mF ($t(13) = 10.7$, $p < 0.001$) between the first ($\overline{x}$ = 284.7± 47.6 N) and last ($\overline{x}$: 192.9 ± 23.5 N) isometric sustained contraction, resulting in a mean drop in force of 32% ± 0.07. As concerns the step-incremental test to induce generalized muscular fatigue with high cardiometabolic effort, the maximal power output reached by the patricians on the ergometer was on average 118.7 ± 23.8 W. The time to exhaustion was on average 574 ± 142 sec. including the 3 min. of warm-up.

The two-way repeated measures ANOVAs showed significant effects for the main factors, Condition and Time, as well as the interactions for the fatigue protocols on $\dot{V}O_2$/kg (Condition: $F_{1,13}$=126.9, P<0.001, η^2= 0.17; Time: $F_{1,13}$=178.5, P<0.001, η^2= 0.53; Condition x Time: $F_{1,13}$=142.2, P<0.001, η^2= 0.17), $\dot{V}CO_2$ (Condition: $F_{1,13}$=122.1, P<0.001, η^2= 0.17; Time: $F_{1,13}$=273.9, P<0.001, η^2= 0.57; Condition x Time: $F_{1,13}$=130.8, P<0.001, η^2= 0.17), $\dot{V}_E$ (Condition: $F_{1,13}$=67.5, P<0.001, η^2= 0.11; Time: $F_{1,13}$=90.1, P<0.001, η^2= 0.58; Condition x Time: $F_{1,13}$=65.8, P<0.001, η^2= 0.10) and HR (Condition: $F_{1,13}$=96.7, P<0.001, η^2= 0.12; Time: $F_{1,13}$=463.0, P<0.001, η^2= 0.64; Condition x Time: $F_{1,13}$=266.9, P<0.001, η^2= 0.13). The GenF protocol induced significant higher responses for all the metabolic parameters compared to LocF (Figure 2.3).

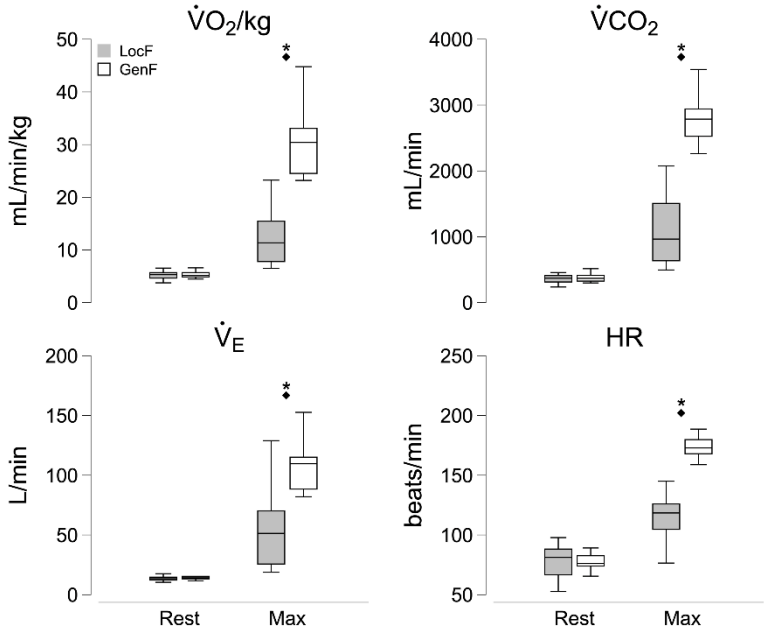

*Figure 2.3 - Metabolic responses ($\dot{V}O_2$/kg, $\dot{V}CO_2$, $\dot{V}_E$, HR) at Rest and to exhaustion (Max) between GenF (white box) and LocF (grey box) fatigue exercises. ◆ Significant effects within Condition factor (GenF vs LocF); * significant effects within Time factor (Rest vs Max). Significance level set at $p < 0.05$.*

The metabolic responses were compared between before (Rest) and after the fatigue exercise, separated into three time point phases of recovery (Post1, Post2 and Post3, see Methods for details) while participants received the pendulum perturbation.

The ANOVAs found significant effects for Condition and Time factors, as well as the interactions on all the considered metabolic responses: $\dot{V}O_2$/kg (Condition: $F_{1,13}$=71.9, P<0.001, η^2= 0.19; Time: $F_{1.5,19.1}$=139.4, P<0.001, η^2= 0.48; Condition x Time: $F_{1.5,19.8}$=56.7, P<0.001, η^2= 0.16); $\dot{V}CO_2$ (Condition: $F_{1,13}$=138.3, P<0.001, η^2= 0.27; Time: $F_{1.5,19.5}$=237.4, P<0.001, η^2= 0.44; Condition x Time: $F_{1.3,16.6}$=88.9, P<0.001, η^2= 0.19); $\dot{V}_E$ (Condition: $F_{1,13}$=112.4, P<0.001, η^2= 0.25; Time: $F_{1.3,17.4}$=117.0, P<0.001, η^2= 0.43; Condition x Time: $F_{1.31,17.1}$=51.8, P<0.001, η^2= 0.14); RR (Condition: $F_{1,13}$=25.6, P<0.001, η^2= 0.08; Time: $F_{1.4,18.3}$=32.6, P<0.001, η^2= 0.28; Condition x Time: $F_{1.6,21.0}$=14.7, P<0.001, η^2= 0.06); HR (Condition: $F_{1,13}$=80.0, P<0.001, η^2= 0.23; Time: $F_{1.8,23.8}$=313.4, P<0.001, η^2= 0.45; Condition x Time: $F_{2,26.4}$=89.9, P<0.001, η^2= 0.11); $[La]_b$ (Condition: $F_{1,13}$=337.1, P<0.001, η^2= 0.48; Time: $F_{2,26}$=216.0, P<0.001, η^2= 0.27; Condition x Time: $F_{3,39}$=159.5, P<0.001, η^2= 0.17). The higher metabolic parameters following the GenF exercise

were maintained during the post phases compared to LocF. Moreover, following exercise, there was a significant decrease in all post-GenF metabolic responses, except for $[La]_b$, which however remained significantly higher compared to Rest even at the last phase (Post3). LocF resulted in a less pronounced decrease in the cardio-metabolic responses during the recovery phases, with a full recovery at the final phase for $\dot{V}CO_2$, RR and $[La]_b$ (Figure 2.4).

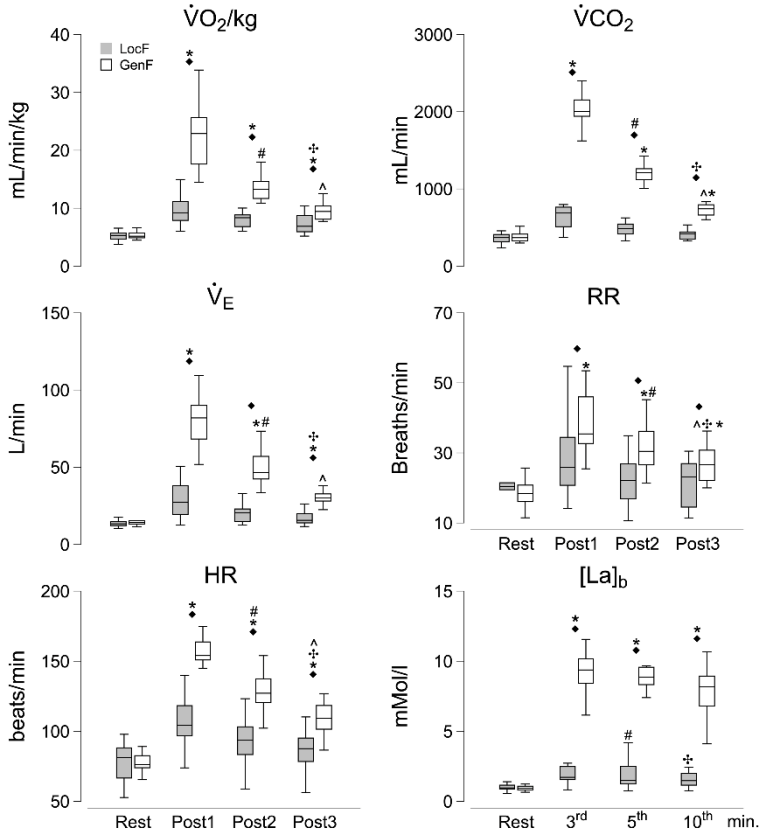

*Figure 2.4 - Metabolic responses ($\dot{V}O_2$/kg, $\dot{V}CO_2$, $\dot{V}_E$, RR, HR and $[La]_b$) between GenF (white box) and LocF (grey box) fatigue exercises at Rest and at the Post phases (Post 1, Post2 and Post3; 3rd, 5th, 10th min. for $[La]_b$) while participants received the pendulum perturbation. ◆ Significant effects within Condition factor (GenF vs LocF); * significant effects between Rest and Post1, Post2 or Post3 (3rd, 5th, 10th min. for $[La]_b$); # significant effect between Post1 and Post2 (3rd and 5th min); ✣ significant effect between Post1 and Post3 (3rd and 10th min); ^ significant effect between Post2 and Post3 (5th min and 10th min). Significance level was set at $p < 0.05$.*

CoP displacement during upright steady-state posture

Root mean square (RMS_{CoP}) and mean velocity (Vel_{CoP}) of the bidirectional CoP displacement before impact with the pendulum (t0) were calculated to assess the effect of fatigue protocols on upright standing posture. The two-way ANOVAs found significant effects of main factor Time on both RMS_{CoP} ($F_{3,38}$=16.0, P<0.001, η^2= 0.25) and Vel_{CoP} ($F_{1.98,25.8}$=17.8, P<0.001, η^2= 0.27). No significant effects

were found for factor Condition and interaction. The pairwise comparisons showed significantly higher RMS_{CoP} and Vel_{CoP} during the three Post phases compared to the Pre condition ($p<0.01$) and between Post2 and Post3 for Vel_{CoP}, indicating that both fatigue exercises induced similar sustained decrease of postural stability in upright standing before the perturbation (Figure 2.5).

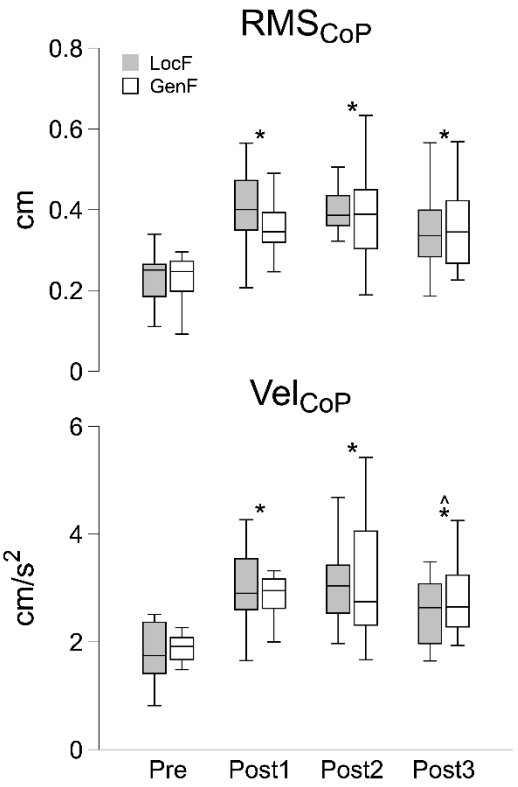

*Figure 2.5 - RMS_{CoP} (on the top) and Vel_{CoP} (at the button) between the pendulum release (t_R) and at the pendulum impact (t_0) before (Pre) and after the fatigue exercise separated by the three Post phases (Post 1, Post2 and Post3). White and grey box indicate the GenF and LocF exercise conditions respectively. * Significant effects between Pre and Post1, Post2 or Post3; ^ significant effect between Post2 and Post3. Significance level was set at $p < 0.05$.*

Kinematic variables

Relative angles in the sagittal plane of ankle (θ_{Ankle}), knee (θ_{Knee}) and hip (θ_{Hip}) joints were computed at three different time points: at the pendulum release (t_R), and at the instant of impact (t_0) and at the maximum shoulder displacement after impact (t_{SBack}).

The ANOVAs found a significant effect for Time factor ($F_{2.1,26.9}=26.3$, $P<0.001$, $\eta^2= 0.07$) on θ_{Hip} at t_R ($F_{2.1,26.9}=26.3$, $P<0.001$, $\eta^2= 0.07$), t_0 ($F_{1.8,23.4}=17.5$, $P<0.001$, $\eta^2= 0.06$) and t_{SBack} ($F_{1.6,21.1}=12.1$, $P<0.001$, $\eta^2= 0.04$), with no statistical effects for Condition and interaction. The post hoc comparisons showed an increase of hip

flexion after the fatiguing exercise protocols for each time points (t_R, t_0 and t_{SBack}) during the three Post phases, as well as between Post1 and Post3 and Post 2 and Post3. No significant effects were found on θ_{Ankle} and θ_{Knee} at the time points t_R and t_0. A significant effect for Time ($F_{3,39}$=3.2, P<0.05, η^2= 0.03) and interaction Condition x Time ($F_{3,39}$=3.3, P<0.05, η^2= 0.02) was found on θ_{Ankle} at t_R. The post hoc comparisons revealed a significant reduced ankle dorsiflexion after the impact at Post1 compared to Pre and Post 3 for the LocF exercise condition (Figure 2.6). There were statistically significant effects for Condition and Time factors on S_{Back} (χ^2_7 = 16.2, p < 0.01). LocF condition induced a greater backward shoulder displacement after impact following fatigue exercise for Post 1 ($\overline{x}$: 4.0 cm ± 0.47 SEM) compared to Pre ($\overline{x}$: 2.0 cm ± 0.55 SEM, p<0.01) and Post3 ($\overline{x}$: 2.2 cm ± 0.75 SEM, p<0.05) (Figure 2.7).

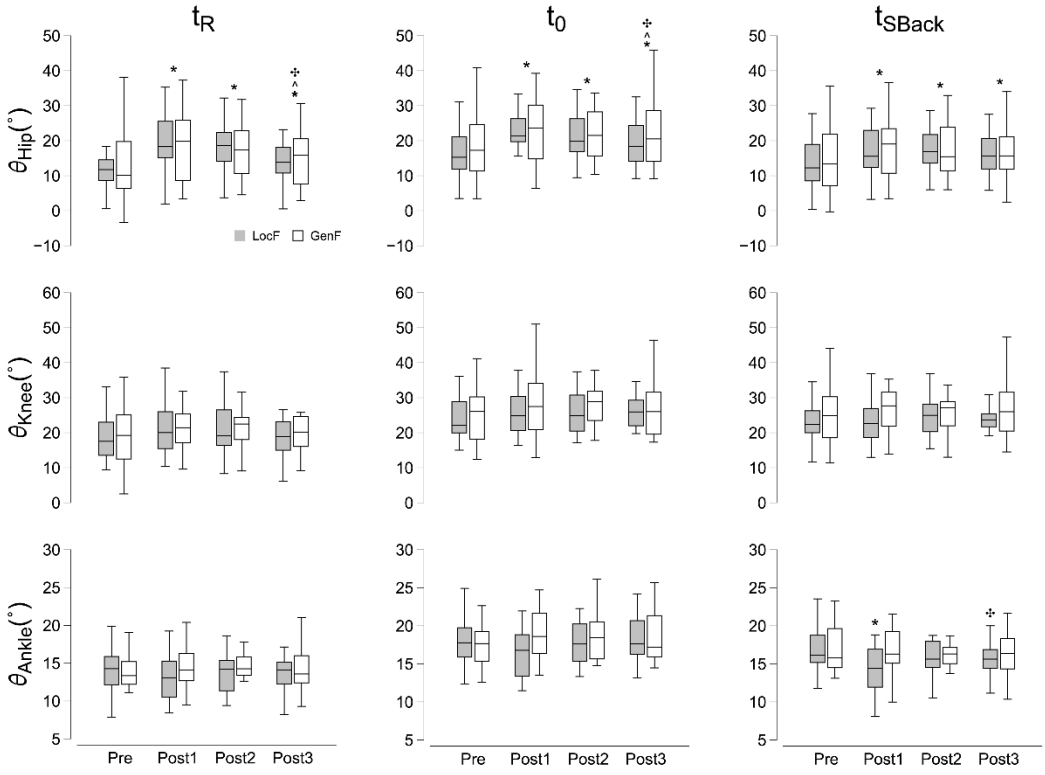

*Figure 2.6 - Relative joint angles (θ_{Ankle}, θ_{Knee}, and θ_{Hip}) at the pendulum release (t_R, panels on the left) at the pendulum impact (t_0, panels in the middle), and at the maximum shoulder displacement after impact (t_{SBack}, panels on the right) before (Pre) and after the fatigue exercise separated by the three Post phases (Post 1, Post2 and Post3). White and grey box indicate the GenF and LocF exercise protocol respectively. * Significant effects between Pre and Post1, Post2 or Post3; ✣ significant effect between Post1 and Post3; ^ significant effect between Post2 and Post3. Significance level was set at p < 0.05.*

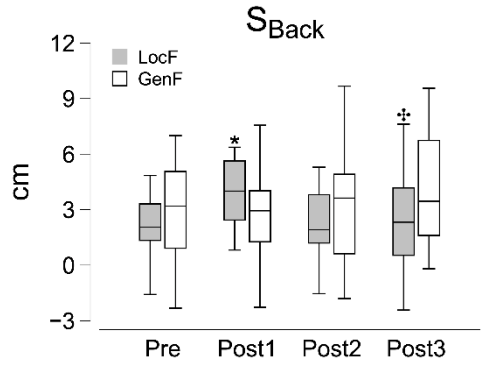

*Figure 2.7 - Maximum shoulder displacement after impact (S_{Back}) before (Pre) and after the fatigue protocol separated by the three Post phases (Post 1, Post2 and Post3). White and grey box indicate the GenF and LocF exercise protocol respectively. * Significant effects between Pre and Post1, Post2 or Post3; ✣ significant effect between Post1 and Post3. Significance level was set at $p < 0.05$.*

Effects of different fatiguing exercise on the anticipatory and compensatory postural EMG activity

Figure 2.8 shows EMG traces of one trial before the fatigue exercise (Pre) for a representative participant. Anticipatory and compensatory activity, seen as bursts in the background EMG activity, was present in the ventral muscles (TA, RF, RA) and ES.

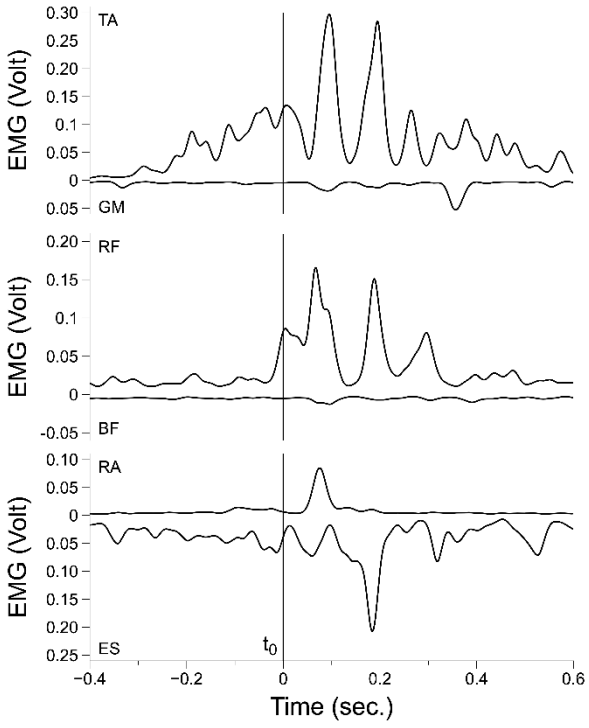

Figure 2.8 - Filtered EMG traces of one trial in the Pre condition for a representative participant. The vertical solid line in the center of each panel corresponds to the impact time of the pendulum (t_0). TA: tibialis anterior; GM: gastrocnemius medialis; RF: rectus femoris; BF: biceps femoris;

RA: rectus abdominis; ES: erector spinae. Dorsal muscle activation patterns (GM, BF, ES) are shown inverted for ease of comparison.

Statistical analysis found significant effects for Condition and Time factor on GM during APA1 ($\chi^2_7 = 13.9$, $p < 0.05$) and APA2 ($\chi^2_7 = 22.4$, $p < 0.01$). Pairwise comparisons found decreased ∫EMG of GM in all the Post time points (Post1, Post2, and Post3) following LocF exercise during both APA1 ($p<0.05$) and APA2 ($p<0.05$). Conversely, GM showed higher activation at Post1 compared Pre and Post 3 after GenF exercise during APA2 ($p<0.01$) (Figure 2.9 and Figure 2.10). There were statistically significant effects for Condition and Time ($\chi^2_7 = 19.0$, $p < 0.01$) on TA during APA2. The anticipatory ∫EMG of TA during APA2 decreased after the LocF exercise in all three Post time points ($p<0.01$), while not difference was observed with GenF exercise condition. Significant effects were also observed for Condition and Time on RF and ES during APA1 (RF: $\chi^2_7 = 26.6$, $p < 0.001$; ES: $\chi^2_7 = 24.9$, $p < 0.001$) and APA2 (RF: $\chi^2_7 = 26.1$, $p < 0.001$; ES: $\chi^2_7 = 23.6$, $p < 0.01$). The post hoc pairwise comparisons showed a decreased ∫EMG of RF in all the Post time points during APA2 ($p<0.010$ and in Post1 phase compared to Pre and Post2 during APA1 ($p<0.01$) after performing the LocF protocol. By contrast, RF ∫EMG increased at Post1 compared to Pre during APA1 ($p<0.05$), as well as compared to Post2 during APA2 following GenF exercise ($p<0.05$). ES muscle deactivation was observed only after LocF exercise for the Post time points during both APA1 ($p<0.05$) and APA2 ($p<0.05$) (Figure 2.9 and Figure 2.10).

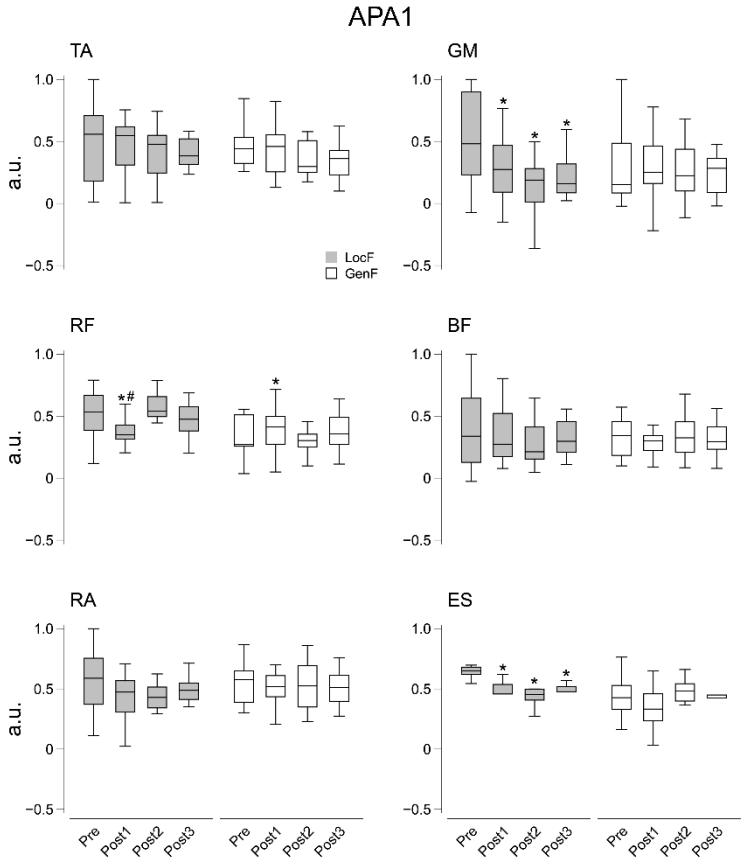

*Figure 2.9 - Integrals of EMG activity (∫ APA1) during APA1 before (Pre) and after the fatigue exercise divided by the three Post time points (Post 1, Post2 and Post3). White and grey box indicate the GenF and LocF exercise protocol respectively. TA: tibialis anterior; GM: gastrocnemius medialis; RF: rectus femoris; BF: biceps femoris; RA: rectus abdominis; ES: erector spinae. * Significant effects between Pre and Post1, Post2 or Post3; # significant effect between Post1 and Post2. Significance level was set at $p < 0.05$.*

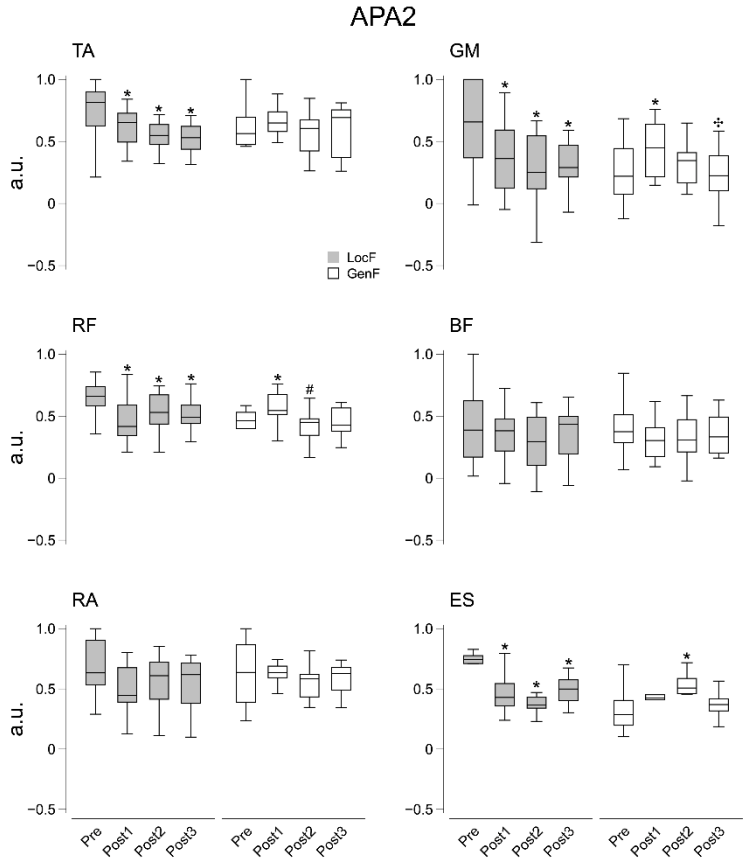

*Figure 2.10 - Integrals of EMG activity (∫ APA2) during APA2 before (Pre) and after the fatigue exercise divided by the three Post time points (Post 1, Post2 and Post3). White and grey box indicate the GenF and LocF exercise protocol respectively. TA: tibialis anterior; GM: gastrocnemius medialis; RF: rectus femoris; BF: biceps femoris; RA: rectus abdominis; ES: erector spinae. * Significant effects between Pre and Post1, Post2 or Post3; # significant effect between Post1 and Post2. Significance level was set at p < 0.05.*

As far it is concerned the compensatory activity (∫CPA), significant effects were found for Condition and Time factors on the ventral muscles RF ($\chi^2_7 = 22.6$, $p < 0.01$) and RA ($\chi^2_7 = 15.9$, $p < 0.05$) during CPA1, and on TA ($\chi^2_7 = 15.9$, $p < 0.05$) and RF (Time: $F_{1.45,18.9}=17.6$, $P<0.001$, $\eta^2= 0.39$) during CPA2. There were statistically significant effects for Condition and Time factors on dorsal muscle GM and ES for both CPA1 (GM: $\chi^2_7 = 18.9$, $p < 0.01$; ES: $\chi^2_7 = 34.0$, $p < 0.001$) and CPA2 (GM: $\chi^2_7 = 15.4$, $p < 0.05$; ES: $\chi^2_7 = 20.6$, $p < 0.01$) epochs. The post hoc showed a systematic significant decrease of ∫CPA after LocF exercise in the three Post time phases for RF ($p<0.01$), RA ($p<0.05$), GM ($p<0.05$), ES ($p<0.01$) muscles during CPA1, and for TA ($p<0.05$) and RF ($p<0.05$) muscles during CPA2 epoch. In addition, decreased ∫CPA in GM and ES muscles was observed for Post 3 compared to Pre during CPA2 ($p<0.05$). GenF exercise resulted in a significant

increase of ∫CPA in the GM muscle for Post 1 compared to Pre and Post3, and only to Post3 during CPA1 ($p<0.01$) and CPA2 ($p<0.01$) epochs respectively. By contrast, there was a decrease of ∫CPA in the ES muscle for Post 1 compared to Pre and Post2 during CPA1 ($p<0.05$) following to GenF exercise (Figure 2.11 and Figure 2.12).

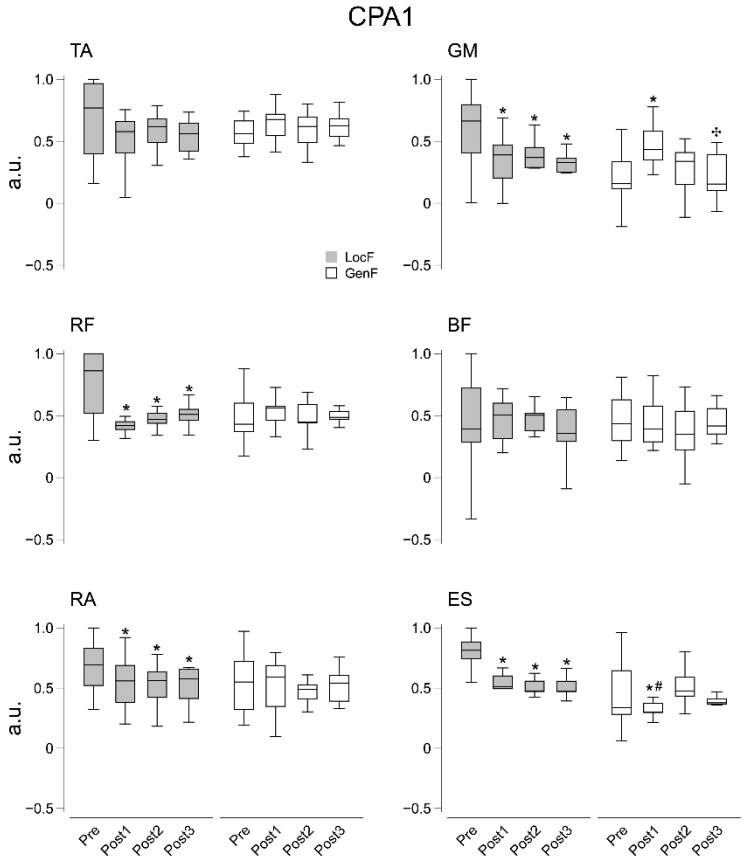

*Figure 2.11 - Integrals of EMG activity (∫ CPA1) during CPA1 before (Pre) and after the fatigue exercise divided by the three Post time points (Post 1, Post2 and Post3). White and grey box indicate the GenF and LocF exercise protocol respectively. TA: tibialis anterior; GM: gastrocnemius medialis; RF: rectus femoris; BF: biceps femoris; RA: rectus abdominis; ES: erector spinae. * Significant effects between Pre and Post1, Post2 or Post3; # significant effect between Post1 and Post2. Significance level was set at $p < 0.05$.*

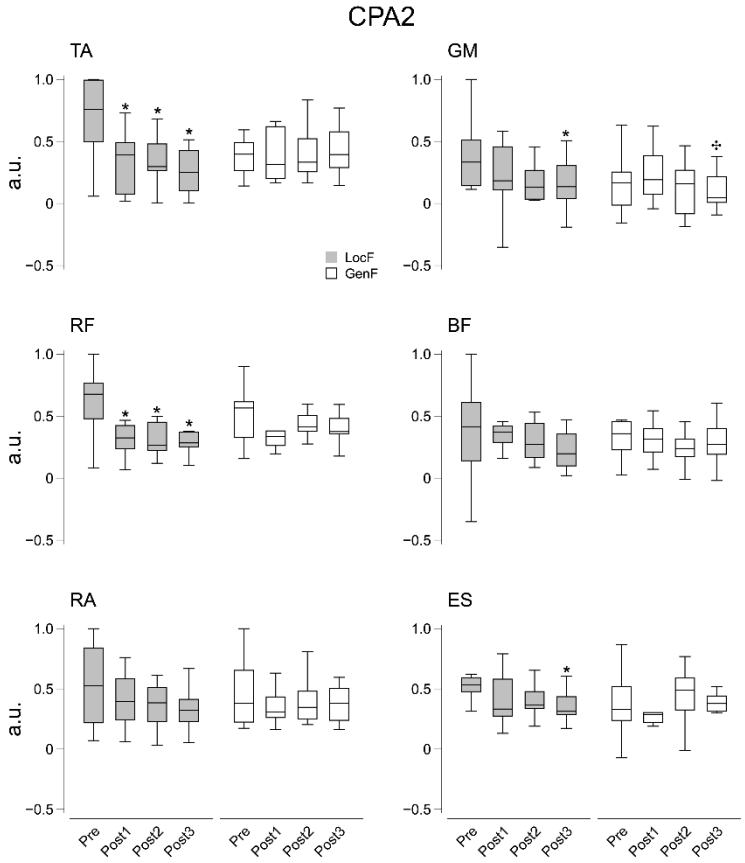

*Figure 2.12 - Integrals of EMG activity (∫ CPA2) during CPA2 before (Pre) and after the fatigue exercise divided by the three Post time points (Post 1, Post2 and Post3). White and grey box indicate the GenF and LocF exercise protocol respectively. TA: tibialis anterior; GM: gastrocnemius medialis; RF: rectus femoris; BF: biceps femoris; RA: rectus abdominis; ES: erector spinae. * Significant effects between Pre and Post1, Post2 or Post3; # significant effect between Post1 and Post2. Significance level was set at p < 0.05.*

Changes in C- and R-Indexes after fatiguing exercise

The repeated measures analysis found significant effects for Condition and Time factor on the C-Index ($\chi^2_7 = 28.6$, $p < 0.001$) and R-Index ($\chi^2_7 = 16.2$, $p < 0.05$) in the TA/GM pair during APA2. The pairwise comparisons showed a decrease in C-Index in the TA/GM muscle pair after LocF exercise over the three Post phases ($p<0.001$), while following GenF exercise there was an increase in C-Index at Post1 compared to Pre and Post 3 ($p<0.01$) (Figure 2.13). It was observed a decrease in R-Index with the GenF at Post1 compared to Pre and Post3 ($p<0.05$) (Figure 2.13). No significant effects were found on C- and R-Index for RF/BF and RA/ES muscle pairs during APA2, as well as for all the muscle pairs during APA1 (Figure 2.13 and Figure 2.14).

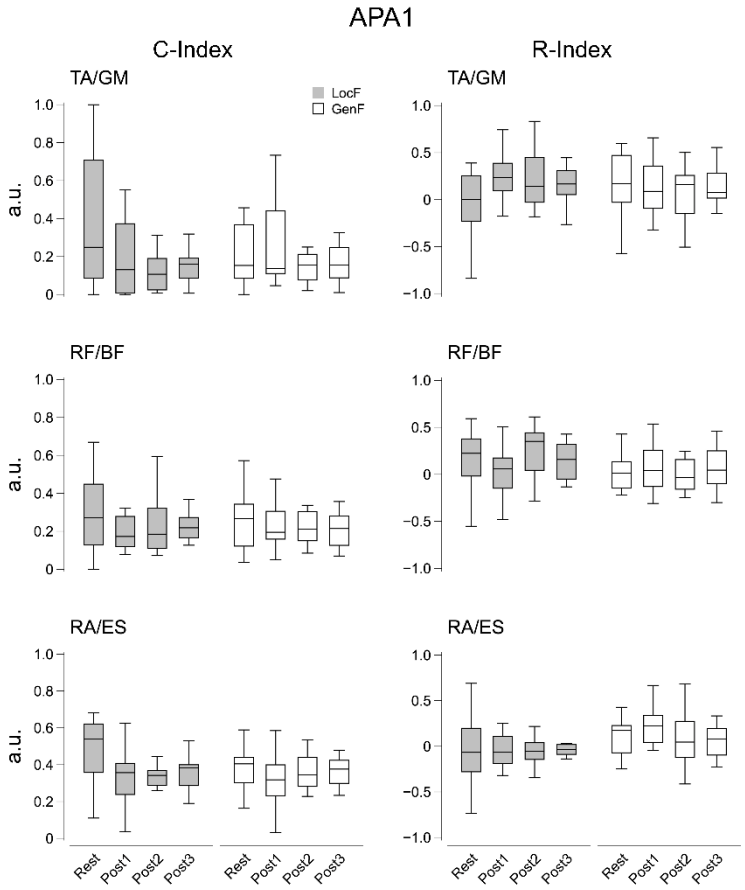

Figure 2.13 - C-Index (left panels) and R-Index (right/panels) values for the agonist–antagonist pairs acting at the ankle (TA/GM), knee (RF/BF), and hip (RA/ES) joints for APA1 before (Pre) and after the fatigue exercise divided by the three Post time points (Post 1, Post2 and Post3). White and grey box plots represent GenF and LocF exercise conditions respectively.

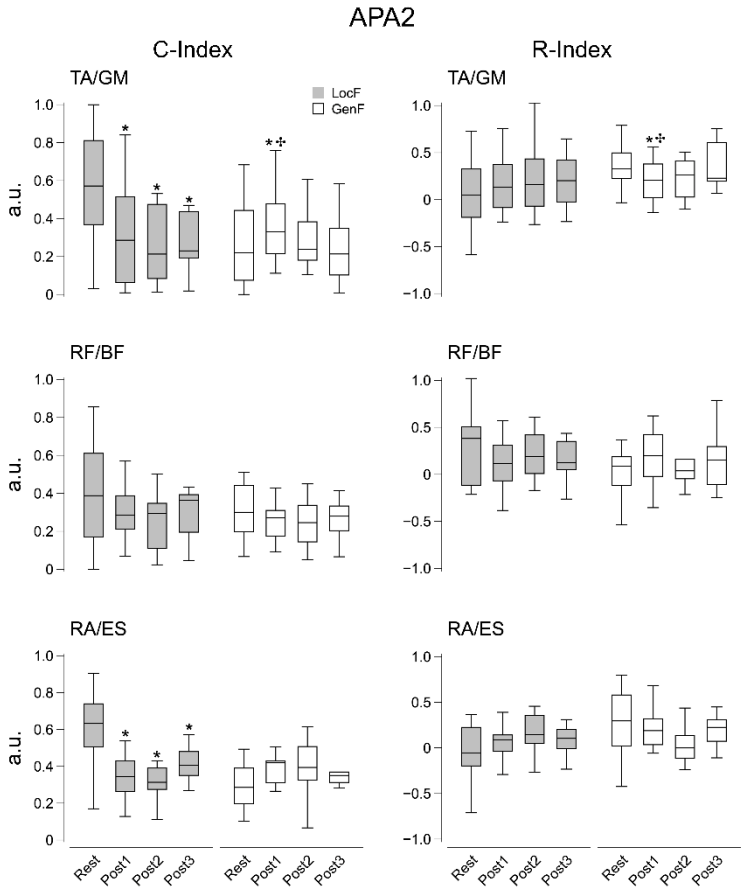

*Figure 2.14 - C-Index (left panels) and R-Index (right/panels) values for the agonist–antagonist pairs acting at the ankle (TA/GM), knee (RF/BF), and hip (RA/ES) joints for APA2 before (Pre) and after the fatigue exercise divided by the three Post time points (Post 1, Post2 and Post3). White and grey box plots represent GenF and LocF exercise conditions respectively. * Significant effects between Pre and Post1, Post2 or Post3; ✣ significant effect between Post1 and Post3. Significance level was set at p < 0.05.*

With regards to the compensatory strategies, Condition and Time factors showed significant effects on the C-Index of TA/GM pairs for CPA1 ($F_{1.8,23.4}$=10.4, P<0.001, η^2= 0.24) and CPA2 (χ^2_7 = 17.3, p < 0.05). During both the CPA1 and CPA2 epochs, TA/GM co-activation decreased over all the Post phases after the LocF exercise (p<0.05) (Figure 2.15 and Figure 2.16). There was a significant effect for Condition and Time on C-Index for RA/ES pair during CPA1 (χ^2_7 = 25.6, p < 0.001) showing a decrease of the co-activation after LocF for the Post phases (p<0.01) (Figure 2.15). The RF/BF muscle pair showed significant effect for Condition and Time on the R-Index for both CPA1 (χ^2_7 = 16.4, p < 0.05) and CPA2 (χ^2_7 = 15.5, p < 0.05), and on the C-Index for CPA2 (χ^2_7 = 22.0, p < 0.01). Post hoc comparisons showed a decrease of reciprocal activation (R-Index) during CPA1

(p<0.05) and CPA2 (p<0.01) at Post 1 and Post2 compared to the Pre condition only following LocF. In addition, it was found a decrease of coactivation index after LocF exercise over the Post phases (p<0.05) (Figure 2.15 and Figure 2.16).

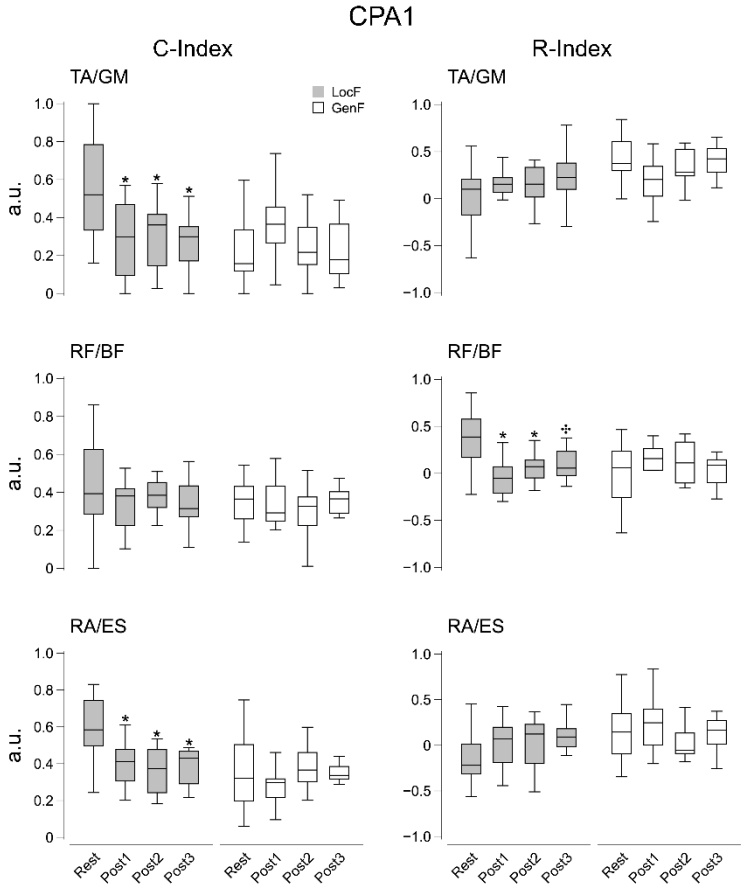

*Figure 2.15 - C-Index (left panels) and R-Index (right/panels) values for the agonist–antagonist pairs acting at the ankle (TA/GM), knee (RF/BF), and hip (RA/ES) joints for CPA1 before (Pre) and after the fatigue exercise divided by the three Post time points (Post 1, Post2 and Post3). White and grey box plots represent GenF and LocF exercise conditions respectively. * Significant effects between Pre and Post1, Post2 or Post3; ✢ significant effect between Post1 and Post3. Significance level was set at p < 0.05.*

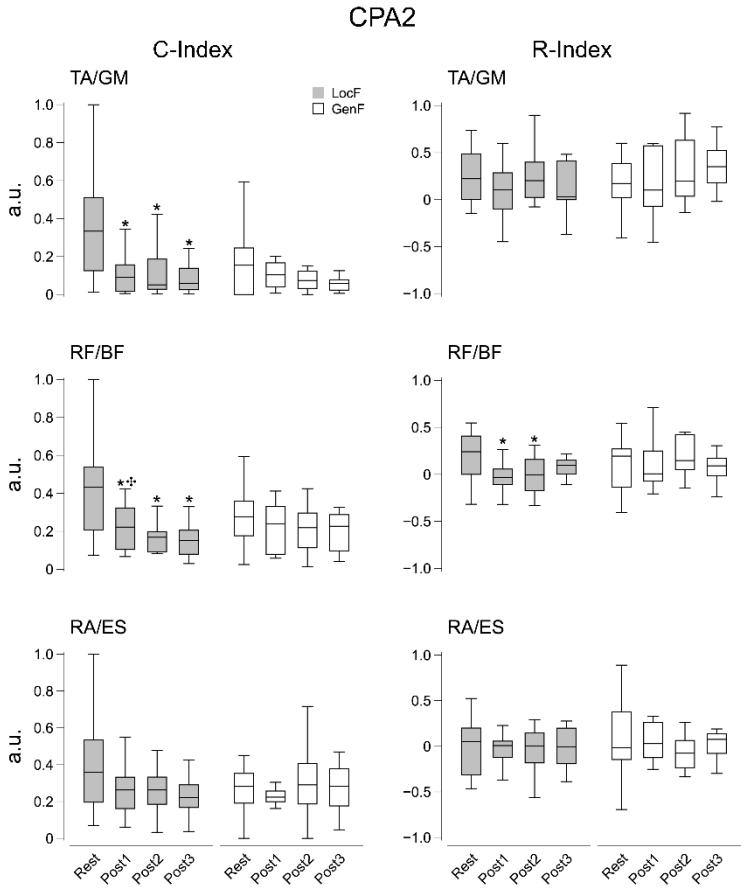

*Figure 2.16 - C-Index (left panels) and R-Index (right/panels) values for the agonist–antagonist pairs acting at the ankle (TA/GM), knee (RF/BF), and hip (RA/ES) joints for CPA2 before (Pre) and after the fatigue exercise divided by the three Post time points (Post 1, Post2 and Post3). White and grey box plots represent GenF and LocF exercise conditions respectively. * Significant effects between Pre and Post1, Post2 or Post3; ✣ significant effect between Post1 and Post3. Significance level was set at $p < 0.05$.*

DISCUSSION

We investigated the effects of different fatiguing exercise protocols on the reorganization of muscles activity at the lower extremity joints during the anticipatory and compensatory phases of postural adjustments. The exercise protocols and modalities were specifically chosen in order to avoid the direct involvement of muscles involved in the task, which may confound the results (Paillard, 2012). Contrary to our first hypothesis, general fatigue showed comparable results to localized in terms of duration of the effects over time. These effects vanish in a short time after the termination of exercise. Since cardiorespiratory and metabolic data remained significantly higher than at rest (pre-exercise) during the whole recovery phase, we suggest the recovery of the two

physiological mechanisms is not directly linked, with a fast recalibration of motor outputs happening within the CNS, as previously suggested (Lyu et al., 2021).

While the postural instability during vertical standing posture (unperturbed) – measured by RMS_{CoP} and Vel_{CoP} – was similarly increased after both exercise protocols, only the LocF condition determined a decrease of APAs. Our interpretation is that while both exercise protocols affected the control of vertical posture and increased instability, participants used different strategies to respond to this instability, increasing muscle activation just for the GenF condition. This seems to be supported also by results for muscle coactivation indexes in postural muscles. C-index exhibited an opposite trend between the two exercises: it significantly decreased after exercise for LocF, in particular at the level of the ankle and knee joints, on the contrary, GenF resulted in an increase of the index at the ankle level in the first phase after exercise. These findings support our second hypothesis, suggesting that localized muscle fatigue not only altered activation patterns of muscle acting at the level of the ankle (TA-GM), where one of the muscles was fatigued and activated less, but interestingly it induced a change in the activation patterns of other postural muscles not involved in the fatiguing exercise (RF-BF). These results are in accordance with previous studies (Singh et al., 2010; Singh and Latash, 2011) and have been interpreted as a recalibration of the commands within CNS, allowing higher variability in muscle activation of non-fatigued muscles to compensate for the ones fatigued (Singh and Latash, 2011), thus lowering the risk of loss of balance (Cesari et al., 2022). Indeed, an increase of muscle co-activation could lead to excessive joint stiffness and result in potential balance instability (Latash, 2018; Yamagata et al., 2019, 2021), which might not be corrected in time due to physiological alterations of muscle response and proprioceptive feedbacks due to fatigue (Gandevia, 2001; Carroll et al., 2017).

Furthermore, as reported in recent studies (Lyu et al., 2021), both fatiguing modalities induced alterations in static postural control which were rapidly compensated. These results suggest that the CNS efficiently and quickly recalibrated sensory inputs to successfully regain postural stability.

The study has some inherent limitations. First of all, the definition itself of localized and general fatigue – although valid for the purpose of the study – is not completely

valid in terms of physiological involvement (Gandevia, 2001; Carroll et al., 2017). In fact, the influence of peripheral afferents (Taylor et al., 2000; Amann et al., 2013) and the cognitive aspects of the exercise and of the task have been demonstrated to alter the perception of effort (Marcora et al., 2009; Tanaka et al., 2012) and consequently influence activity and response even of hierarchically higher structures within the CNS (Taylor et al., 2016; Martin et al., 2018). Secondly, we tested participants during the recovery phase after fatigue, averaging results across pre-determined time-windows. Physiologically, NMF is a transient mechanism and its recovery starts right after the termination of the exercise (Carroll et al., 2017), thus the effects of NMF might be blurred and vanish in time. However, due to the nature of the postural task and to the fact that few participants in pilot tests experienced light-headed state after switching from GenF protocol to a standing static position, we saw no viable alternatives.

Despite the mentioned limitations, the main findings are in accordance with a reorganization in the motor commands to the muscle, driven by different adaptations within the CNS mechanisms.

CHAPTER 3 – EXPERIMENTAL RESEARCH: STUDY 2

Localized neuromuscular fatigue of postural muscles is efficiently compensated during a force-field motor adaptation task

Mauro Nardon[1], Matteo Bertucco[1], Tarkeshwar Singh[2]

[1]Department of Neurosciences, Biomedicine and Movement Sciences, University of Verona

[2]Department of Kinesiology, The Pennsylvania State University, USA

ABSTRACT

Motor adaptation processes allow humans to adapt their actions to unexpected perturbations via an error-driven correction of the motor output. These processes imply an efficient compensation of performance errors, achieved by refining and updating motor commands and integrating error-based predictions. Neuromuscular fatigue (NMF) transiently affects the execution of movement through different mechanisms at several level in the sensorimotor system. Performing reaching movements while standing requires not only the selection of the correct motor command for the movement itself, but also a general postural control. The study aim was to determine how localized NMF of postural muscles affects the motor adaptation processes during a standing reaching task in a force-field. Twenty-eight participants (14 females) were randomly assigned to either Fatigue (FAT) or Control (CON) group and exposed to a motor adaptation paradigm using a robotic handle to deploy a curl force-field during reaching tasks. Participants performed ankle-dorsiflexion isometric exercise with tibialis anterior (TA) muscles before each block of reaching tasks after baseline (unperturbed trials). Exercise intensity differed between groups (FAT: 65±5%; CON; 7.5±5% of their maximal voluntary contraction – MVC). TAs MVC decreased by 32 ± 4% in FAT group after exercise. Handle kinematics, body kinetics and electromyographic (EMG) data were collected. Both groups showed visible adaptation curves for hand movement error (HME). However, HME remained significantly higher in FAT compared to CON during the late adaptation phase. As expected, postural stability deteriorated when force-field perturbation was introduced, and then gradually recovered throughout

the trials, with similar trends between groups. Patterns of muscle activation were significantly different between groups across the considered time-windows (anticipatory activity and reactive responses). Noteworthily, differences were present not only at the level of lower limbs, but also at the level of shoulder muscles. The results suggest NMF induced the adoption of different motor strategies between groups, which persisted even after the removal of the force-field perturbation, suggesting that different internal models were formed when fatigued, to optimize performance. Overall, the CNS effectively compensates for a transient perturbation like NMF. However, differences in muscle activation patterns suggest NMF affects the exploration and retention of alternative or sub-optimal strategies.

INTRODUCTION

Everyday life requires a wide range of skilled movements, most of which we are not even aware of (e.g., grasping a pen falling from the table). The effectiveness of these actions relies on our ability to predict and compensate for external dynamics either produced by our own movement or by the interaction with other people and/or with moving objects (Bertucco et al., 2021).

When the forces are expected and predictable, movement initiation is usually preceded by anticipatory postural adjustments (APAs) which can be measured by changes in the activation levels of postural muscles (Belen'kiĭ et al., 1967; Massion, 1992; Aruin et al., 1998). The optimal modulation of APAs is a crucial factor in reducing online corrective responses to account for errors in movement planning. The presence of APA is usually associated to familiarity with the action or well-practiced movements, thus resulting from a long-term learning process. In this framework, motor adaptation is a behavioral process that adjusts an already well-practiced motor task in order to maintain performance, despite a sudden change in the body or environment (e.g., walking with unusual shoes, changing mouse cursor's sensitivity). In all these cases, the motor command yielding optimal performance in normal conditions might be inefficient and require a modification, which is typically a process that follows an error-based exponential-shaped time profile and usually its rate scales with error (Krakauer et al., 2019). In the case of a standing task such as reaching, if a perturbation acting at the level of the upper limb

is introduced during the movement, both the motor command for reaching and the command that ensure postural control need to be adjusted in order to successfully reach for the object and maintain balance. In fact, the control of vertical posture is a non-trivial issue due to the biomechanical and physical constraints of human body (high center of mass, multiple joints and muscle acting at different levels in the lower limbs). In this context, changes in external forces acting on the body represent an additional challenge to the maintenance of balance. In this complex framework, it has been suggested that neuromuscular fatigue (NMF) – here defined as an exercise-related, transient reduction in force or power generation (Gandevia, 2001; Enoka and Duchateau, 2008) – could be used as a tool in understanding posture-movement coordination in motor adaptation processes (Monjo et al., 2015). Acute and prolonged effects of NMF have been extensively studied relative to exercise physiology (Amann et al., 2013; Taylor et al., 2016; Laginestra et al., 2021), sport performance and postural control (Vuillerme et al., 2002; Strang and Berg, 2007; Paillard, 2012). Effects of NMF on motor learning and skill acquisition however, are still debated and inconsistent (Takahashi et al., 2006; Branscheidt et al., 2019). Previous results could also be affected by the confounder of fatiguing a muscle directly involved in the learned skill (Branscheidt et al., 2019). Moreover, we aimed to separately assess task performance and postural control in the same task. The choice of a standing reaching task was done in order to have a functional task which might better translate to daily life situations.

For this purpose, in our study we applied a localized muscle fatigue protocol that targeted tibialis anterior (TA) muscles: they represent the main foot dorsiflexor and are primarily involved in the control of standing posture, whereas it is not directly involved in the successful execution of the reaching task. Since NMF is a transient phenomenon (Carroll et al., 2017), fatiguing exercise was repeated multiple times throughout the experiment, in order to maintain a sufficient level of fatigue and limit recovery. Timing of the experiment was based on pilot tests, where we observed a substantial and persistent drop in force production for ~8 min after exercise termination.

In order to assess the effects of NMF on motor adaptation processes, we computed performance variables, variables concerning postural control and EMG anticipatory

(APAs) and corrective responses – here we define EMG activity occurring after movement initiation as *early*- and *voluntary Reactive Responses* since the force-field perturbation allows for voluntary feedback-mediated (visual, proprioceptive) online corrections to the movement trajectory (Scott et al., 2015), in contrast with traditional discrete-perturbation paradigms (e.g., pendulum) (Santos et al., 2010a; Cesari et al., 2022; Pascucci et al., 2023), where this activity is referred as compensatory postural adjustments (CPAs).

Our hypotheses were that: 1) NMF would have detrimental effects on performance error; 2) measures of postural stability – as a result of the EMG activity imbalance of postural muscles controlling ankle joints – would decrease in the Fatigue group, in accordance with previous work on condition with increased risk of falling (Cesari et al., 2022); 3) NMF would affect afferent feedback loops in the fatigued muscles, resulting in lower EMG anticipatory activity and an increase in the activation of other, non-fatigued muscle to stabilize performance.

MATERIALS AND METHODS

Participants

Twenty-eight right-handed, healthy young adults (14 males; 14 females) were recruited for this study and randomly assigned to the fatigue (FAT) or control (CON) group. Participants were screened for exclusion criteria: 1) history of neurological or 2) musculoskeletal disorders, 3) cardiovascular disease, 4) conditions of the vestibular system or 5) medications affecting balance. The study protocol conformed to the most recent principles of the Declaration of Helsinki and was approved by the Institutional Review Board (IRB) of The Pennsylvania State University (IRB Study N° 00020213). Participants provided written informed consent before taking part in the study. Due to task constrains, FAT group was tested before CON group (details in ISOMETRIC TASK). Right-handed only participants were recruited, due to limitations of the robot used in the experiments. Participants demographics is reported in Table 3.1.

Group (F/M)	Age (years)	Weight (kg)	Height (cm)
FAT (7/7)	22.4 ± 2.9	69.3 ± 13.4	171.9 ± 10
CON (7/7)	22.3 ± 4	67.2 ± 12.9	169.6 ± 7.9

Table 3.1: Participants demographics. Values are reported as mean ± SD. F: Females, M: Males, FAT: Fatigue, CON: Control.

Apparatus

Experiments were carried out employing a KINARM robot (BKIN Technologies Ltd, Kingston, Canada). The system consisted of a height-adjustable KINARM End-Point robot with a handle for right-handed subjects. The KINARM was equipped with a horizontal screen system, used to overlay images of targets and cursors in the plane of the movements, at the same time preventing participants from viewing their arm directly. The laboratory was also equipped with a floor-embedded force plate (FP4060-07-TM, Bertec, Columbus, OH, USA) which signal was integrated and synchronized to the system. The force plate was positioned in front of the center of the robot screen and an overhead metal rack, equipped with carabiners for connecting a full-body safety harness (max operating weight and height range: 163 kg and 97-213 cm, respectively) was present, allowing safe testing of participants while standing even in case of increased risk of falling.

A customized frame equipped with a uniaxial strain-gauge force sensor (Model S-AL-A, Deltatech, Sogliano al Rubicone, Italy) was used during the *isometric task* (see later in Protocol) to measure isometric force in ankle dorsiflexion. Force data were collected using a custom LabVIEW VI (National Instruments) software at 500 Hz sampling rate.

Electromyographic (EMG) activity of twelve muscles – four in the upper right limb (*anterior deltoid (AD), posterior deltoid (PD), brachioradialis (BR) and triceps brachii (TR)*) and four in the lower limbs, bilaterally (*rectus femoris (RF), biceps femoris – long head (BF), tibialis anterior (TA), gastrocnemius medialis(GM)*) – was sampled using wireless EMG sensors (Trigno, Delsys Inc., Natick, MA, USA). EMG sensors were positioned over the muscle bellies, following recommendations (Hermens et al., 2000) and signal baseline noise and signal-to-noise ratio were inspected using a dedicated software (EMGWorks, Delsys Inc.) to ensure high EMG signal quality. EMG signals were digitalized and synchronized with robot kinetics and kinematics, and with force-plate data through a A/D converter

(National Instruments) and automatically streamed to the computer running the robot data-acquisition software (Dexterit-E™, BKIN Technologies Ltd, Kingston, Canada). All signals during the reaching task were sampled at 1000 Hz and later exported to Matlab software (R2023a, version 9.14.0, MathWorks, Natick, MA, USA) for offline analysis.

Procedures

Participants were shown a brief introductory presentation of the outline of the experiment with a few demonstrative videos about the reaching task, safety-ensuring procedures and task-specific instructions: 1) avoid leaning their forehead on or holding with their hand onto the robot structure, 2) avoid grasping and pulling downward the robot handle. After making sure participants understood the instructions, they were granted 10 (unperturbed) trials to familiarize with the reaching task. Prior to the execution of the successive blocks of reaching task, participants performed 10 trials (*normTrials*) where they had to maintain the hand cursor over a circle-shaped target (1.5 cm radius) and a background constant load of –10 N was applied in the backward direction. These trials were used during data analysis to normalize EMG data participant-wise.

REACHING TASK

Participants stood barefoot on the force plate, in front of the robot screen. Feet position was checked and marked on the force platform to ensure consistency across experimental blocks. Participants were then connected to the safety harness by one of the experimenters to minimize risks of accidental falls. The task consisted of quick planar reaching movements in the medio-lateral direction. Participants hold the robot handle with their right, dominant hand in a neutral position (elbow joint angle ~90° in starting position). KINARM screen and handle height was adjusted to each participant's height to ensure comfortable range of movement.

Participants were required to match the position of the virtual cursor (1 cm radius) – representing handle position – to the location of the visual targets on the screen. The starting position (*start_tg*) consisted of a red circle (1.5 cm radius, positioned 5cm left from the mid-sagittal plane, ~40 cm from the participant's chest) and the reaching target (*final_tg*) consisted in a red circle (1.5 cm radius) located 30 cm to

the right in the horizontal plane Figure 3.1(Panel **A**). Both targets turned to green color when reached by the participant. Targets were within reach of the participant and did not require trunk movement.

Data acquisition started when participants reached *start_tg*. They were instructed to maintain the cursor in this location until a second target (*final_tg*) appeared to their right, and only then reach for it as fast and accurate as possible. The code was programmed to display *final_tg* after cursor position matched *start_tg* for 1.5 s, to this time a random delay (1–500ms) was added in the appearance of the target to avoid predictability of the stimulus. Trial was aborted and restarted in the case participants moved away from *start_tg* before the *final_tg* appeared. Participants' vision of the hand was occluded by the screen during the trials. Return movement to starting position was not recorded and participants were invited to do it at a comfortable pace.

Immediately after familiarization, participants performed a block (n= 30 trials) of unperturbed (*null*) reaching task (baseline). Learning phase consisted in 240 trials divided into four successive blocks (n= 60 trials; adaptation), in which the robot simulated a viscous curl field (*force-field*) by generating a force F on the handle that was perpendicular (clockwise) to the direction and proportional to the magnitude of the instantaneous velocity V of the robot handle *(Eq*. 1). Thus, during a rightward reaching movement (+x), the robot generated backward perturbing forces (–y) depending on the field gain k = 0.2 N*s/cm.

$$\begin{bmatrix} Fx \\ Fy \end{bmatrix} = k \begin{bmatrix} 0 & -1 \\ 1 & 0 \end{bmatrix} \begin{bmatrix} Vx \\ Vy \end{bmatrix} \qquad \textit{(Eq. 1)}$$

Catch trials – trials where force-field was turned off) – were introduced during the perturbed blocks (three out of 30 trials in each *force-field* block). The last block (60 trials) of the protocol were unperturbed trials (washout). Based on pilot tests, participants were allowed a short break (<1min) to relax their arm and move their lower limbs halfway (after 30 trials) in learning and washout phase blocks in order to avoid fatigue in the upper limb. Participants performed an isometric exercise (see *ISOMETRIC TASK*) prior to each of the blocks except for *BASE* block. Handle position, velocity and force applied at the handle, force plate ground reaction forces (GRF), center of pressure (COP) and surface EMG data were recorded during each trial.

Performance, COP, kinematics and EMG data were compared at six phases of the experiment Figure 3.1(Panel **C**): late baseline (LB; last 10 trials in baseline phase); early adaptation (EA; 1st trial in learning phase); late adaptation – 1st chunk (LA_1; last 3 trials of the first half of the first block in learning phase – i.e. 27th–30th trial); late adaptation – final block (LA_{end}; last 5 trials in learning phase); early washout (EW; 1st trial in washout phase); late washout (LW; last 5 trials in washout phase); Two separate planned comparisons: 1) LB, EA, LA_1, LA_{end}; and 2) LB, EW, LW, were made to assess learning and washout phases effects, respectively, in accordance with similar studies (Ahmed and Wolpert, 2009; Pienciak-Siewert et al., 2016, 2020). A schematic outline of the experiment is shown in Figure 3.1 (Panel **C**).

ISOMETRIC TASK

Participants were seated on a height-adjustable chair with their feet fastened to a customized metal frame through two adjustable, inextensible straps, placed proximal to the metatarsophalangeal joints (Figure 3.1, Panel **B**). Knee and ankle joint angles were maintained at approximately 90° and 110°, respectively and the position did not change throughout the entire experimental session. To avoid the involvement of other postural and upper limb muscles, participants were not secured to the chair backrest and were instructed to place and keep their hands prone on their thighs.

Participants were firstly asked to perform three ~5 seconds maximal voluntary contractions (MVCs) in isometric dorsiflexion of the ankles, using both their TAs muscles. MVCs were inspected and the highest value was used to set the relative exercise intensity. To ensure maximal effort and avoid errors in the MVC determination, in the case one of the MVCs value differed more than 10% from the others, the value was discarded and an additional MVC was performed. Participants rested for >1 min between consecutive MVCs.

Sustained, cyclical isometric exercise protocol (40 seconds; 75% duty cycle) was set relative to each participant's MVC value and differed between groups (FAT: 65±5%; CON: 7.5±5% MVC). A computer monitor (22"; viewable diagonal screen size 54.8 cm), placed ~1 m away from the chair at participant's eye level provided visual feedback on the real-time force production during the exercise while the

sounds of a timer set the pace of the exercise-rest phases of the protocol. Participants were asked to keep their isometric force – shown as a black dot – within the target force boundaries, displayed on the monitor screen as a green-shaded area throughout the entire exercise phase (30s) of the cycle and successively relax for the remaining 10s of the cycle. Participants in the FAT group were considered fatigued and stopped when their force did not reach and sustain for >1s the target force for two consecutive cycles despite continuous encouragement. Few seconds after, participants were asked to produce an additional MVC to measure the drop in force from pre-exercise and then asked to move back to the KINARM system and immediately perform the subsequent reaching task block (≤30 s).

Mean exercise time for each bout (each exercise in-between blocks of reaching task) of isometric task of the FAT group was calculated and rounded up to the nearest cycle (40s). These exercise times were later used to stop participants in the CON group (exercising around 7.5% MVC). The rationale for this criterion was to ensure both groups exercised for a similar time duration and required FAT group to be tested before CON. Participants in both groups were stopped by the experimenter and were blind to exercise intensity (%MVC), termination criteria and exercise bouts duration. Isometric exercise setup was positioned ~1.5 meters away from the robot to ensure rapid transitions between the tasks.

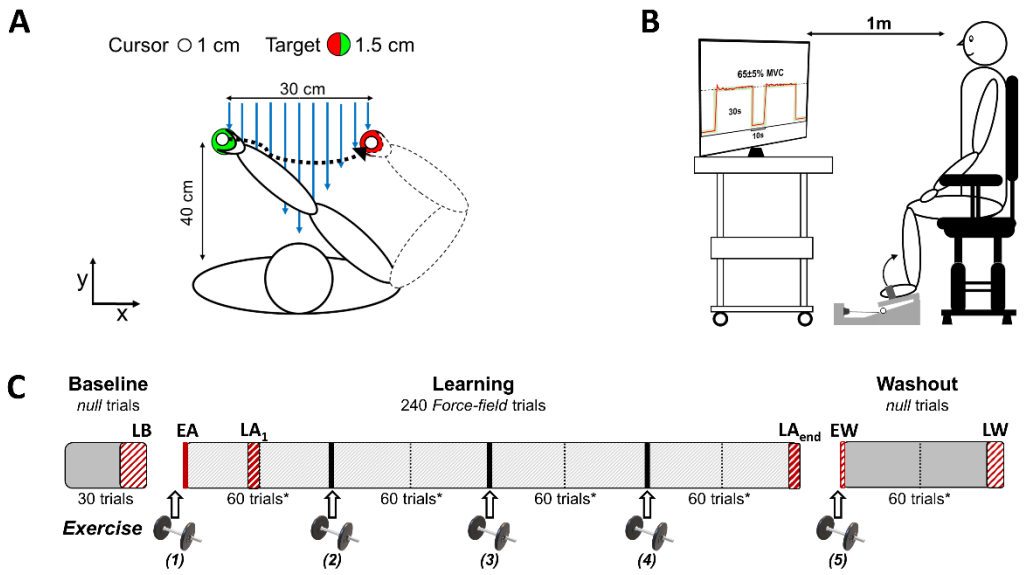

*Figure 3.1 Schematic representation of the experimental setup. **A**. Illustration of the reaching task on the KINARM robot screen (vison from above). White-filled circles represent the cursor (handle) position. Both initial position (start_tg) and reaching (final_tg) targets appeared as red-filled circles on the screen, that turned to green once reached. Blue, vertical arrows represent the force-field*

perturbation, acting in the direction of the arrows, while the black dotted line with final arrow represents the hypothetical cursor trajectory during a force-field trial. Axes orientation is shown at the bottom-left corner of the panel. ***B****. Isometric exercise setup illustration. Knee and ankle joint angles were kept ~90° and 110° throughout the exercise. Visual feedback of the real-time isometric force production was provided by a monitor, which also displayed a green-shaded area corresponding to the required force target (FAT= 65±5%, CON= 7.5±5% MVC).* ***C****. Schematic outline of the experiment: baseline phase consisted in 30 unperturbed (null) reaching trials, learning phase consisted of 240 perturbed (force-field) trials divided into 4 blocks of 60 trials and washout phase consisted in 60 null trials. *A short break (<1min) was allowed between two "chunks" of 30 trials during learning and washout phase (thin, black-dashed vertical lines). After baseline phase, each of the following blocks was preceded by a bout of isometric exercise (represented by a dumbbell in the graph), where the intensity (%MVC) varied between groups (see: ISOMETRIC TASK in the text). Experimental phases used in the analyses to compare variables are highlighted in red: LB= late baseline (last 10 trials of baseline phase), EA= early adaptation (1st trial of learning phase), LA_1= late adaptation – first chunk (27th to 30th trials in the first "chunk of the first block during learning phase), LA_{end}= late adaptation – final block (last 5 trials in the adaptation phase), EW= early washout (1st trial of washout phase), LW= late washout (last 5 trials of washout phase).*

Data analysis

Datasets were anonymized and exported to be offline preprocessed in MATLAB software (R2023a, version 9.14). Handle kinematics and force plate signals were filtered with a 10 Hz low-pass, 6th order, zero-phase digital Butterworth filter. EMG signals were detrended, band-pass filtered with a 20–450 Hz, 4th order, zero-phase digital Butterworth filter and rectified, then a 57–63 Hz, band-stop, 4th order filter was applied to remove electrical power line noise. For each trial, the instant of *final_tg* display and the instant of its reach by participants were retrieved from the KINARM events output. To define hand movement onset, defined as time zero (t0), we calculated the point in time when hand force profile in the mediolateral direction crossed 5% of its peak value (Sinha et al., 2023). Individual trials EMG, hand kinematics and force plate signals were then aligned at t0 and stored in matrices ranging from 500ms before- to 1s after t0 for further analyses. EMG signals from *normTrials* were similarly preprocessed and stored separately.

Movement variables

Reaction time (RT) was calculated for each trial as the time between the target presentation on the screen and t0. Movement time (MT) was computed as the time between t0 and the instant when the cursor reached *final_tg*. Both variables were computed to control for possible cognitive and motivational effects of fatigue on the responsiveness and attention of participants which might influence the interpretation of performance variables. Hand movement error (HME) was calculated as the signed maximum perpendicular deviation of the hand from a

straight line connecting the two targets (Ahmed and Wolpert, 2009). Positive HME values represent an error in the backward direction (towards participant's chest). As a measure of hand trajectory corrections, absolute peak hand velocity in the anteroposterior direction (Peak Hand velocity$_{AP}$) was computed during the movement phase.

Postural variables

Center of pressure (COP) two-dimensional position was computed from GRF and force plate moments according to Winter (Winter, 2009). COP position was then normalized to the mean value of COP during the first 5 samples of the trial. Maximal backward displacement of the COP during movement (COP$_{back}$) was calculated as the lowest COP value in the anteroposterior direction (negative values represent backward displacement from initial position). Anticipatory postural control (APC – Ahmed and Wolpert, 2009) was quantified as the mean COP velocity in the anteroposterior direction over a 150 ms time window starting 100 ms prior- and ending 50 ms after t0. The time-window was based on earlier work (Horak and Nashner, 1986) and consistent with previous motor adaptation studies (Ahmed and Wolpert, 2009). Reactive postural control (RPC) was calculated as the maximum absolute COP velocity in the anteroposterior direction over the remaining time-window (from 50ms after t0 until the end of the trial) and is considered an index of postural corrections, where higher values indicate increased postural corrections during movement (Ahmed and Wolpert, 2009). We calculated 95% confidence interval of COP area (COP Area (95% CI)) during movement according to Danion and Latash (Danion and Latash, 2010) using the following computation in MATLAB:

$$[\mathrm{vec}, \mathrm{val}] = \mathrm{eig}\big(\mathrm{cov}(\mathrm{COPap}, \mathrm{COPml})\big);$$

$$\mathrm{COP\ Area\ (95\%\ CI)} = \mathrm{pi} * \mathrm{prod}\Big(2.4478 * \mathrm{sqrt}\big(\mathrm{svd}(\mathrm{val})\big)\Big);$$

Where COPap and COPml represent COP anteroposterior and mediolateral coordinates of each trial, respectively.

EMG variables

Linear envelope of pre-processed EMG signals (both for reaching and *normTrials*) were computed for each EMG channel by applying a 100 Hz low-pass, 4th order, zero-phase digital Butterworth filter. The resulting aligned linear envelopes were then averaged participant-wise across the first/last three consecutive trials for each experimental phase (Krishnan et al., 2012), respectively (e.g., for LB: average of last 3 trials; for EA: average of first 3 trials). EMG envelopes of *normTrials* were averaged across all the 10 trials, yielding a single averaged signal for each muscle. Phase-averaged EMG signals were then integrated at the level of each muscle using a trapezoidal numerical integration (function "trapz" in MATLAB).

Anticipatory Postural Adjustments (APA) were defined from –150 to + 50 ms with respect to t0, early Reactive Responses ($_e$RR) were defined over a 100 ms window from + 50 to+ 150 ms with respect to t0, while voluntary Reactive Responses ($_v$RR) were defined over a 300 ms window from + 150 to+ 450 ms with respect to t0. Time-windows for EMGs integration were chosen based on the nature of the reaching task and on the continuous rather than discrete perturbation. Reactive responses windows differentiate on the physiological nature of the activity: the first window ($_e$RR) mainly represents spinal circuit and stretch reflexes responses (Scott et al., 2015), while the second conveys information about voluntary, visually-driven EMG activity to ensure online trajectory correction, which are characterized by longer latencies (~120 to 200 ms in the lower limbs), as shown in previous work (Nardone and Schieppati, 1988).

Integrals, identified as ∫APA, ∫$_e$RR and ∫$_v$RR (*Eq. 2*), were further normalized for each participant by dividing it by the integral of the averaged EMG activity during *normTrials* (∫normTrials; integrated over a 100 ms time-window, starting 100 ms after the force was applied):

$$\int APA = \frac{\int_{-100}^{50} EMG_{reaching}(i)}{\left(\left(\int_{100}^{200} normTrials\right) \times 1.5\right)}$$

$$\int eRR = \frac{\int_{50}^{150} EMG_{reaching}(i)}{\int_{100}^{200} normTrials}$$

$$\int vRR = \frac{\int_{150}^{450} EMG_{reaching}(i)}{\left(\left(\int_{100}^{200} normTrials\right)\times 3\right)} \quad \textit{(Eq. 2)}$$

We further normalized the EMG values by dividing integrated EMG values of each time-window (i.e. APA, $_{e}$RRs and $_{v}$RRs) for each experimental phases (i.e. EA, LA1, LAend, EW, LW) by the integrated EMG in the same time-window during LB – similarly to (Pienciak-Siewert et al., 2020) – to control for baseline differences and explore changes in muscle activation across phases during APAs $_{e}$RRs and $_{v}$RRs.

Finally, we computed indexes of co-activation (C-index) and reciprocal activation (R-index) within agonist–antagonist muscle pairs (Left TA/GM, Right TA/GM, Left RF/BF, Right RF/BF and AD/PD) acting at joint level within the framework of the equilibrium-point hypothesis (Feldman, 1986). Indexes were computed using EMG integrals of ventral and dorsal muscles (before normalization by LB) for each time-epoch (Slijper and Latash, 2000, 2004; Bertucco et al., 2021; Cesari et al., 2022). Specifically, R-Index = ($\int EMG_{ventral}$ - $\int EMG_{dorsal}$) and C-Index = 0 if $\int EMG_{ventral}$ and $\int EMG_{dorsal}$ had different signs; C-Index = min $\{|\int EMG_{ventral}|;|\int EMG_{dorsal}|\}$ if $\int EMG_{ventral}$ and $\int EMG_{dorsal}$ had the same signs (Piscitelli et al., 2017; Cesari et al., 2022).

Statistical analysis

Jamovi statistical software (The jamovi project (2023). jamovi (Version 2.3.28) [Computer Software]. Retrieved from https://www.jamovi.org) was used for all statistical analyses. All data in the text, Tables, and Figures – unless otherwise stated – are presented as mean ± 1 standard deviation (SD). For all comparisons, statistical significance was set at an α of 0.05. Data distribution (skewness and kurtosis) was assessed, the normality of the data was assessed by the Shapiro–Wilk test and confirmed by the inspection of density and Q–Q plots. When normality assumption was violated, non-parametric statistical tests were performed

(Friedman's test with pairwise Durbin-Conover comparisons) Successively, non-parametric independent samples t-test (Welch-test) was used for pairwise comparisons between groups.

To test the effects of the isometric exercise protocol, group differences in MVC changes from initial (pre-exercise) to final (post-exercise) were assessed using a two-way mixed-design ANOVA (group–time). To test the effects of fatigue on the adaptation process, a two-way mixed-design ANOVA (Phase as a repeated measure factor) was used to assess group differences in performance and postural variables across four experimental phases (LB, EA, LA_1, LA_{end}). Similarly, to test the effects of fatigue on the washout process, a two-way mixed-design ANOVA (Phase as a repeated measure factor) was used to assess group differences in performance and postural variables across three experimental phases (LB, EW, LW). Assumptions of sphericity were explored using Mauchly's test and controlled for using the Greenhouse–Geisser adjustment in instances where Mauchly's test was significant ($\alpha < 0.05$) and relative corrected degrees of freedom (DOF) are reported in results. In the event of a significant interaction or main effect, post hoc comparisons were performed using Holm-Bonferroni correction. Non-parametric independent-sample t-tests (Welch-test) were used to assess between-group differences if Levene's test revealed unequal variance. Integrated EMG time-windows were compared between groups using a two-way mixed-design ANOVA where Phase levels were *N*-1 due to the normalization to LB values (Phase as a repeated measure factor). In order to test differences within groups between LB and the other phases, a one-way repeated measure ANOVA (Phase as a repeated measure factor) was performed for each group (Fatigue/Control), separately.

RESULTS

Isometric force

Isometric exercise duration was on average 4:15 ± 2:59 min:s (number of cycles: 6.6 ± 3.2), with a trend for a reduction across bouts (bout1: 7:56 ± 4:14 min:s, bout2: 4:04 ± 1:47 min:s, bout3: 3:30 ± 1:41 min:s, bout4: 3:19 ± 1:37 min:s, bout5: 2:27 ± 1:58 min:s). Maximal voluntary contraction (MVC) isometric force prior to the exercise did not differ between groups (FAT: 264.3 ± 78.2 N, CON: 261.8 ± 86.1

N; p>.05). The fatiguing exercise led to a significant drop in tibialis anterior MVC isometric force for Fatigue group (FAT: -32 ± 4%, CON: 1 ± 3%, p<.001). Figure 3.2 shows pre-post exercise difference in isometric force (calculated as the difference from the mean force during 1st cycle to the force during last cycle of each bout).

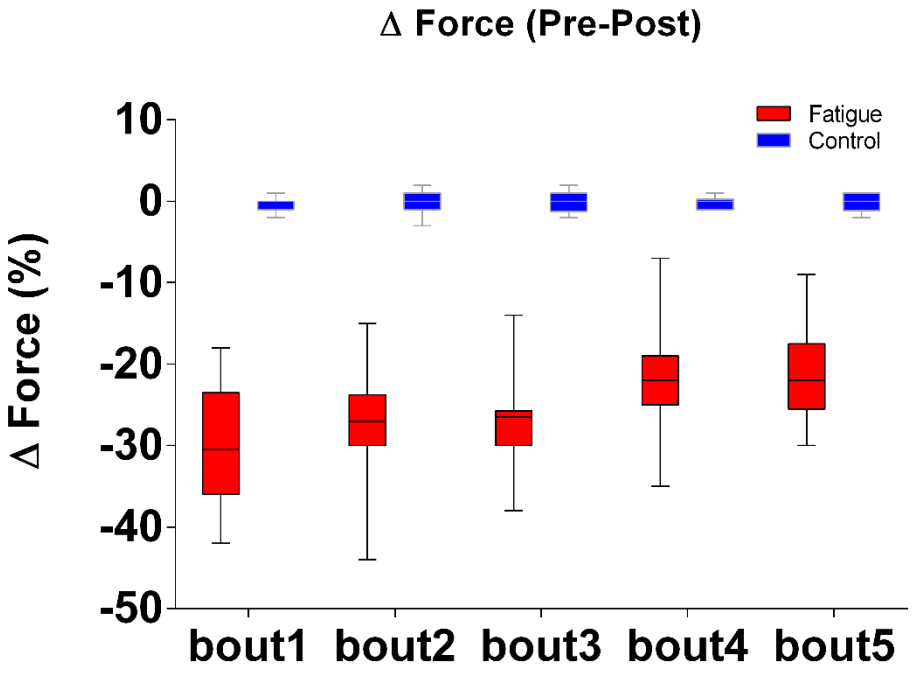

Figure 3.2 Pre- to post differences in isometric force (expressed as %) from the first to the last exercise cycle within each bout. Data in box-plots represent 5th – 95th percentiles of values and median is marked by the horizontal black line.

Task parameters

Prior to the first isometric exercise bout (LB), participants performed the reaching movement with an average movement time (MT) of 430 ± 90 ms. There was a significant effect of experimental phase on MT, which differed across all phases (EA: 813 ± 132, LA_1: 506 ± 104, LA_{end}: 454 ± 97, EW: 513 ± 99, LW: 400 ± 88 ms; p<.01) except for LB–LW, LB–LA_{end}, and LA_1–EW pairwise comparisons. However, aside from the sharp MT increase during the first trial where force-field perturbation was introduced (EA), the difference in MT across all the other phases is negligible (20–80ms). MT values across phases are presented in Figure 3.3 (Panel **A**). Reaction time (RT) – calculated as the time between the presentation of the target on the screen and the onset of the hand movement – values did not differ

across phases (LB: 265 ± 43; EA: 291 ± 62, LA_1: 277 ± 50, LA_{end}: 269 ± 34, EW: 324 ± 93, LW: 271 ± 42 ms; p>.05). Data are presented in Figure 3.3 (Panel **B**).

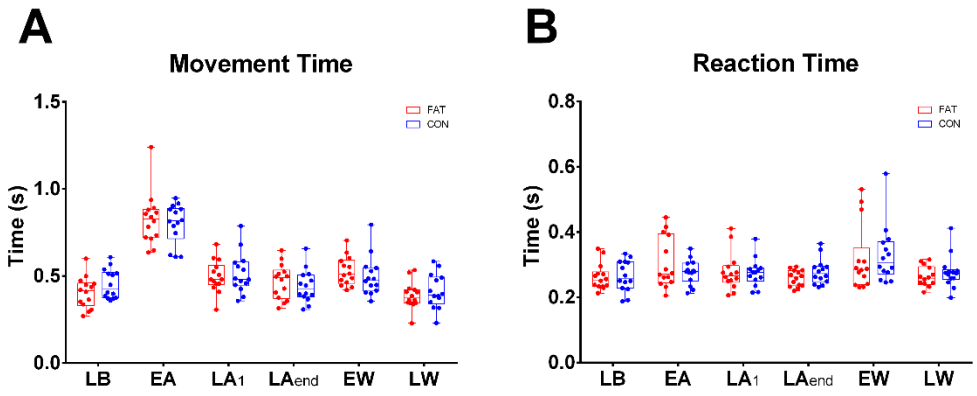

*Figure 3.3 Box-plots with individual data across experimental phases divided by groups. Boxes comprise 25th to 75th percentiles, whiskers represent min to max values. Median value is shown by the thin horizontal line. **A** Movement time (MT) values; **B** Reaction time (RT) values.*

Performance variables

Figure 3.4 illustrates the average reaching performance – quantified by the hand movement error (HME) – of the two groups across the whole experiment (HME was averaged in batches of 3 trials). Participants in both groups were able to improve in the performance outcome with practice.

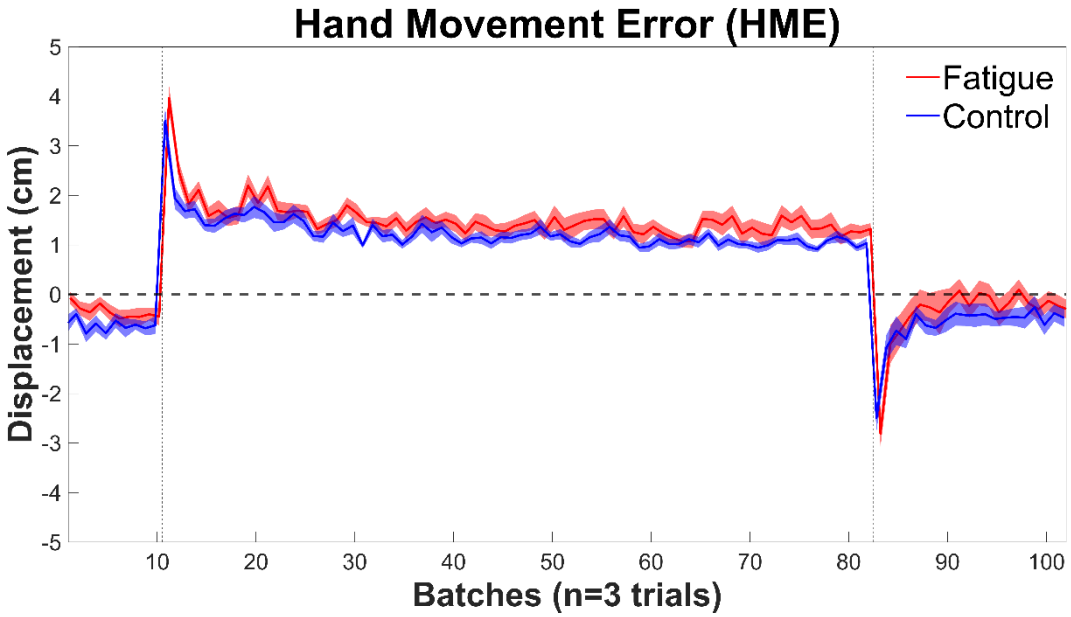

Figure 3.4 Hand movement error (HME) averaged for each group during the whole experiment. HME was averaged per batches of 3 consecutive trials. A positive value of HME represent a backward displacement. Vertical dashed lines represent changes in experimental phases (baseline

– learning – washout). Solid lines represent MEAN values and shaded areas represent ±1 standard error (SE).

Learning phase

There was a significant main effect of experimental phase (χ^2 (3) = 73.6, p < 0.001 for all pairwise comparisons) on HME between each comparison. Figure 3.5 shows as HME increased from LB to EA, then it decreased during LA_1 and LA_{end} still remaining higher than LB. Welch's t-test resulted in a statistically significant difference in HME between groups both at LA_1 (FAT: 2.06 ± 0.93 CON: 1.08 ± 0.98; t (-2.739) = 25.9, p = .011, d = 1.035) and at LA_{end} phases (FAT: 0.85 ± 0.77 CON: 0.17 ± 0.74; t (25.9) = -2.385, p = .025, d = .902).

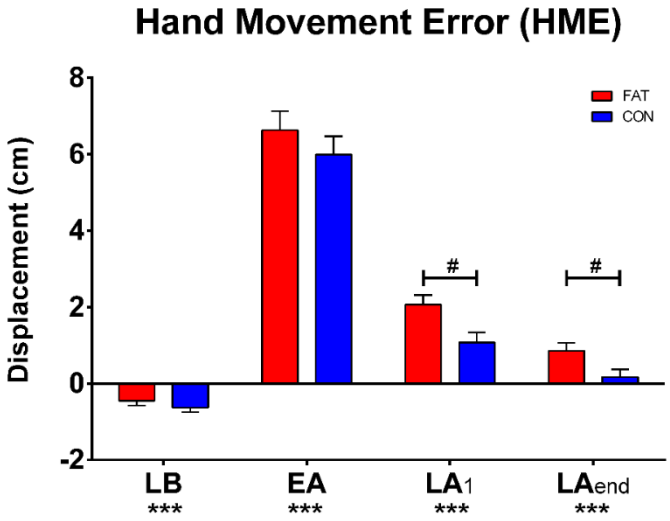

*Figure 3.5 Hand movement error (HME) across learning phase. Positive values represent backward displacement. *** significant effects at p < 0.001, # significant effects between groups (p < 0.05). Data are presented as mean value and standard error (SE)*

Peak hand velocity in the anteroposterior direction (Peak Hand $velocity_{AP}$) demonstrated a trend similar to HME throughout the experiment. Phase significantly affected Peak Hand $velocity_{AP}$ (χ^2 (3) = 65.2, p < 0.001 for all pairwise comparisons). Friedman's tests were performed also on separated groups: in this case LA_1-LA_{end} Durbin-Conover pairwise comparison was significant only for Fatigue group (p<.01). Welch's t-test resulted in a statistically significant difference in Peak Hand $velocity_{AP}$ between groups at LA_1 (FAT: 0.21 ± 0.08 CON: 0.16 ± 0.05; t (21.9) = -2.296, p = .003, d = 0.87).

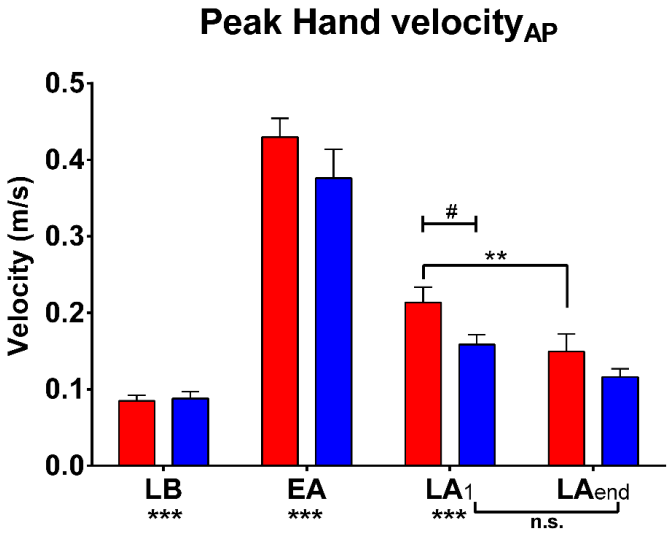

*Figure 3.6 Peak Hand velocity$_{AP}$ across learning phase. ** significant effects at p < 0.01, *** significant effects at p < 0.001, # significant effects between groups (p < 0.05), n.s.= not statistically significant. Data are presented as mean value and standard error (SE)*

Washout phase

During the washout phase, performance immediately decreased and then quickly returned to baseline values, showing an inverse trend compared to learning phase Figure 3.4. Repeated measures ANOVA found a main effect of phase (F(1.35, 35.22) = 194.26, p = <.001). Holm-Bonferroni post hoc pairwise tests indicated HME was higher during the first trial after the removal force-field perturbation (EW) compared to the other two conditions (EW: -3.46 ± 0.97: LW -0.38 ± 0.68; LB: -0.54 ± 0.46; p<.001), whereas it did not differ between LB and LW (p>.05). HME at the end of the washout phase (LW) did not differ from LB (p>.05). There were no significant effect of group and Phase*Group interaction.

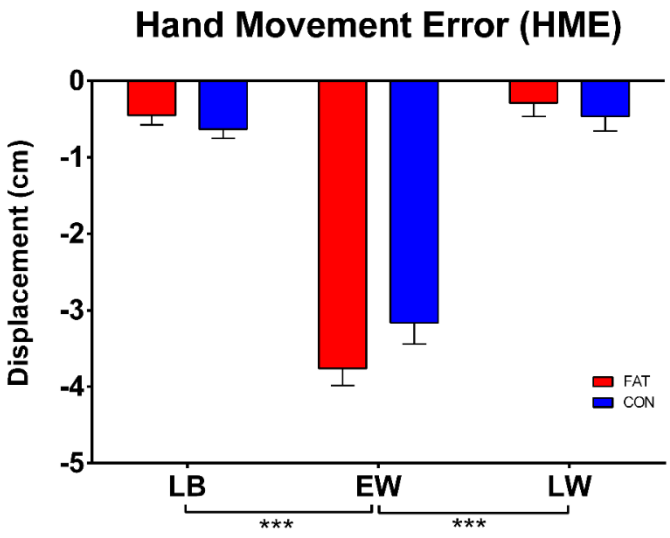

*Figure 3.7 Hand movement error (HME) across washout phase. Negative values represent forward displacement. *** significant effects at p < 0.001. Data are presented as mean value and standard error (SE)*

Peak Hand velocity$_{AP}$ demonstrated a similar behavior also during washout phase. Phase significantly affected Peak Hand velocity$_{AP}$ (χ^2 (2) = 42.3, p < 0.001). Pairwise Durbin-Conover comparisons indicated velocity was higher in EW compared to the other conditions (EW: 0.29 ± 0.12: LW 0.09 ± 0.03; LB: 0.09 ± 0.03; p<.001). Welch's t-test resulted in a significant difference in Peak Hand velocity$_{AP}$ between groups at EW (FAT: 0.33 ± 0.13 CON: 0.24 ± 0.09; t (22.6) = -2.1206, p = .045, d = 0.8).

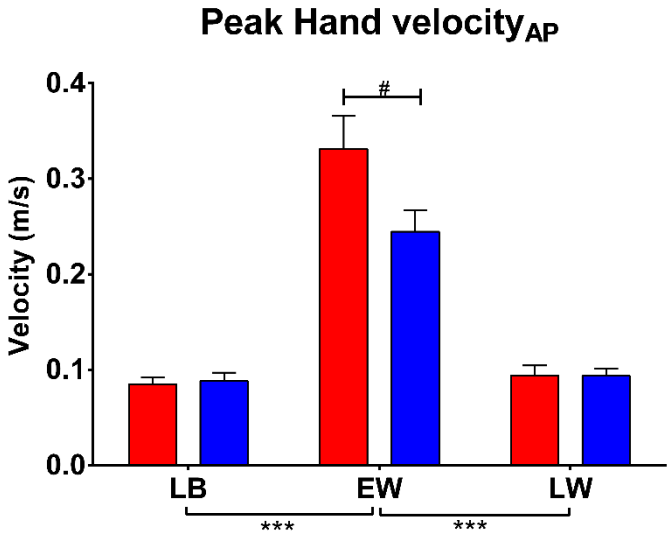

*Figure 3.8 Peak Hand velocity$_{AP}$ across washout phase. *** significant effects at p < 0.001, # significant effects between groups (p < 0.05). Data are presented as mean value and standard error (SE)*

Center of Pressure and postural variables

Learning phase

Repeated measures ANOVA revealed a main effect of phase on COP Area ($F(1.59, 39.7) = 47.96$, $p = <.001$, $\eta^2 = 0.505$). Holm-Bonferroni post hoc pairwise tests indicated COP Area was different across each condition ($p<.001$; Figure 3.9 – upper left corner). Similar results were obtained for COP_{back} ($F(2.23, 55.73) = 171.95$, $p = <.001$, $\eta^2 = 0.766$), where Holm-Bonferroni post hoc pairwise comparisons were significant for each condition ($p<.001$; $p = 0.012$ for LA_1–LA_{end}; Figure 3.9 – upper right corner). An effect of phase was found also for APC ($F(1.93, 48.36) = 4.7$, $p = 005$, $\eta^2 = 0.093$), where Holm-Bonferroni post hoc pairwise comparisons revealed statistical differences only between LB–LA_1 and LB–LA_{end} comparisons (LB: 0.0115 ± 0.005: LA_1 0.0177 ± 0.012; LA_{end}: 0.205 ± 0.017; $p = 0.045$; Figure 3.9 – lower left corner). Finally, the effect of phase was statistically significant also for RPC ($F(1.9, 47.61) = 82.8$, $p < .001$, $\eta^2 = 0.589$). Holm-Bonferroni post hoc pairwise comparisons were significant for each condition ($p<.001$; $p = 0.037$ for LA_1–LA_{end}; Figure 3.9 – lower right corner).

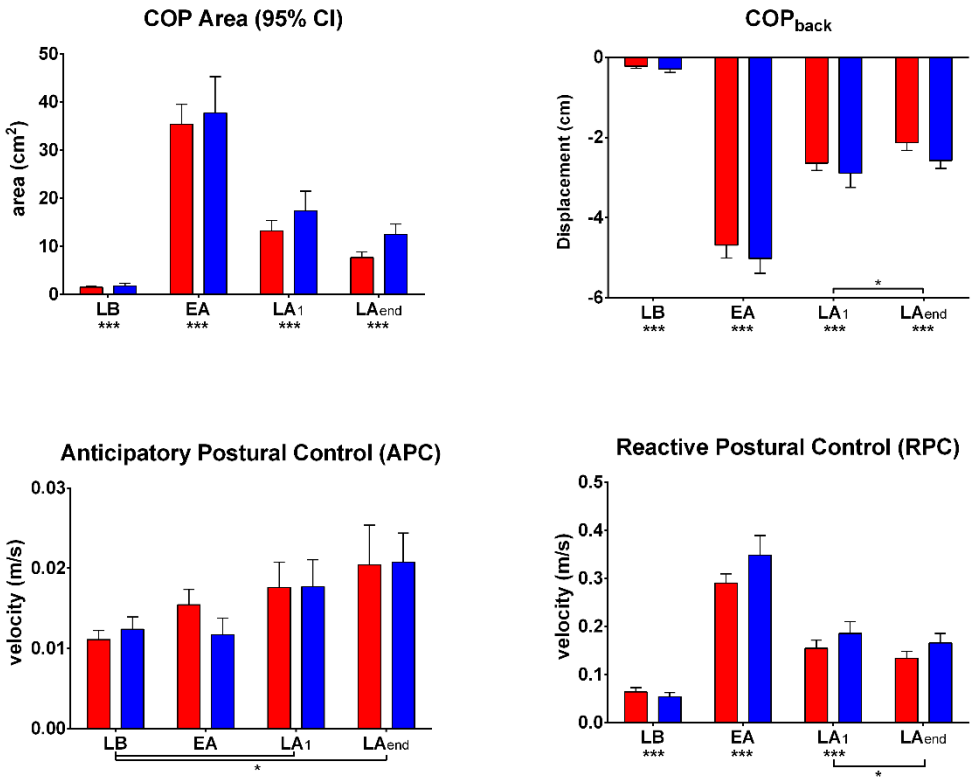

*Figure 3.9 Variables of postural control during learning phase. Upper left panel: 95% Confidence intervals for COP area covered during the movement. Upper right: value of maximal backward displacement of the COP during movement (COP_{back}). Bottom left: Anticipatory postural control (APC) – mean velocity of COP in anteroposterior direction during preparatory phase (100 ms before- 50 ms after t0). Bottom right: reactive postural control (RPC) – peak velocity of COP in anteroposterior direction during movement (from 50 ms after t0) * Significant effects at $p < 0.05$, *** significant effects at $p < 0.001$. Data are presented as mean value and standard error (SE).*

Washout phase

During washout, a significant main effect of phase Area ($F(1.05, 26.14) = 39.44$, $p = <.001$, $\eta^2 = 0.462$) and phase*group interaction ($F(1.05, 26.14) = 3.9$, $p = 0.027$, $\eta^2 = 0.046$) were found for COP Area. Holm-Bonferroni post hoc pairwise tests indicated COP Area differed across conditions in the FAT group, while it was close to significance in CON ($p<.001$ and $p = 0.57$, respectively; Figure 3.9 – upper left corner). For COP_{back} it was found a significant effect of phase ($F(1.06, 27.46) = 33.34$, $p = <.001$, $\eta^2 = 0.406$), where Holm-Bonferroni post hoc pairwise comparisons were significant for each condition ($p<.001$; $p = 0.031$ for LB–LW; Figure 3.9 – upper right corner). A main effect of phase was found also for APC ($F(1.09, 28.27) = 13.712$, $p < .001$, $\eta^2 = 0.244$), where Holm-Bonferroni post hoc pairwise comparisons revealed statistical differences only between LB–EW and

EW–LW comparisons (LB: 0.012 ± 0.005: EW: 0.025 ± 0.018; LW: 0.011 ± 0.004; $p < .01$; Figure 3.9 – lower left corner). Finally, the effect of phase was statistically significant also for RPC ($F(1.09, 28.30) = 88.33$, $p < .001$, $\eta^2 = 0.622$). Holm-Bonferroni post hoc pairwise comparisons were significant only between LB–EW and EW–LW comparisons (LB: 0.059 ± 0.032: EW: 0.259 ± 0.118; LW: 0.061 ± 0.029; $p < .01$; Figure 3.9 – lower right corner).

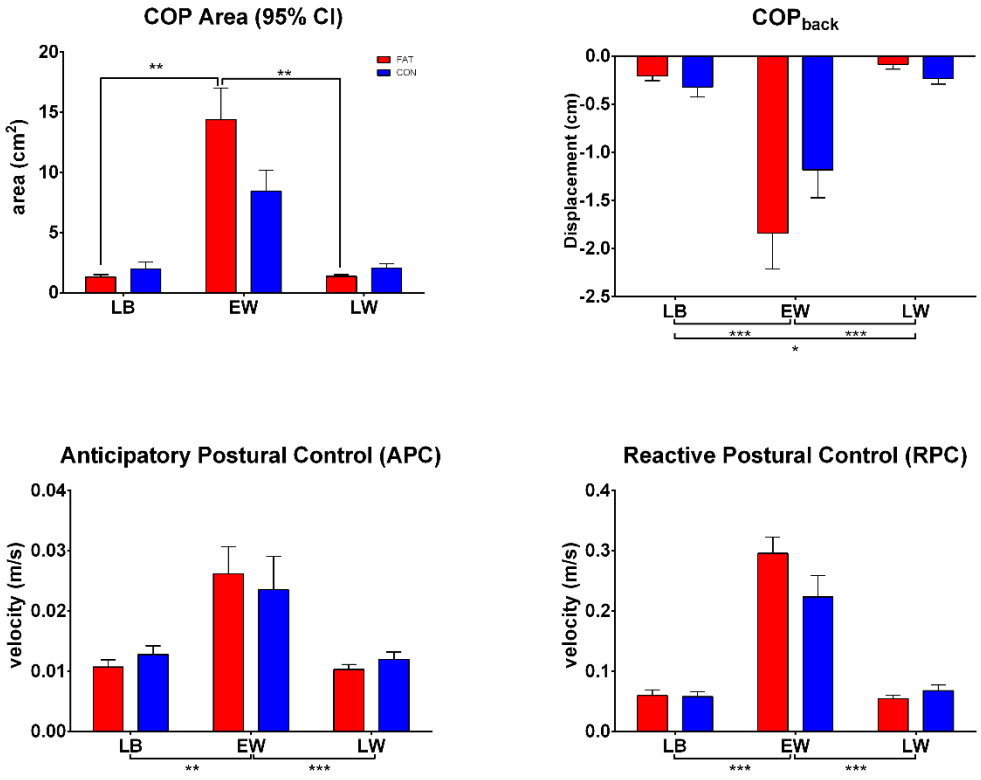

*Figure 3.10 Variables of postural control during washout phase. Upper left panel: 95% Confidence intervals for COP area covered during the movement. Upper right: value of maximal backward displacement of the COP during movement (COP_{back}). Bottom left: Anticipatory postural control (APC) – mean velocity of COP in anteroposterior direction during preparatory phase (100 ms before- 50 ms after t0). Bottom right: reactive postural control (RPC) – peak velocity of COP in anteroposterior direction during movement (from 50 ms after t0). * Significant effects at $p < 0.05$, ** significant effects at $p < 0.01$, *** significant effects at $p < 0.001$. Data are presented as mean value and standard error (SE)*

Muscle activity

Learning phase

Considering the EMG activation of postural and effector (e.g., shoulder) muscles during the course of learning phase, notable changes in the patterns are seen across experimental phases (EA, LA_1 and LA_{end}) in both groups, supposedly reflecting strategies to reduce performance errors. Furthermore, significant differences

between groups – Fatigue (FAT) and Control (CON) – are seen in particular in APA and $_{e}$RR windows at the level of AD, TAs and RFs muscles. The most interesting results, are reported in Figure 3.11 for AD muscle, Figure 3.12 for Left TA (left panel) and Figure 3.14 for Left RF muscle (left panel).

In details, the repeated measures analysis (Friedman's test – considering participants in both groups) found significant effects for Phase on the APA (χ^2_2 = 15.4, $p < .001$) in the AD muscle. Running the analysis with separate groups resulted in the significant decrease for FAT from $LA_{1\ to}\ LA_{end}$ ($p < .01$). Welch's paired t-test resulted in a significant difference between groups in APA at LA_1 ($p = 0.036$), while it was close to significance at EA ($p = 0.051$). Welch's paired t-test resulted in a significant difference between groups in $_{e}$RR across each phase ($p < .001$, $p = 0.042$ and $p = 0.002$ for EA, LA_1 and LA_{end}, respectively). Friedman's test resulted in a phase effect on $_{v}$RR ($\chi^2_2 = 16.2$, $p < .05$ – just for CON group), where Durbin-Conover pairwise comparisons reported a decrease in $_{v}$RR between EA–LA_1 and EA–LA_{end} ($p < .001$). Welch's paired t-test resulted in significant differences between groups at LA_1 and LA_{end} ($p = 0.013$ and $p = 0.025$, respectively).

Friedman's test for Left TA muscle resulted in a phase effect on $_{v}$RR ($\chi^2_2 = 42.7$, $p < .001$) and pairwise confirmed the effect across all phases ($p < .001$). Friedman's test on separate groups for Left TA muscle resulted in a phase effect on $_{e}$RR ($\chi^2_2 = 6.14$, $p = 0.043$) for FAT group, Durbin-Conover pairwise comparisons yielded significance for LA_1–LA_{end} ($p < .05$). Welch's paired t-test found significant differences between groups at LA_{end} ($p < .05$) for APA; EA, LA_1 and LA_{end} ($p < .01$, $p < .05$, and $p < .01$, respectively) for $_{e}$RR; and at LA_{end} ($p < .01$) for $_{v}$RR. Left TA muscle data are shown in Figure 3.12 (left panel).

Friedman's test for Left GM muscle resulted in a phase effect on all EMG windows: APA, $_{e}$RR and $_{v}$RR ($\chi^2_2 = 28.8$, $p < .001$, $\chi^2_2 = 13$, $p = 0.002$, and $\chi^2_2 = 15.1$, $p < .001$, respectively). Pairwise comparisons for APA were significant between EA–LA_1 and EA–LA_{end} ($p < .001$). Pairwise comparisons for $_{e}$RR were significant between EA and LA_{end} ($p < .005$), while EA–LA_1 and LA_1–LA_{end} comparisons were significant only for FAT and CON group, respectively ($p < .01$ and $p < .05$). Pairwise comparisons for $_{v}$RR were significant between EA and LA_{end} ($p < .005$),

while EA–LA_1 and LA_1–LA_{end} comparisons were significant only for FAT and CON group, respectively ($p < .05$), similarly to the results for $_eRR$. Welch's paired t-test found significant differences between groups only in $_vRR$, especially at EA and LA_1 ($p < .05$). Left GM data are shown in Figure 3.12 (right panel).

Friedman's test for Left RF muscle resulted in a phase effect on $_eRR$ and $_vRR$ ($\chi^2_2 = 7.36$, $p = 0.025$ and $\chi^2_2 = 31.7$, $p < .001$, respectively). Durbin-Conover pairwise comparison in $_eRR$ was significant only for EA–LA_1 ($p = 0.007$). Pairwise comparison in $_vRR$ resulted always significant ($p < .001$). Running Friedman's test on separate groups resulted in a significant decrease in $_vRR$ only for FAT group ($\chi^2_2 = 22.4$, $p < .001$) between LA_1–LA_{end} ($p < .001$). Welch's paired t-test found significant differences between groups across all phases for $_eRR$ ($p < .05$), while $_vRR$ was different only at LA_{end} ($p < .01$). Left RF muscle data are shown in Figure 3.14 (left panel).

All the other significant results for EMG activity windows at the level of individual muscles during learning phase are reported with relative symbols (legend in each figure caption) in Figure 3.11–3.15. Note that significant differences from late baseline values (LB; equals to dashed horizontal line =1 in figures) – resulting from a one-way mixed ANOVA – are shown in graphs.

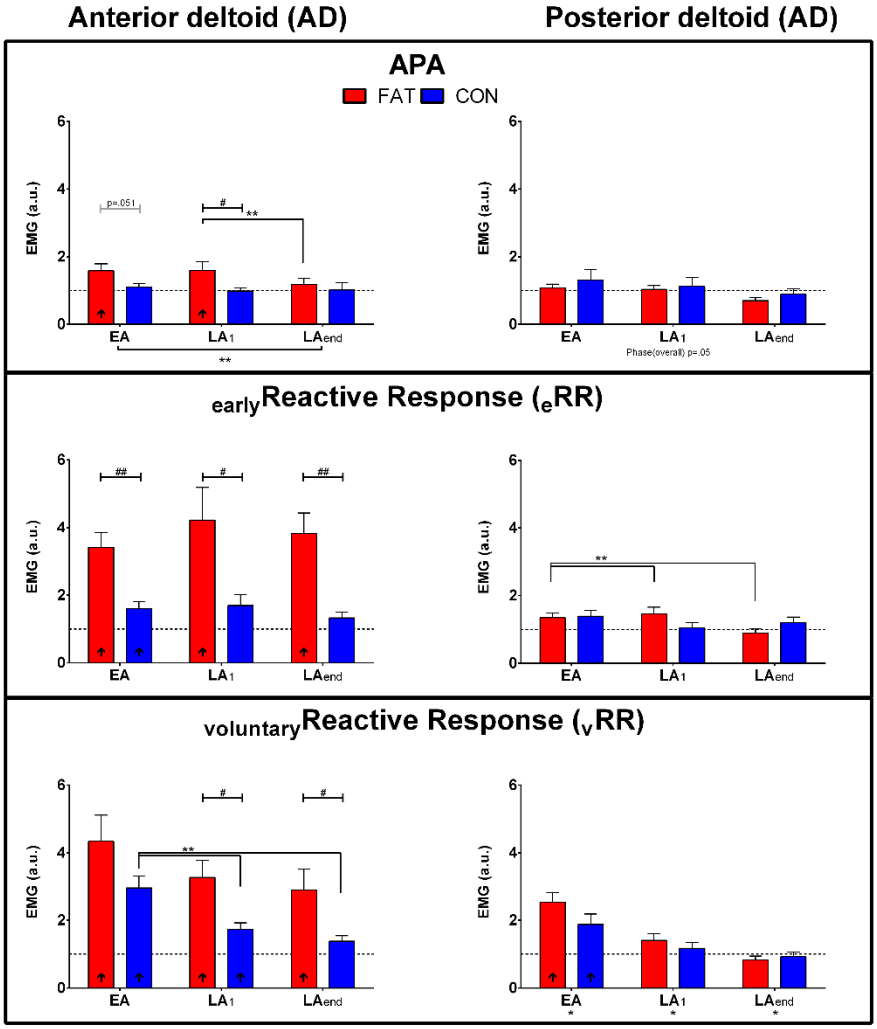

*Figure 3.11 EMG integrals of muscles acting at the shoulder level (Anterior deltoid (AD) and posterior deltoid (PD)) over the selected time-windows for learning phase. Anticpatory Postural Adjsutment – APA (upper box), early Reactive Response – eRR (central box) and voluntary Reactive Response – vRR (bottom box). EMG data are in arbitrary units and normalized subject-wise by late baseline (LB) values: value=1 represents no change from baseline (horizontal dashed line). Data are presented as mean value and standard error (SE). ↑ significant difference from LB(p <0.05), * significant effects at p < 0.05, ** significant effects at p < 0.01, *** significant effects at p < 0.001, # significant effects between groups (p < 0.05), # significant effects between groups (p < 0.05), ## significant effects between groups (p < 0.01), n.s.= not statistically significant*

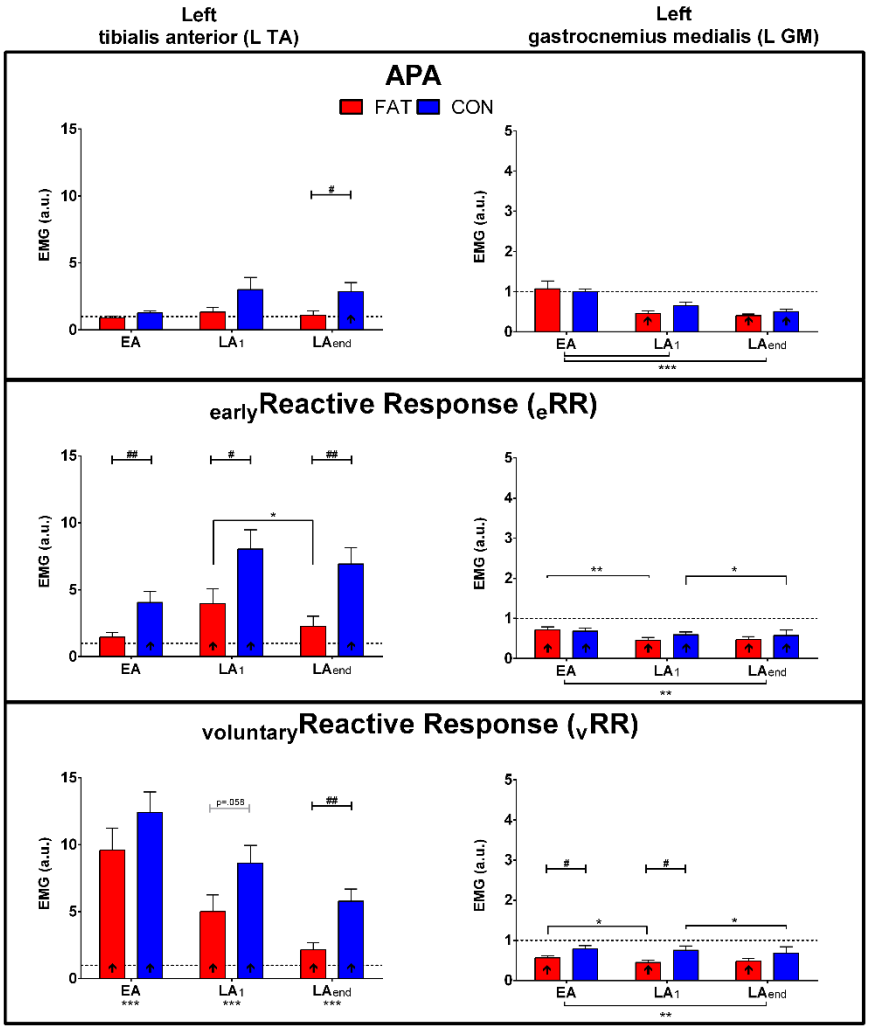

*Figure 3.12 EMG integrals of the muscles acting at the level of the left ankle joint (Left tibialis anterior (TA) and Left gastrocnemius medialis (GM)) over the selected time-windows for learning phase. Anticpatory Postural Adjsutment – APA (upper box), early Reactive Response – eRR (central box) and voluntary Reactive Response – vRR (bottom box). EMG data are in arbitrary units and normalized subject-wise by late baseline (LB) values: value=1 represents no change from baseline (horizontal dashed line). Data are presented as mean value and standard error (SE). Note the difference in y-axis limits between the two muscles. ↑ significant difference from LB(p <0.05), * significant effects at p < 0.05, ** significant effects at p < 0.01, *** significant effects at p < 0.001, # significant effects between groups (p < 0.05), # significant effects between groups (p < 0.05), ## significant effects between groups (p < 0.01), n.s.= not statistically significant*

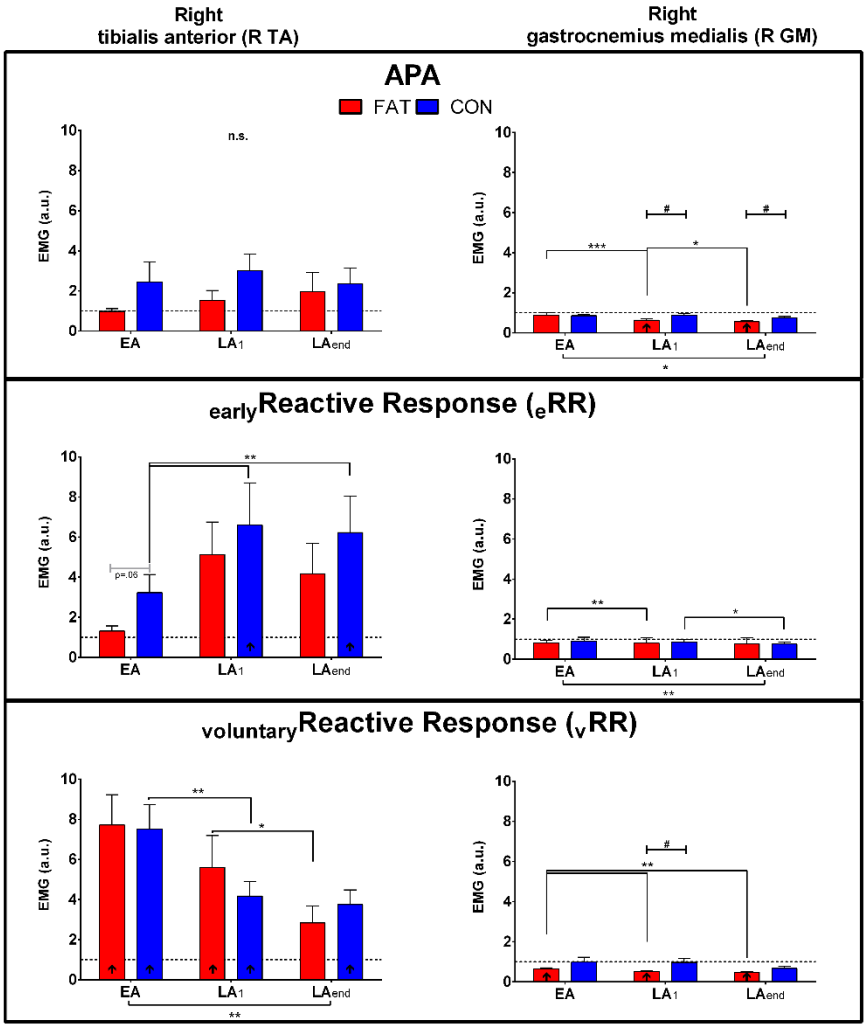

*Figure 3.13 EMG integrals of the muscles acting at the level of the right ankle joint (Right tibialis anterior (TA) and Right gastrocnemius medialis (GM)) over the selected time-windows for learning phase. Anticpatory Postural Adjsutment – APA (upper box), early Reactive Response – eRR (central box) and voluntary Reactive Response – vRR (bottom box). EMG data are in arbitrary units and normalized subject-wise by late baseline (LB) values: value=1 represents no change from baseline (horizontal dashed line). Data are presented as mean value and standard error (SE). ↑ significant difference from LB(p <0.05), * significant effects at p < 0.05, ** significant effects at p < 0.01, *** significant effects at p < 0.001, # significant effects between groups (p < 0.05), # significant effects between groups (p < 0.05), n.s.= not statistically significant*

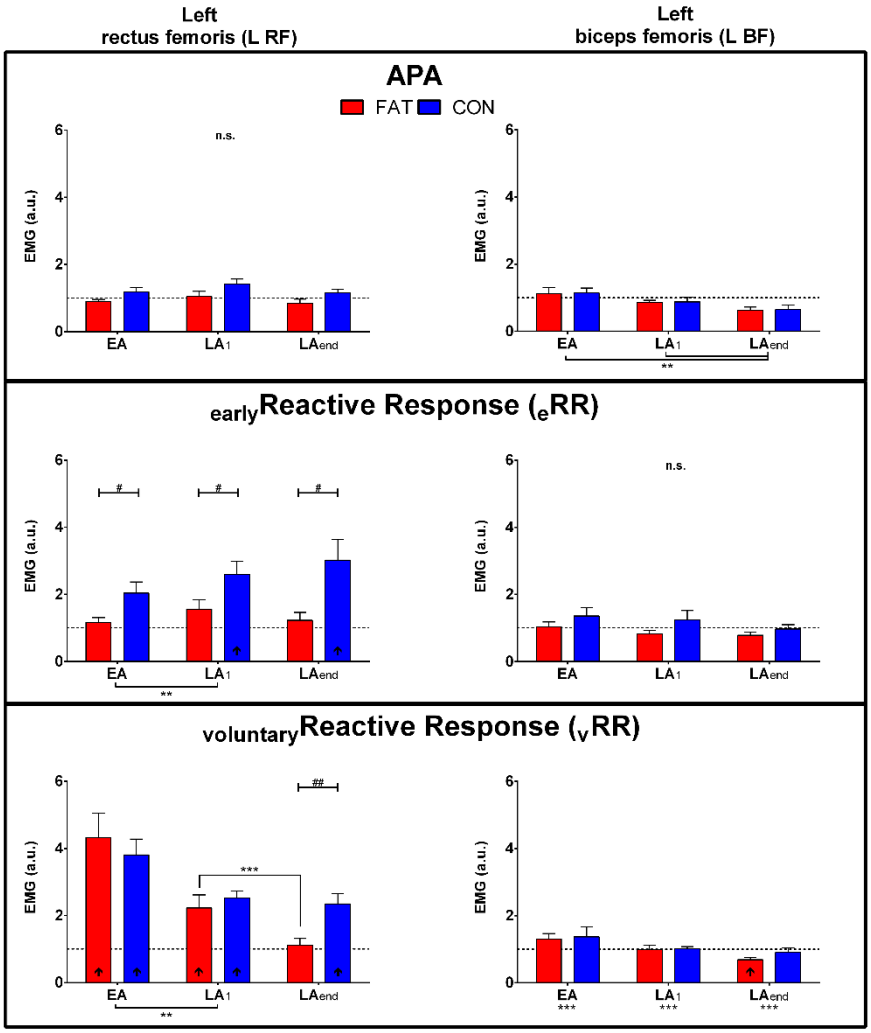

*Figure 3.14 EMG integrals of the muscles acting at the level of the left knee joint (Left rectus femoris (RF) and Left biceps femoris (BF)) over the selected time-windows for learning phase. Anticpatory Postural Adjsutment – APA (upper box), early Reactive Response – eRR (central box) and voluntary Reactive Response – vRR (bottom box). EMG data are in arbitrary units and normalized subject-wise by late baseline (LB) values: value=1 represents no change from baseline (horizontal dashed line). Data are presented as mean value and standard error (SE). ↑ significant difference from LB(p <0.05), ** significant effects at p < 0.01, *** significant effects at p < 0.001, # significant effects between groups (p < 0.05), ## significant effects between groups (p < 0.01), n.s.= not statistically significant*

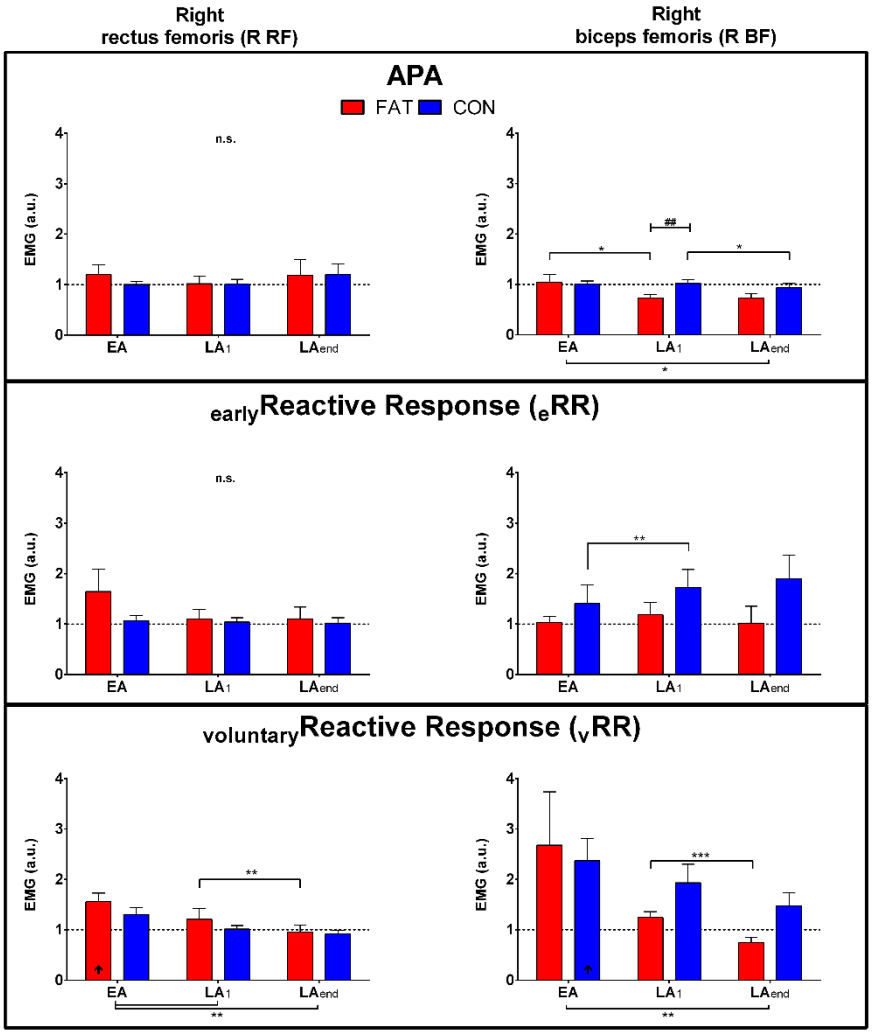

*Figure 3.15 EMG integrals of the muscles acting at the level of the right knee joint (Right rectus femoris (RF) and Right biceps femoris (BF)) over the selected time-windows for learning phase. Anticpatory Postural Adjustment – APA (upper box), early Reactive Response – eRR (central box) and voluntary Reactive Response – vRR (bottom box). EMG data are in arbitrary units and normalized subject-wise by late baseline (LB) values: value=1 represents no change from baseline (horizontal dashed line). Data are presented as mean value and standard error (SE). ↑ significant difference from LB($p < 0.05$), ** significant effects at $p < 0.01$, *** significant effects at $p < 0.001$, ## significant effects between groups ($p < 0.01$), n.s.= not statistically significant*

Washout phase

Results of EMG activity during washout phase partially reflect learning phase, following a general trend of de-learning or re-adapting to unperturbed conditions, with a tendency of returning to late baseline (LB) values. Significant differences between groups are appreciable in APA, $_{e}$RR and $_{v}$RR windows at the level of AD, TAs and RFs muscles. The most interesting results are reported in Figure 3.16 (left

panel), Figure 3.17 (left panel) and Figure 3.19 (left panel) for AD, Left TA and Left RF muscle, respectively.

In details, Friedman's repeated measures analysis for AD muscle found significant effects for phase on APA, $_{e}$RR and $_{v}$RR only when considering just the FAT group (χ^2_1 = 7.14, p = 0.008, χ^2_1 7.14, p = 0.008, and χ^2_1 7.14, p = 0.008, respectively). Welch's paired t-test results for EW was close to significance in APA (p = 0.07), while in the same EMG window differences between groups were significant for $_{e}$RR (p = 0.003) and $_{v}$RR (p = 0.04). A similar trend was observed also in PD muscle (Figure 3.16).

Friedman's test for Left TA muscle, found a significant effect for phase on $_{v}$RR only when considering just the FAT group (χ^2_1 = 13.4, p < .001), while the effect was significant in $_{e}$RR only for CON (χ^2_1 = 9.31, p < .001). Welch's paired t-test found significant higher TA muscle activity in CON group during LW for APA (p < .001) and $_{v}$RR (p = 0.027), For $_{e}$RR, both Welch's paired t-test found TA to be higher in CON group both during EW and LW (p = 0.029 and p = 0.007, respectively). Left TA results are shown in Figure 3.17 (left side).

Friedman's test for Left RF muscle, resulted in a phase effect on all the EMG windows: APA, $_{e}$RR and $_{v}$RR (χ^2_1 = 11.6, p < .001, χ^2_1 = 11.6, p < .001, and χ^2_1 = 5.14, p = 0.023, respectively). As confirmed by the results of Welch's paired t-tests, EMG activity of Left RA was significantly higher in CON across all phases and time windows (p < .05; Figure 3.19 (left side)).

All the other significant results for EMG activity windows at the level of individual muscles during washout phase are reported with relative symbols (legend in each figure caption) in Figure 3.16–3.20. Note that significant differences from late baseline values (LB; equals to dashed horizontal line =1 in figures) – resulting from a one-way mixed ANOVA – are shown in graphs.

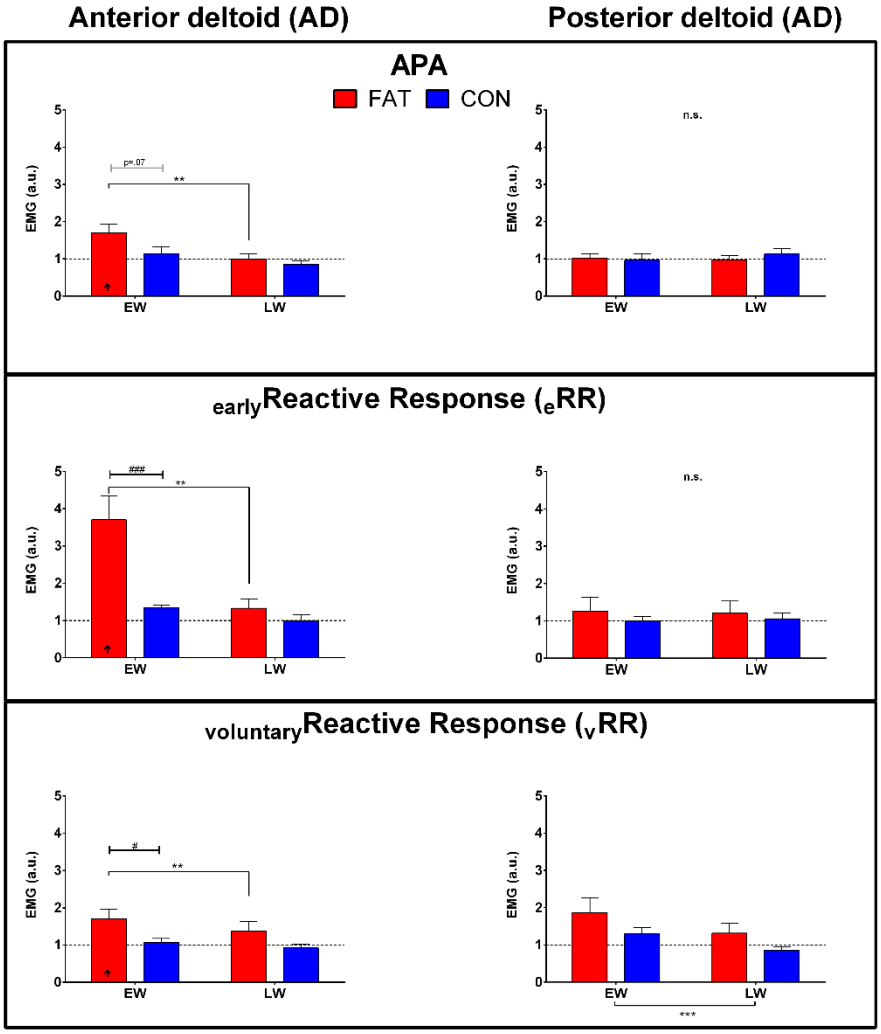

*Figure 3.16 EMG integrals of muscles acting at the shoulder level (Anterior deltoid (AD) and posterior deltoid (PD)) over the selected time-windows for washout phase. Anticpatory Postural Adjsutment – APA (upper box), early Reactive Response – eRR (central box) and voluntary Reactive Response – vRR (bottom box). EMG data are in arbitrary units and normalized subject-wise by late baseline (LB) values: value=1 represents no change from baseline (horizontal dashed line). Data are presented as mean value and standard error (SE). ↑ significant difference from LB(p <0.05), ** significant effects at p < 0.01, *** significant effects at p < 0.001, # significant effects between groups (p < 0.05), # significant effects between groups (p < 0.05), ## significant effects between groups (p < 0.01), ### significant effects between groups (p < 0.001), n.s.= not statistically significant*

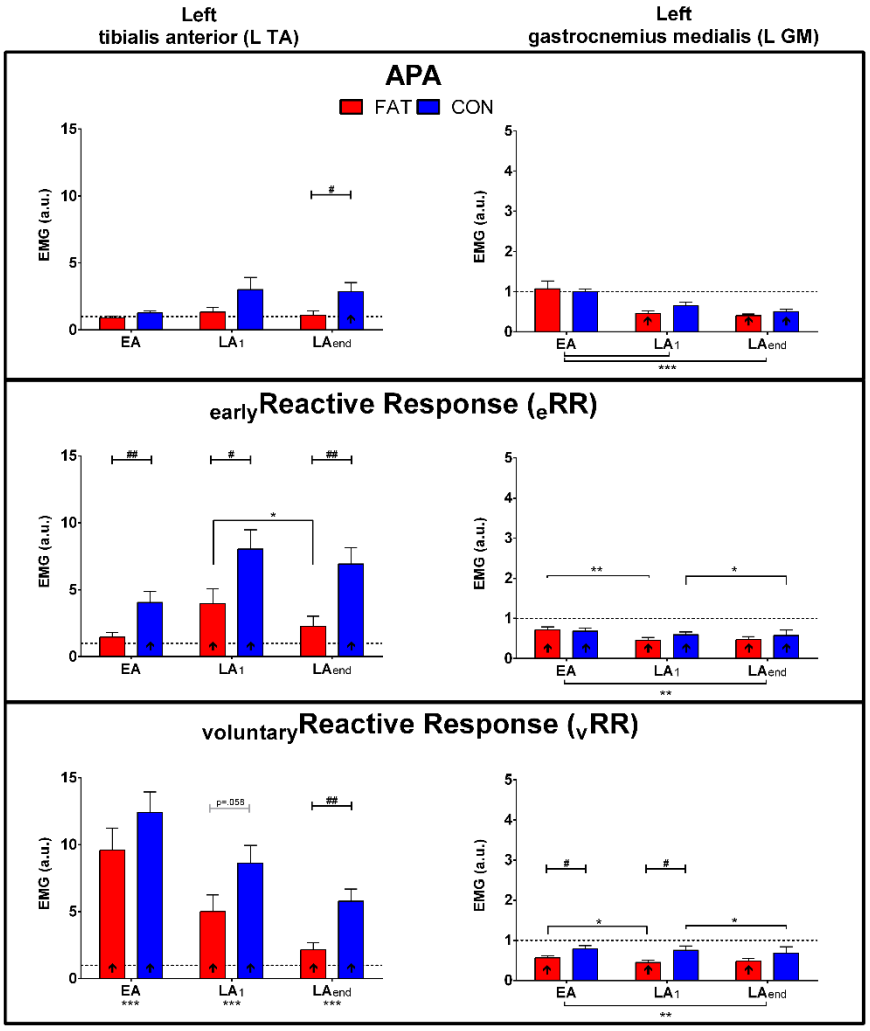

*Figure 3.17 EMG integrals of the muscles acting at the level of the left ankle joint (Left tibialis anterior (TA) and left gastrocnemius medialis (GM)) over the selected time-windows for washout phase. Anticpatory Postural Adjsutment – APA (upper box), early Reactive Response – eRR (central box) and voluntary Reactive Response – vRR (bottom box). EMG data are in arbitrary units and normalized subject-wise by late baseline (LB) values: value=1 represents no change from baseline (horizontal dashed line). Data are presented as mean value and standard error (SE). Note the difference in y-axis limits between the two muscles. ↑ significant difference from LB(p <0.05), * significant effects at p < 0.05, *** significant effects at p < 0.001, # significant effects between groups (p < 0.05), ## significant effects between groups (p < 0.01), ### significant effects between groups (p < 0.001), n.s.= not statistically significant*

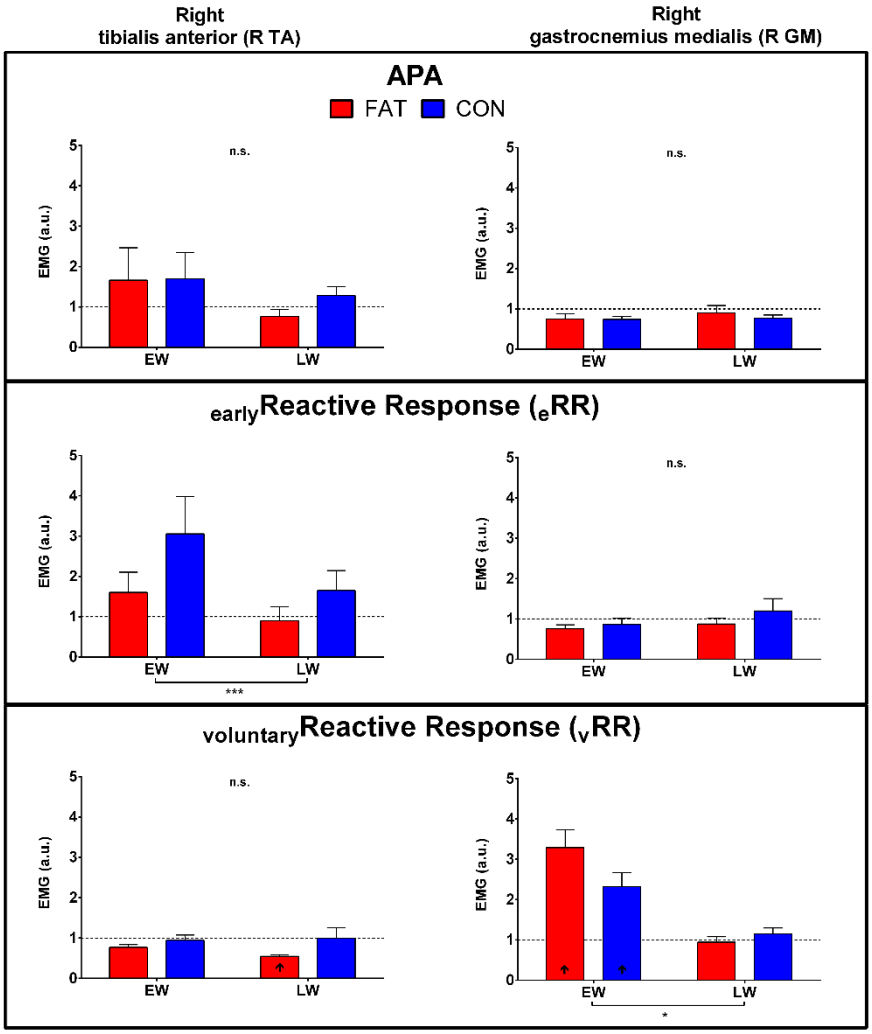

*Figure 3.18 EMG integrals of the muscles acting at the level of the right ankle joint (Right tibialis anterior (TA) and Right gastrocnemius medialis (GM)) over the selected time-windows for washout phase. Anticpatory Postural Adjsutment – APA (upper box), early Reactive Response – eRR (central box) and voluntary Reactive Response – vRR (bottom box). EMG data are in arbitrary units and normalized subject-wise by late baseline (LB) values: value=1 represents no change from baseline (horizontal dashed line). Data are presented as mean value and standard error (SE). ↑ significant difference from LB($p < 0.05$), * significant effects at $p < 0.05$, *** significant effects at $p < 0.001$, n.s.= not statistically significant*

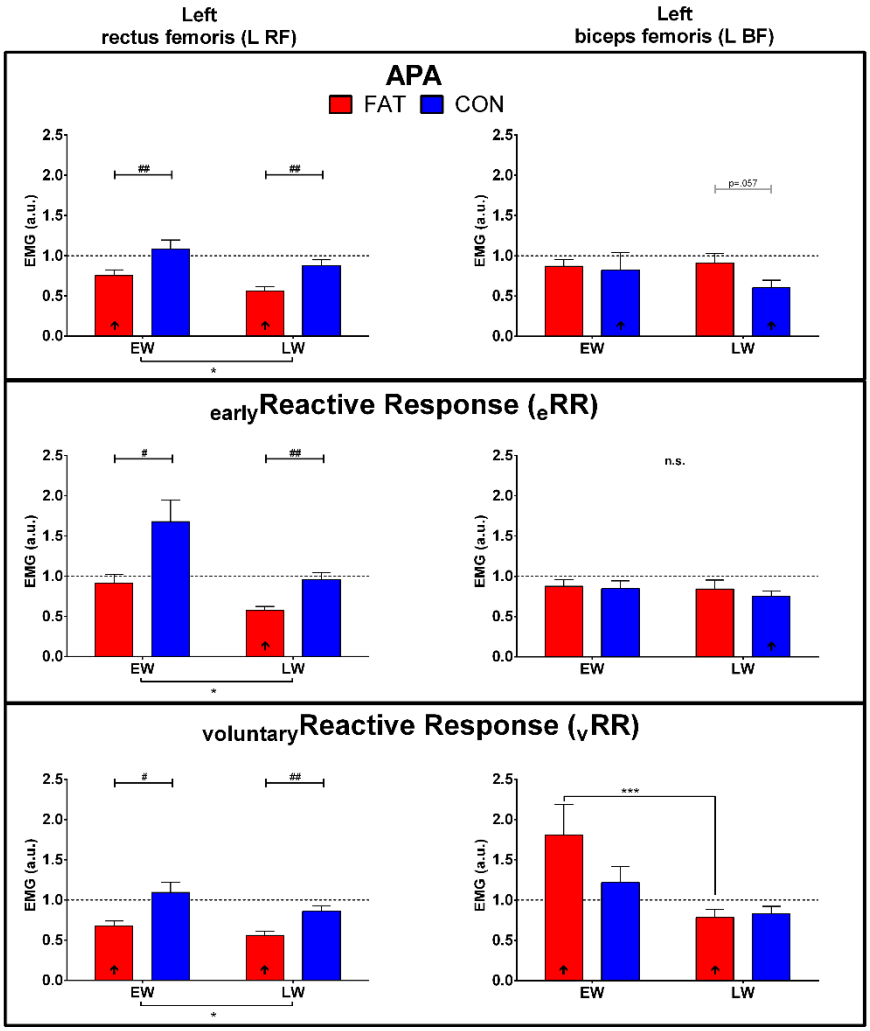

*Figure 3.19 EMG integrals of the muscles acting at the level of the left knee joint (Left rectus femoris (RF) and left biceps femoris (BF)) over the selected time-windows for washout phase. Anticpatory Postural Adjsutment – APA (upper box), early Reactive Response – eRR (central box) and voluntary Reactive Response – vRR (bottom box). EMG data are in arbitrary units and normalized subject-wise by late baseline (LB) values: value=1 represents no change from baseline (horizontal dashed line). Data are presented as mean value and standard error (SE). ↑ significant difference from LB(p <0.05), * significant effects at p < 0.05, *** significant effects at p < 0.001, # significant effects between groups (p < 0.05), ## significant effects between groups (p < 0.01), n.s.= not statistically significant*

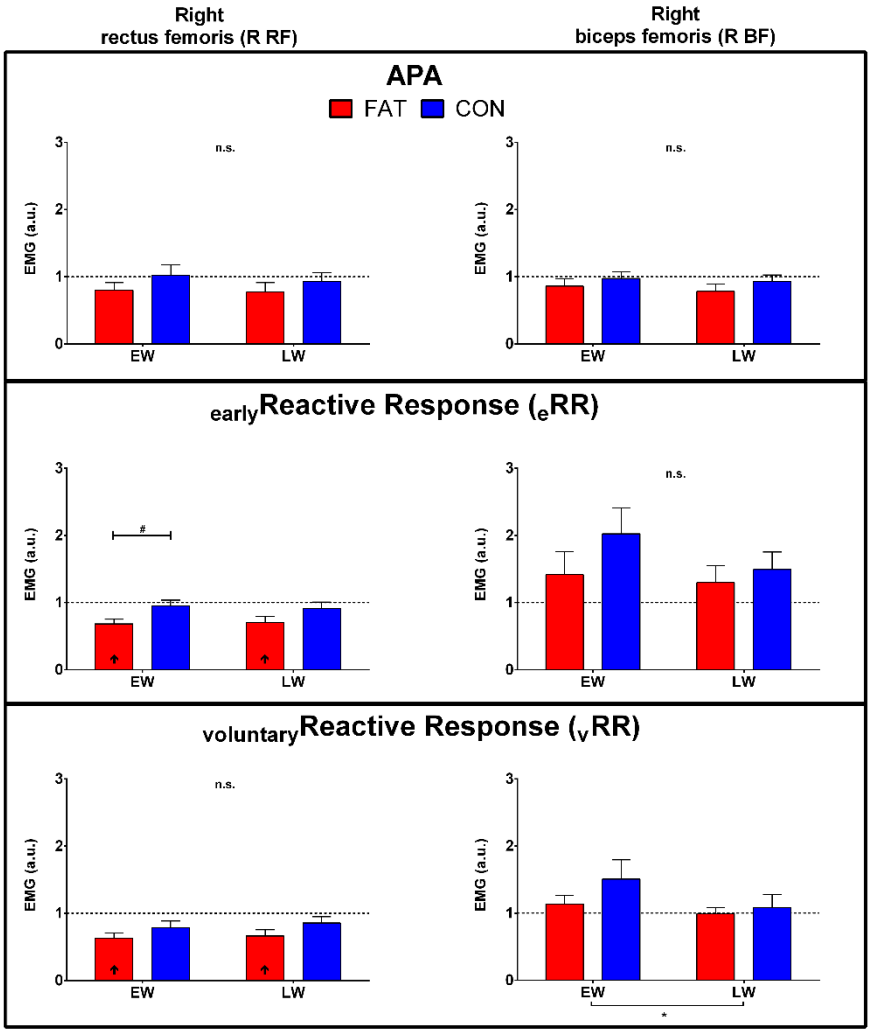

*Figure 3.20 EMG integrals of the muscles acting at the level of the right knee joint (Right rectus femoris (RF) and Right biceps femoris (BF)) over the selected time-windows for washout phase. Anticpatory Postural Adjsutment – APA (upper box), early Reactive Response – eRR (central box) and voluntary Reactive Response – vRR (bottom box). EMG data are in arbitrary units and normalized subject-wise by late baseline (LB) values: value=1 represents no change from baseline (horizontal dashed line). Data are presented as mean value and standard error (SE). ↑ significant difference from LB($p < 0.05$), * significant effects at $p < 0.05$, # significant effects between groups ($p < 0.05$), n.s.= not statistically significant.*

EMG activation indexes

EMG activation indexes were computed at the level of muscle agonist-antagonist pairs at the level of a joint. Indexes, compared to individual muscles, may convey more information about the strategy the CNS utilizes – namely the increase in activation of the agonist or the co-activation of both agonist-antagonist muscles to increase joint stiffness – to stabilize the posture within a pre-determined time window. Patterns of changes seen at individual muscles level are here confirmed,

especially regarding the difference in terms of C-index modulation in different joints across groups. Interestingly, some of these changes seem to persist even after the removal of perturbation.

Learning phase

The repeated measures analysis (Friedman's test – considering participants in both groups) found significant effects for Phase on C-index during the $_{e}$RR ($\chi^2_3 = 23.7$, $p < .001$) for the AD-PD muscle pair. Durbin-Conover pairwise comparisons reported a difference between LB and EA. Running the analysis with separate groups resulted in the significant increase of the index for FAT from LB to LA_1 and LA_{end}, and from EA to LA_1 ($p < .001$). Friedman's test resulted in a phase effect on C-index during $_{v}$RR ($\chi^2_3 = 42.7$, $p < .001$), increasing from LB once the perturbation is presented, and then slowly returning to those values at LA_{end}. Durbin-Conover pairwise comparisons reported significant differences across phases ($p = 0.016$ to $p < .001$) except between LB and LA_{end} ($p > .05$). Data are presented in Figure 3.21 (left panel).

Friedman's test for C-index at the level of the Left ankle joint resulted in a phase effect on APA ($\chi^2_3 = 5.36$, $p = 0.049$), $_{e}$RR ($\chi^2_3 = 28.9$, $p < .001$) and $_{v}$RR ($\chi^2_3 = 55.2$, $p < .001$). Pairwise Durbin-Conover found both main effects of phases and effects on the individual group (Figure 3.22 for details). Welch's paired t-test found significant differences between groups in APA and $_{e}$RR at LA_{end} ($p < .05$), in $_{v}$RR at EA, LA_1 and LA_{end} ($p < .05$).

Friedman's test for C-index at the level of the Left knee joint, resulted in a phase effect on APA ($\chi^2_3 = 12.1$, $p = 0.007$), $_{e}$RR ($\chi^2_3 = 10.5$, $p < .015$) and $_{v}$RR ($\chi^2_3 = 40.5$, $p < .001$). Pairwise Durbin-Conover found both main effects of phases and effects on the individual group (Figure 3.24 for details). Welch's paired t-test found significant differences between groups in APA at LA_{end} ($p < .05$), in $_{e}$RR ($p < 0.05$, all phases), and $_{v}$RR at LA_1 and LA_{end} ($p < .05$).

All the other significant results for EMG activity windows at the level of individual muscles during learning phase are reported with relative symbols (legend in each figure caption) in Figure 3.21–3.25.

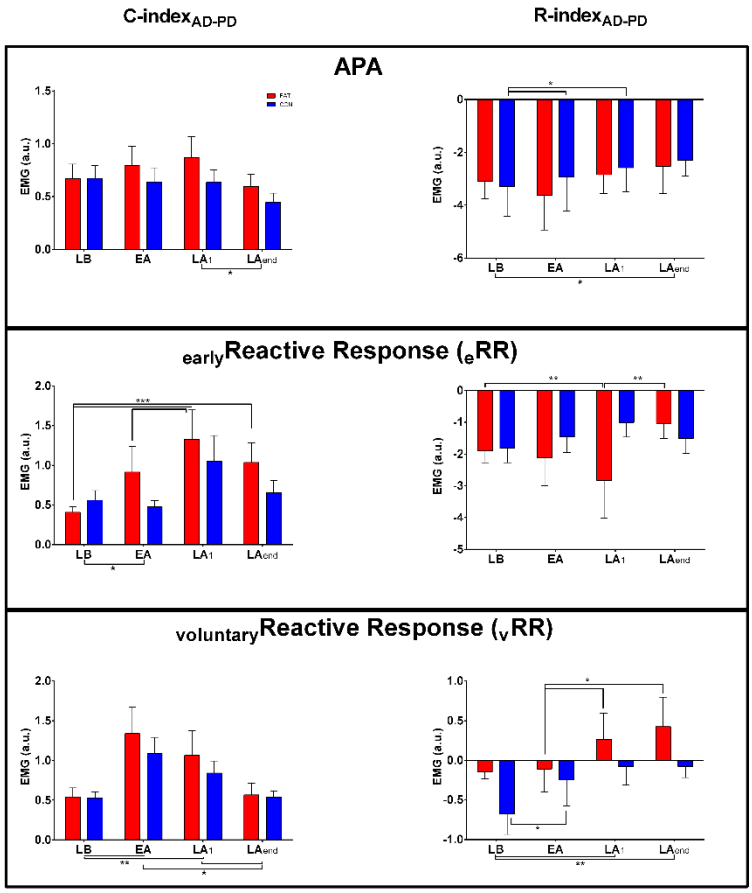

*Figure 3.21 C-index (left) and R-index (right) and C-index values for the agonist–antagonist pairs acting at the shoulder joint (AD–PD), over the selected time-windows for learning phase. Anticpatory Postural Adjsutment – APA (upper box), early Reactive Response – eRR (central box) and voluntary Reactive Response – vRR (bottom box). EMG data are in arbitrary units and presented as mean value, while errorbars represent 1 standard error (SE). * significant effects at p < 0.05, ** significant effects at p < 0.01, *** significant effects at p < 0.001.*

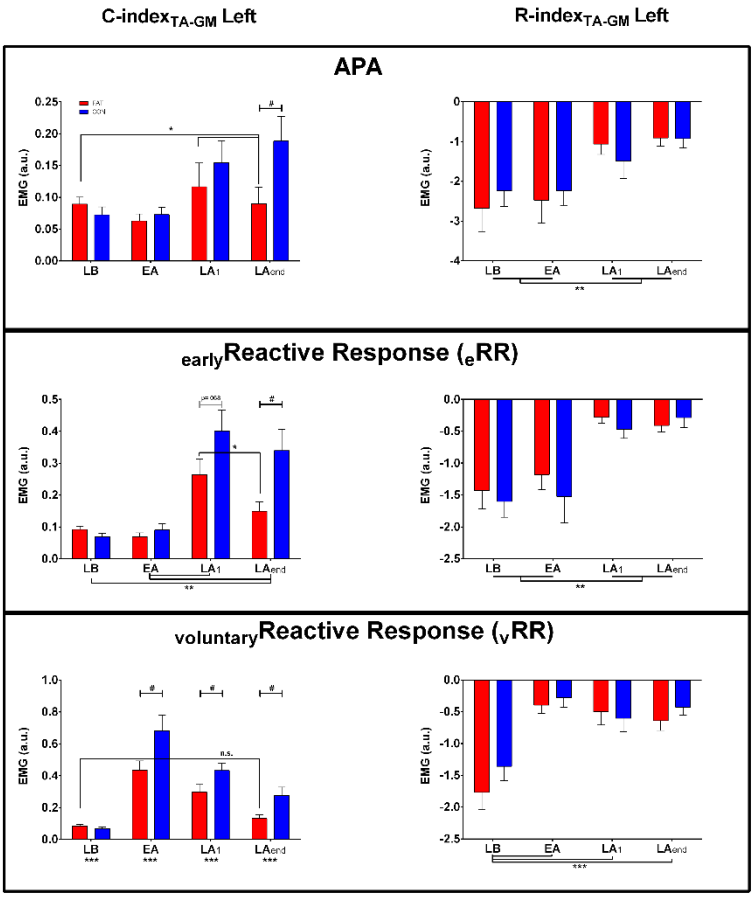

*Figure 3.22 C-index (left) and R-index (right) and C-index values for the agonist–antagonist pairs acting at the left ankle joint (TA–GM Left), over the selected time-windows for learning phase. Anticpatory Postural Adjsutment – APA (upper box), early Reactive Response – eRR (central box) and voluntary Reactive Response – vRR (bottom box). EMG data are in arbitrary units and presented as mean value, while errorbars represent 1 standard error (SE). * significant effects at p < 0.05, ** significant effects at p < 0.01, *** significant effects at p < 0.001, # significant effects between groups (p < 0.05).*

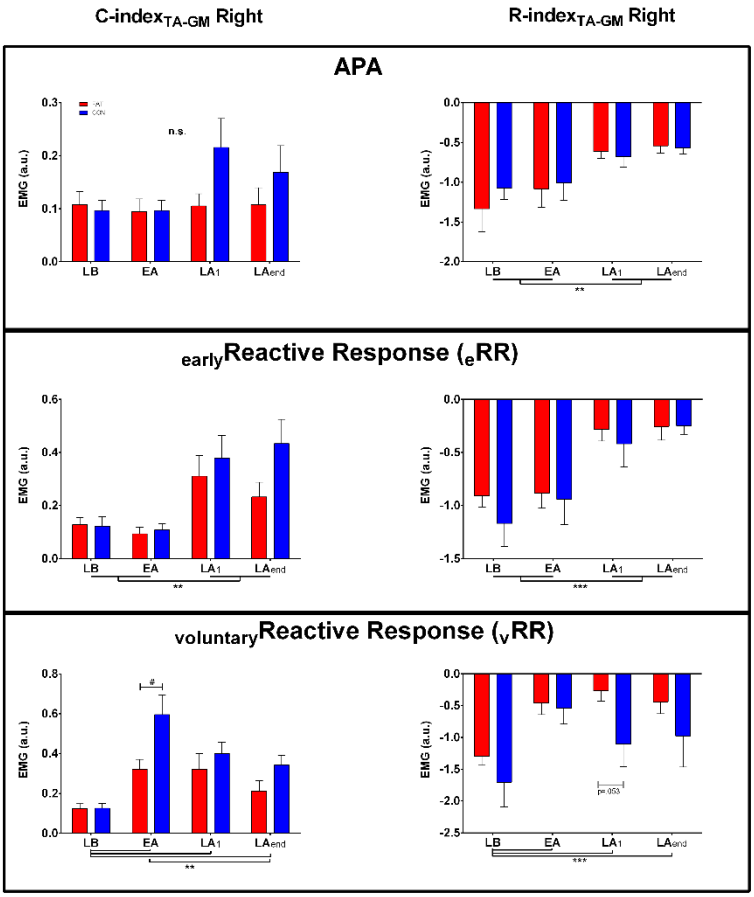

*Figure 3.23 C-index (left) and R-index (right) and C-index values for the agonist–antagonist pairs acting at the right ankle joint (TA–GM Right), over the selected time-windows for learning phase. Anticpatory Postural Adjsutment – APA (upper box), early Reactive Response – eRR (central box) and voluntary Reactive Response – vRR (bottom box). EMG data are in arbitrary units and presented as mean value, while errorbars represent 1 standard error (SE). * significant effects at p < 0.05, ** significant effects at p < 0.01, *** significant effects at p < 0.001, n.s.= not statistically significant.*

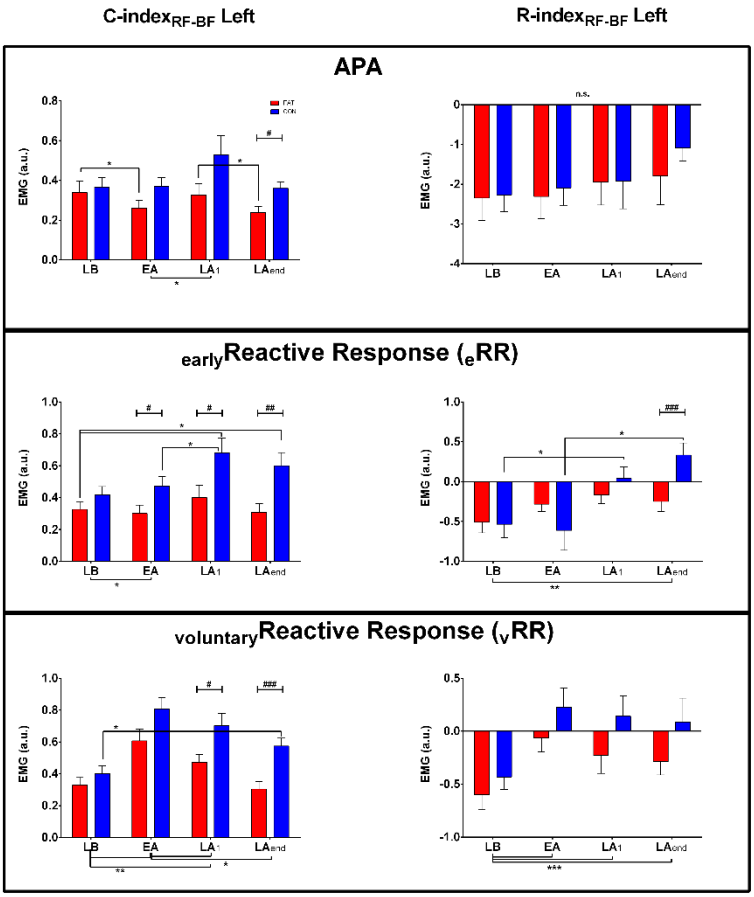

*Figure 3.24 C-index (left) and R-index (right) and C-index values for the agonist–antagonist pairs acting at the left knee joint (RF–BF Left), over the selected time-windows for learning phase. Anticpatory Postural Adjsutment – APA (upper box), early Reactive Response – eRR (central box) and voluntary Reactive Response – vRR (bottom box). EMG data are in arbitrary units and presented as mean value, while errorbars represent 1 standard error (SE). * significant effects at p < 0.05, ** significant effects at p < 0.01, *** significant effects at p < 0.001, # significant effects between groups (p < 0.05), ## significant effects between groups (p < 0.01), ### significant effects between groups (p < 0.001), n.s.= not statistically significant.*

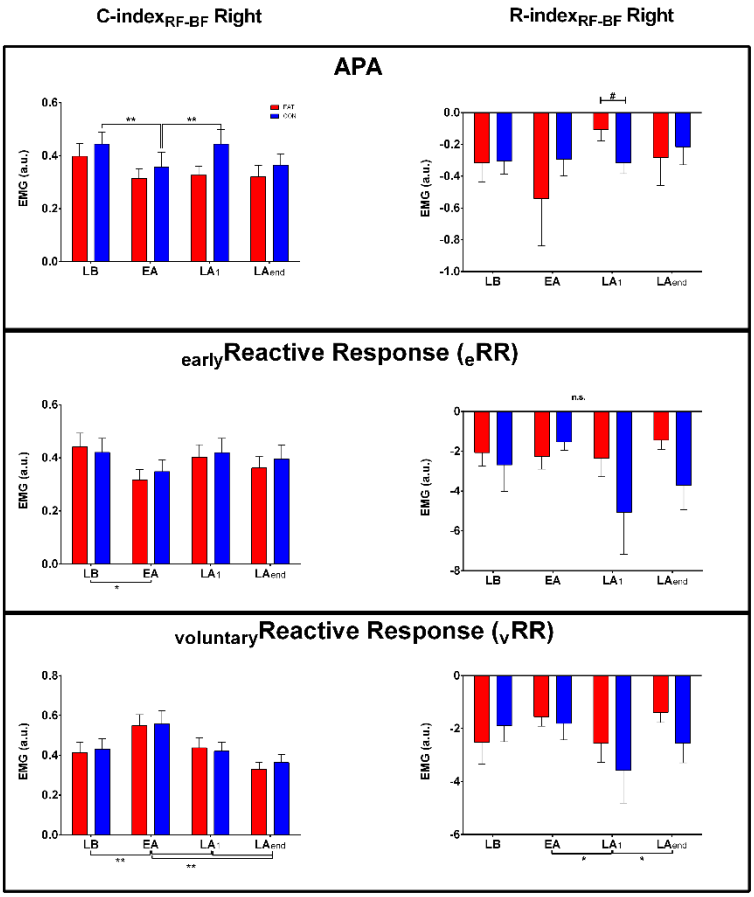

*Figure 3.25 C-index (left) and R-index (right) and C-index values for the agonist–antagonist pairs acting at the right knee joint (RF–BF Right), over the selected time-windows for learning phase. Anticpatory Postural Adjsutment – APA (upper box), early Reactive Response – eRR (central box) and voluntary Reactive Response – vRR (bottom box). EMG data are in arbitrary units and presented as mean value, while errorbars represent 1 standard error (SE). * significant effects at p < 0.05, ** significant effects at p < 0.01, # significant effects between groups (p < 0.05), n.s.= not statistically significant.*

Washout phase

Friedman's test run on separate groups found significant effects for Phase on C-index of FAT group only during the $_{e}$RR ($\chi^2_2 = 9.93$, $p = 0.007$) for the AD-PD muscle pair.

Friedman's test for C-index at the level of the Left ankle joint, resulted in a phase effect on APA ($\chi^2_2 = 15.6$, $p < .001$), $_{e}$RR ($\chi^2_2 = 23.8$, $p < .001$) and $_{v}$RR ($\chi^2_2 = 32.4$, $p < .001$). Pairwise Durbin-Conover found APA difference during LB–EW and LB–LW statistically significant ($p < .001$; Figure 3.27 – left panel). Pairwise comparisons for $_{e}$RR were statistically different at LB–EW and EW–LW ($p < .001$). Pairwise comparisons for $_{v}$RR statistically differed at LB–EW and EW–LW ($p <$

.01). Welch's paired t-test found significant differences between groups in C-index during $_{e}$RR only at EW phase ($p < 0.05$).

Friedman's test for C-index at the level of the Left knee joint, resulted in a phase effect on APA, decreasing only on FAT group ($\chi^2_2 = 15.9$, $p < .001$). Welch's paired t-test found significant differences between groups at EW and LW in APA ($p < .05$). Friedman's test on separated groups for left knee C-index in $_{e}$RR found a significant LB–LW decrease in FAT ($p < 0.01$), and a decrease in EW–LW ($p < 0.05$) for CON group. Welch's paired t-test found significant differences between groups at EW and LW in $_{e}$RR ($p < .05$), which were higher for CON. Relative to $_{v}$RR, Friedman's test found a significant effect of phase ($\chi^2_2 = 17.3$, $p < .001$) only for FAT. Pairwise Durbin-Conover comparisons were all significant ($p < .01$), with a decreasing trend from LB to LW just in FAT group. Welch's paired t-test found significant differences between groups at EW and LW in $_{v}$RR ($p < .05$; Figure 3.29) All the other significant results for EMG activity windows at the level of individual muscles during learning phase are reported with relative symbols (legend in each figure caption) in Figure 3.26–3.30.

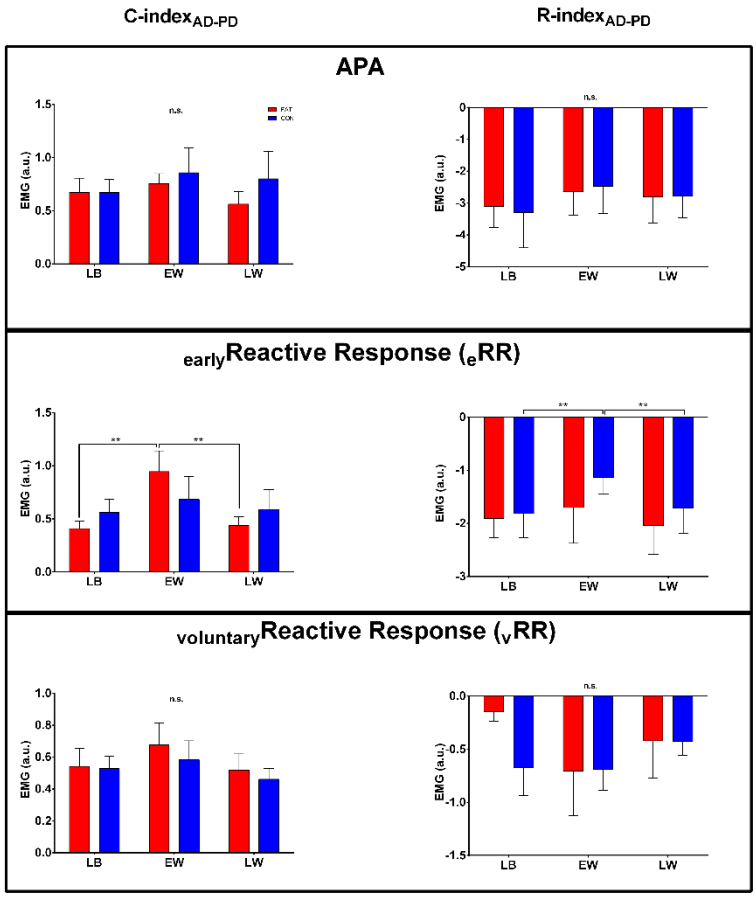

*Figure 3.26 C-index (left) and R-index (right) and C-index values for the agonist–antagonist pairs acting at the shoulder joint (AD–PD), over the selected time-windows for washout phase. Anticpatory Postural Adjsutment – APA (upper box), early Reactive Response – eRR (central box) and voluntary Reactive Response – vRR (bottom box). EMG data are in arbitrary units and presented as mean value, while errorbars represent 1 standard error (SE). * significant effects at p < 0.05, ** significant effects at p < 0.01, n.s.= not statistically significant.*

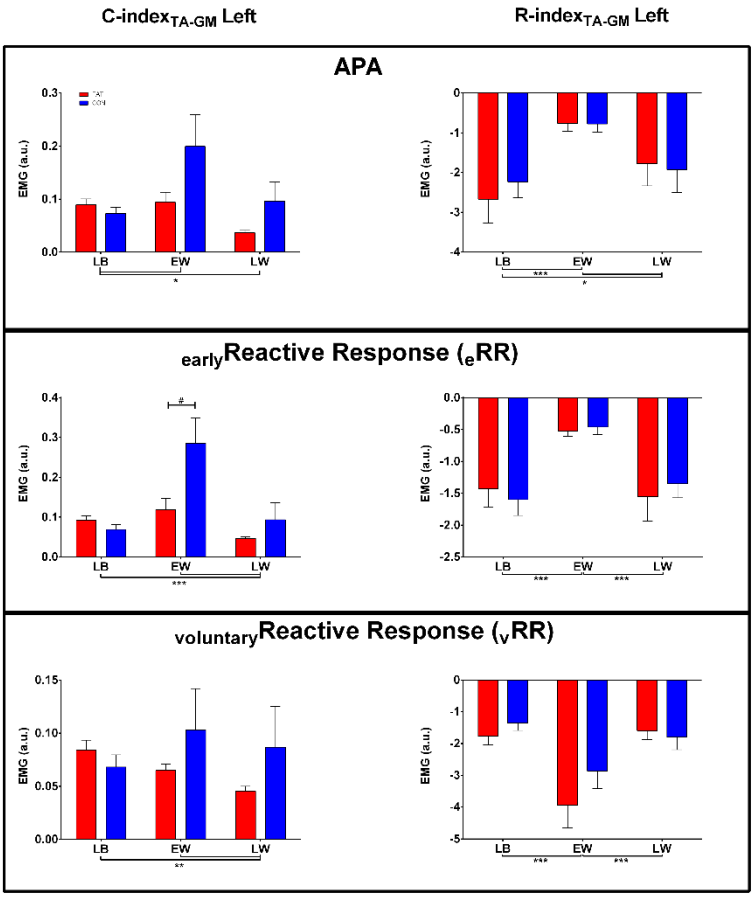

*Figure 3.27 C-index (left) and R-index (right) and C-index values for the agonist–antagonist pairs acting at the left ankle joint (TA–GM Left), over the selected time-windows for washout phase. Anticpatory Postural Adjsutment – APA (upper box), early Reactive Response – eRR (central box) and voluntary Reactive Response – vRR (bottom box). EMG data are in arbitrary units and presented as mean value, while errorbars represent 1 standard error (SE). * significant effects at p < 0.05, ** significant effects at p < 0.01, *** significant effects at p < 0.001.*

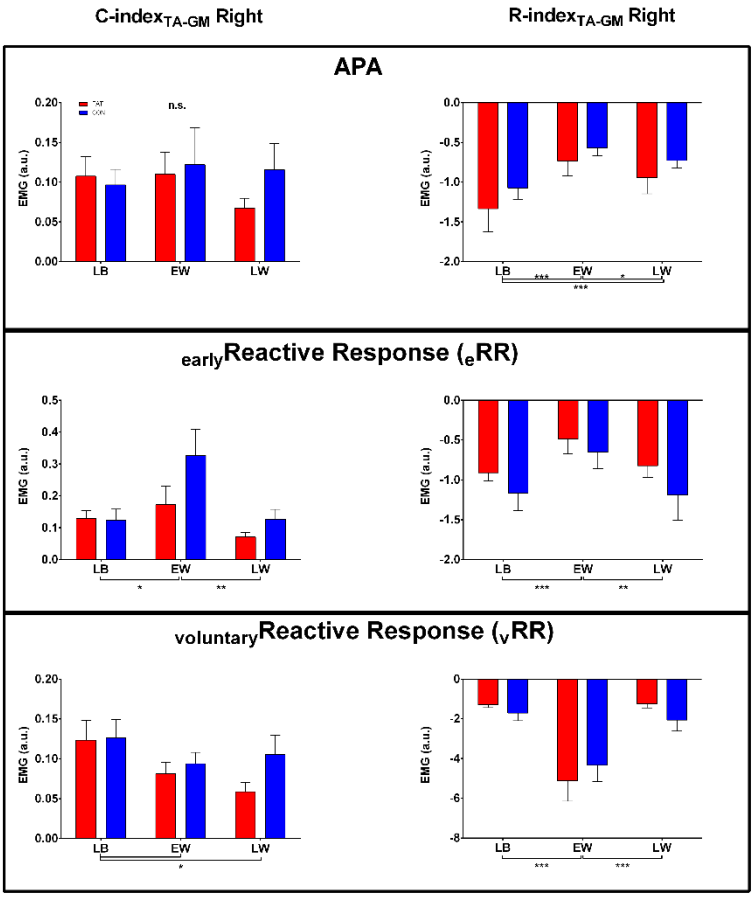

*Figure 3.28 C-index (left) and R-index (right) and C-index values for the agonist–antagonist pairs acting at the right ankle joint (TA–GM Right), over the selected time-windows for washout phase. Anticpatory Postural Adjsutment – APA (upper box), early Reactive Response – eRR (central box) and voluntary Reactive Response – vRR (bottom box). EMG data are in arbitrary units and presented as mean value, while errorbars represent 1 standard error (SE). * significant effects at p < 0.05, ** significant effects at p < 0.01, *** significant effects at p < 0.001, n.s.= not statistically significant.*

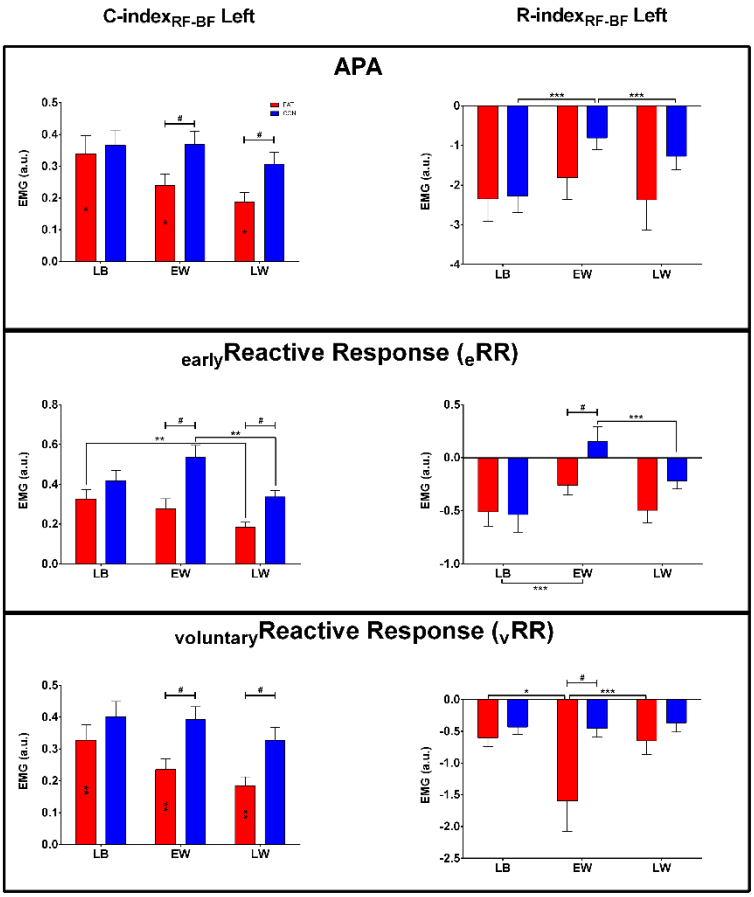

*Figure 3.29 C-index (left) and R-index (right) and C-index values for the agonist–antagonist pairs acting at the left knee joint (RF–BF Left), over the selected time-windows for washout phase. Anticpatory Postural Adjsutment – APA (upper box), early Reactive Response – eRR (central box) and voluntary Reactive Response – vRR (bottom box). EMG data are in arbitrary units and presented as mean value, while errorbars represent 1 standard error (SE). * significant effects at p < 0.05, ** significant effects at p < 0.01, *** significant effects at p < 0.001, # significant effects between groups (p < 0.05), n.s.= not statistically significant.*

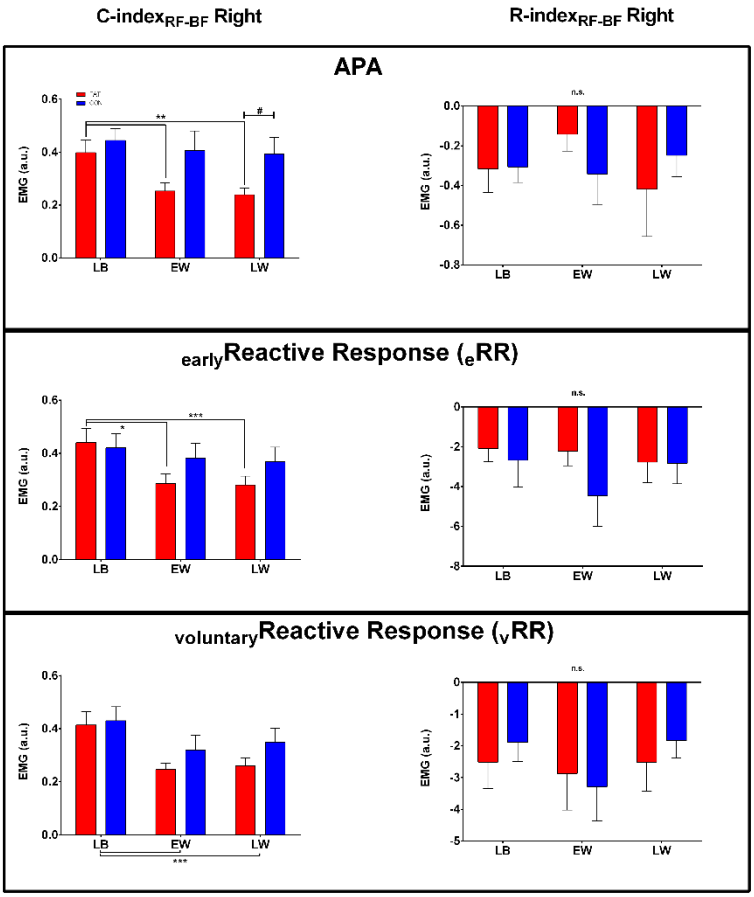

*Figure 3.30 C-index (left) and R-index (right) and C-index values for the agonist–antagonist pairs acting at the right knee joint (RF–BF Right), over the selected time-windows for washout phase. Anticpatory Postural Adjsutment – APA (upper box), early Reactive Response – eRR (central box) and voluntary Reactive Response – vRR (bottom box). EMG data are in arbitrary units and presented as mean value, while errorbars represent 1 standard error (SE). * significant effects at $p < 0.05$, ** significant effects at $p < 0.01$, *** significant effects at $p < 0.001$, # significant effects between groups ($p < 0.05$), n.s.= not statistically significant.*

DISCUSSION

Overall, the study results demonstrate that the CNS efficiently adapted to a force-field perturbation even in a physiologically perturbed state such as localized NMF in postural muscles, which alters muscle properties, perception of effort and proprioceptive feedback loops. Despite a similar behavior between groups in the overall postural control and maintenance of balance, we observed two distinct and opposite strategies in terms of patterns of muscle activation.

Effects of neuromuscular fatigue on task performance

The results of the present study are in line with previous studies which assessed motor adaptation using similar task paradigms (Takahashi et al., 2006; Ahmed and Wolpert, 2009; Pienciak-Siewert et al., 2016, 2020). Perturbation-driven error in task performance significantly reduced throughout the protocol, following appreciable adaptation curves in both Fatigue and Control group (Figure 3.4). The comparable profiles in HME reduction between groups suggest localized NMF is efficiently compensated and did not preclude motor adaptation of performance-related variables even in presence of fatigued postural muscles. However, when comparing HME values between groups at specific experimental phases, those remained significantly higher during the late adaptation phase (LA_1 and LA_{end}) in the FAT group (Figure 3.5). These results are partially in contrast to what has been previously found in another study, where fatiguing exercise did not alter adaptation processes during subsequent practice (Takahashi et al., 2006). Our interpretation is that the difference arising in the present study are due to the more controlled fatiguing protocol and suggest practicing in a fatigued state led to a slower adaptation rate in FAT group. In previous studies, effects of practicing in a fatigued state arose only during a subsequent re-exposure to the same task (Takahashi et al., 2006; Branscheidt et al., 2019).

The same trend was evident from hand velocity profiles in anteroposterior direction (Peak Hand $velocity_{AP}$), which showed a more rapid decrease in the CON group (Figure 3.6). This result, corroborated by the increase in the activation in upper limb muscles, support the interpretation that participants in the FAT group tended to rely more on upper-limb strategies to control for the perturbation, resulting in greater hand trajectory corrections. Current findings are in accordance with previous studies (Takahashi et al., 2006; Branscheidt et al., 2019), where detrimental effects of NMF where reported during a second re-exposure to the task. However, it is worthwhile to note that in the mentioned study (Takahashi et al., 2006) participants were exposed to fatigue in muscles directly used during the reaching task itself, thus the increase in performance error might be influenced by incapability of muscles to counteract the robot force or impaired proprioception. In our study we specifically avoided fatiguing the effector muscle involved in the execution of the reaching task

to limit these potential biases. Washout phase results are in line – and opposite in sign – with the learning phase, confirming the greater involvement of adjustments at the level of the hand by the FAT group, as shown by the difference between groups in Peak Hand velocity$_{AP}$ on the first trial after the removal of perturbation (EA; Figure 3.8). Overall, participants in both groups were able to adapt to the force-field perturbation, but their rate was different, with a slower trend following localized fatigue.

Effects of neuromuscular fatigue on postural control

Surprisingly, measures of postural control showed similar trends between the two groups. This is in contrast with findings from other studies in literature (Nardone et al., 1997; Gribble and Hertel, 2004; Davidson et al., 2009). However, many of the studies which reported an increase in postural instability after fatigue, consisted in static or passive tasks (Nardone et al., 1997; Gribble and Hertel, 2004). Indeed, it is worth noting that, by the nature of the dynamic task in the present study, the COP was required to allow for some displacement in the mediolateral direction in order to switch the bodyweight left to right during reaching movements. Similarly, in a recent study, measuring postural balance during a dynamic balance performance task, the authors found no differences in dynamic balance performance despite a reduction in EMG activation in soleus muscle (Marcolin et al., 2022). Furthermore, the displacement in the anteroposterior direction was affected by the effects of the robot force generated during the task itself, which were velocity-dependent, thus similar between groups (Movement time was the same between groups; Figure 3.3). Another possible explanation might be the nature of the task itself: performance was controlled at the level of the hand, so participants might have adopted different strategies in terms of body sway, which was not controlled or provided as feedback during the task. Additionally, the heterogeneity of trial's execution at the level of COP sway might have masked differences in the postural destabilization during movement in the FAT group.

Changes in EMG activation patterns following neuromuscular fatigue

Our findings demonstrate the remodulation of motor commands to the muscles (individual muscles) and to the muscles acting at the level of a single joint (R- and C-indexes; (Slijper and Latash, 2000)). In both groups reactive responses – driven by both stereotyped and voluntary correction during the movement – tended to reduce across learning phase, indicating an effective refinement of CNS anticipatory strategies to counteract the perturbation (Kanekar et al., 2008; Santos et al., 2010b, 2010a). Specifically, participants seem to adapt in different and opposite ways depending on their physiological state (fatigued/not fatigued). When participants were fatigued, they tended to maintain stable or reduce muscle activation of most of the postural muscles – except for TAs, which were fundamental for the control of standing posture in the task. The findings at individual muscle level are further confirmed by the trends in muscles activation patterns at joint level. In details, C-indexes (muscle co-activation) of muscle agonist-antagonist pairs were reduced in the FAT group, but not in CON (Figure 3.22 and Figure 3.24), where they remained constant or increased with learning phase. Trends in the CON group are in line with earlier studies (Slijper and Latash, 2000, 2004; Piscitelli et al., 2017), where an upward modulation in co-activation was seen in conditions of task modification and predictability of perturbations. On the other hand, we observed an increase in EMG activation at the level of the upper limb muscles (AD and PD), which was significantly higher in FAT compared to CON group. Once again, the findings were confirmed by looking at C-index (AD-PD), which significantly increased for FAT, interpreted as a recalibration of the commands within CNS, allowing higher variability in muscle activation of non-fatigued muscles to compensate for the ones fatigued, as reported by previous studies (Singh et al., 2010; Singh and Latash, 2011). Evidences of fatigue-induced effects at the level of muscles not involved in the task have been reported in several other studies (Danna-Dos-Santos et al., 2007; Kanekar et al., 2008; Strang et al., 2009). Interestingly, FAT group did not show noticeable increase in APAs except for AD muscle. Furthermore, activation in the same muscle, and in its relative C-index (AD-PD) was higher even in the reactive response phases (both $_{e}$RR and

$_{v}$RR), suggesting participants, when fatigued, relied more on visual and proprioceptive feedback than on anticipatory strategies.

CHAPTER 4 – EXPERIMENTAL RESEARCH: STUDY 3

Effects of muscle fatigue on motor adaptation and savings using a novel postural-task paradigm.

ABSTRACT

Neuromuscular fatigue (NMF) influences and disrupts movement execution through different mechanisms, from modification of muscles' mechanical properties at peripheral level to changes in the gain and sensitivity of proprioceptive feedback loops at central level. It has been recently demonstrated that NMF affects adaptation processes by inducing a change in EMG activation patterns in both fatigued and non-fatigued muscles to stabilize performance.

The goal of this study was to determine how localized NMF of postural muscles during adaptation to a novel standing postural perturbation task affects motor adaptation processes both at short- and long-term (savings). Twenty-three participants (12 females) were randomly assigned to Fatigue (FAT) or Control (CON) group and exposed to a motor adaptation paradigm using a standing postural task consisting in keeping the center of pressure (COP) anteroposterior coordinates within a selected position, while a mechanical perturbation pulled the participant's body backwards. To induce motor learning, the magnitude of the mechanical perturbation was changes during the task – from 4% of bodyweight (BW) during baseline, to 8% BW during subsequent adaptation, and back to 4% BW in washout phase – without participant's knowledge. Participants performed two sessions (Day 1, Day 2; 72h apart), where prior to each of the adaptation and washout trials, participants performed an isometric exercise with the tibialis anterior (TA) muscles. Exercise intensity differed between groups at Day 1 (FAT: 65±5%; CON; 7.5±5% of maximal voluntary contraction – MVC). At Day 2, both groups exercised at 7.5±5% MVC. COP data were collected during the task. TAs MVC decreased by 32 ± 4% in FAT group on Day 1. Participants in both groups showed comparable adaptation curves for performance error at Day1. Interestingly, when participants were re-exposed to the same task (Day2), FAT group exhibited a slower learning rate and reduced savings compared to CON. The results suggest NMF induced the adoption of different motor strategies between groups, which persisted even at re-

exposure, where both groups were not fatigued. We hypothesize the internal models formed during the fatigued state, result in suboptimal commands which are not as effective when recalled at Day2, when muscular conditions are different from Day1.

INTRODUCTION

Neuromuscular fatigue (NMF) is known to influence and disrupt the execution of movement through different mechanisms, from the transient induced changes in physiological state and mechanical properties of the muscles (Gandevia, 2001; Taylor et al., 2016) to the feedback-mediated effects on CNS descending drive to the muscle itself (Carroll et al., 2017). We recently demonstrated that NMF affects the adaptation processes by inducing remodulation in EMG activation patterns in both fatigued and non-fatigued postural muscles, in order to stabilize performance. Similar results have been reported both in motor adaptation (Takahashi et al., 2006) and even in tasks with non-changing perturbations (Strang et al., 2009; Singh et al., 2010; Singh and Latash, 2011). The maintenance of a standing posture in perturbation conditions requires the effective timing of activation across muscle pairs acting at each joint in order to counteract joint torques. The process of learning a novel postural strategy to counteract a postural perturbation in a fatigued condition might have long-term effects on the retention of the strategy and its following recall (Takahashi et al., 2006). Recent evidence from Branscheidt et al., suggested that NMF negatively affects motor skill learning by inducing long-lasting detrimental changes (Branscheidt et al., 2019). In their study, however, they isometrically fatigued hand muscles, which are also task relevant. This detail could be a possible confounder, since it is not clear whether the effects of NMF are due to the inherent inability of the muscle to contract properly in the execution of the task. For this reason, in our study we chose to induce localized fatigue in postural muscles in the lower limbs, which are essential for standing postural control. The specific goal of the present study was to determine how the presence of NMF throughout the adaptation phase in the first exposure to a standing postural task affects the motor adaptation processes both at short- (same session) and long-term (savings during next session). Based on previous research in the field of motor learning (Takahashi et al., 2006; Branscheidt et al., 2019), our hypotheses were that

1) NMF would impact motor adaptation processes in the short term period, resulting in difference in the performance error between groups; 2) Experiencing and learning a novel task in a fatigued state would impact the strategies used by participants to contrast perturbation, impacting savings and learning rate during a second exposure to the task.

MATERIALS AND METHODS

Participants

Twenty-three right-handed, healthy young adults (11 males; 12 females) were recruited for this study. Participants had normal or corrected to normal vision and were screened for exclusion criteria: 1) history of neurological or 2) musculoskeletal disorders, 3) cardiovascular disease, 4) conditions of the vestibular system or 5) medications affecting balance. The experimental protocol was approved by the Ethical Committee of the University of Verona and performed in accordance with the most recent principles of Helsinki Declaration. Participants provided written informed consent before taking part in the study. Participants. Participants anthropometrics is reported in Table 4.1.

Group (*n*)	**Age (years)**	**Weight (kg)**	**Height (cm)**
FAT (*12*)	21.8 ± 1.6	71.8 ± 12.6	176.3 ± 9.3
CON (*11*)	23.4 ± 3.3	62 ± 11.5	168 ± 10.2

Table 4.1 Participants demographics. Values are reported as mean ± SD. FAT: Fatigue, CON: Control.

Apparatus

Experiments were carried in the local Biomechanics laboratory, equipped with a floor-embedded force plate (model OR-5, AMTI, USA; size: 90 x 90 cm) for the recording of the three components of the ground reaction forces (GRFs). An Arduino One microcontroller was used to control power supply of two cylindrical electromagnets via a button-shaped switch. A square-like signal generated by the Arduino board when the switch was activated, was fed back to the data acquisition system (hardware: MX Control, VICON, Oxfordshire, UK) and used as the trigger

to start data acquisition and align the signals in Vicon Nexus software (Nexus 2, version 2.12, Vicon Motion Systems ltd, UK).

A customized frame equipped with a uniaxial strain-gauge force sensor (Model S-AL-A, Deltatech, Sogliano al Rubicone, Italy) was used during the *localized isometric exercise* (see dedicated paragraph) to measure isometric force in ankle dorsiflexion. Force data were collected using a computer-based data acquisition and analysis system (hardware: PowerLab 16/30; ML880, ADInstruments, Colorado Springs, CO and software: LabChart 8, ADInstruments, Colorado Springs, CO) at 1000 Hz sampling rate.

GRF Kinetics data were sampled at 2000 Hz and synchronized using a hardware device (MX Control, VICON, Oxfordshire, UK). Data were later exported to Matlab software (R2023a, version 9.14.0, MathWorks, Natick, MA, USA) for offline analysis.

Study Design

Participants were randomly assigned to the fatigue (FAT) or control (CON) group before being admitted to the study, and fatigue group was tested before control group (details in *Localized Isometric Exercise*). Participants were asked to visit the laboratory for two consecutive experimental sessions (*Day1*, *Day2*), lasting ~3 hours each. Visits were scheduled with a 48–72-hour interval to avoid accumulation and/or long-lasting effects of fatigue. During each session, participants were exposed to the same paradigm of mechanical perturbation to the standing posture. During the first visit, participants were granted – based on pilot tests – 40 trials of familiarization with the task.

Postural task

Participants were asked to stand barefoot at the center of the laboratory ground-embedded force plate with their knees slightly bent and feet in parallel at hip width. Feet position was marked on the surface of the force plate to ensure consistency across the trials. A 22-inch monitor positioned ~1.8 m in front of the participants was used to provide visual feedback. Participants held a horizontal handle bar at mid-chest level, with their elbows fully extended. The handle was connected to an adjustable system consisting of iron cables and pulleys, that allowed to connect two

mechanical loads: one in front of the participant and the other was behind the participant's body (Figure 4.1, Panel A). At both ends of the inextensible iron cables, cylindrical electromagnets were used to connect with pre-assembled load plates. Load plates were "blinded" to the participants by a tissue masking that covered the volume and prevented from the visualization of the contained loads. Handle bar was equipped with a button-shaped switch that was connected to a controller (Arduino Uno): its press turned off the electromagnet in front of the participant, causing the release of the load and leading to a mechanical perturbation in the opposite direction (i.e., the handle bar was pulled backwards). Both loads were equivalent in weight, having no effects on posture when the system was in balance. Height of the structure was adjusted to participant's height to have the pulley system acting at mid-chest level and to have the feedback monitor at participant's eye level. The mechanical perturbation paradigm was developed based on a modified version of the setup used in a recent study (Piscitelli et al., 2017).

A calibration trial was conducted at the very beginning of each session to determine the average COP position in the anteroposterior direction (COP_{AP}) during natural standing. Participants were asked to stand and fixate a point on the screen, hands were positioned on the handle with arms fully extended and parallel to the ground. COP_{AP} position was recorded for 5 seconds, visually inspected offline to control for abnormal spikes and then averaged for the entire time window. This value ($COP_{AP\text{-}Target}$) was then saved and used 1) to set the zero target for the online visual feedback in the successive postural task and 2) to normalize COP position data during offline analysis of the trials.

During postural task, participants were cued to assume the starting position (hands on the handle, arms fully extended, knees slightly bent). $COP_{AP\text{-}Target}$ was projected on the screen as a thin white horizontal line enclosed by a ±2 cm green-shaded area. Real-time COP_{AP} position was superimposed on the screen by means of a thick, horizontal blue line. Participants were aware of the nature of the feedback and were instructed to maintain their COP_{AP} within the green-shaded area. After a "ready" cue, the feedback was turned off following a random delay and participants were required to press as fast as possible the switch that released the load. Visual representation of participant's COP_{AP} displacement from $COP_{AP\text{-}Target}$ was provided

right after the trial termination ($COP_{feedback}$). Value (cm) and sign of the COP_{AP} error was reported by an arrow superimposed on the $COP_{AP\text{-}Target}$ (Figure 4.1, Panel A). If the error was within $COP_{AP\text{-}Target}$ ±2 cm (green-shaded area), values and arrow were shown in black color, otherwise the display color was red. Data were collected for a 4-s window centrally aligned on the instant the switch was pressed (*t0*; i.e., 2 seconds before/after pressing the button). $COP_{feedback}$ was automatically computed by a customized script in MATLAB (R2018a, version 9.4; MathWorks Inc., MA, Natick, USA) which was developed to access real-time COP data through Nexus SDK files. When trial acquisition ended and the file was saved, offline COP_{AP} displacement computation was performed ($COP_{feedback} = COP_{AP} - COP_{AP\text{-}Target}$). Participant's goal was to minimize COP_{AP} displacement. Average trial duration was ~10 seconds.

Participants were given 40 familiarization trials to understand the task and stabilize their performance, immediately followed by the first experimental block (trials n = 30; *baseline*). During these trials the loads in the plates were set to 4% of participant's body weight (BW). Following baseline block, each successive block was preceded by a protocol of isometric exercise (details in *Localized Isometric Exercise*). During the trials in the successive six blocks (*adaptation*), another set of loads (8% of participant's BW) were used, without participants awareness of the change. During the final two blocks (*washout*) loads were switched back to initial values (4% BW). The choice of loads in percentage to BW was done to control the amount of perturbation and scale it to BW-differences among participants. Percentage values are chosen to produce a consistent, yet controllable perturbation, based on pilot tests where multiple combinations were tested. Sessions were identical in structure, except for familiarization, which was performed only at *Day1*. An outline of the experimental protocol is shown in Figure 4.1 (Panel C).

Localized isometric exercise

Participants seated on a customized height-adjustable wooden-box with their feet fastened to a customized metal frame through two adjustable, inextensible straps, placed proximal to the metatarsophalangeal joints Figure 4.1(Panel B). Knee and ankle joint angles were maintained at approximately 90° and 110°, respectively and the position did not change throughout the exercise. To avoid the involvement of

other postural and upper limb muscles, participants were not allowed to hold or use their hands. Sustained, cyclical isometric exercise protocol for *Day1* was based on our previous study (Study 2), where it has already been detailed (CHAPTER 2).

In the present study, real-time visual feedback of their force throughout the exercise was provided through a 22-inch monitor ~1.5 m in front of participants, connected to the computer-based data acquisition software (LabChart 8, ADInstruments, Colorado Springs, CO). Time and force values on the axes were removed to ensure participants did not try to use pacing strategies.

Exercise time in the FAT group was averaged within each bout (each exercise in-between blocks of postural task) and rounded up to the nearest cycle (40s). These averaged exercise bout durations were successively used to stop participants in the CON group. Participants in both groups were stopped by the experimenter and were blind to exercise intensity (%MVC), termination criteria and exercise bouts duration. Transition time between protocols (i.e., from isometric exercise to postural task) was minimized (<15s).

During *Day2*, the exercise intensity was the same in both groups (7.5 ± 5% MVC). Exercise durations were based on individual values during *Day1* for participants in FAT group, whereas for CON, the same *Day1* group-averaged values were used.

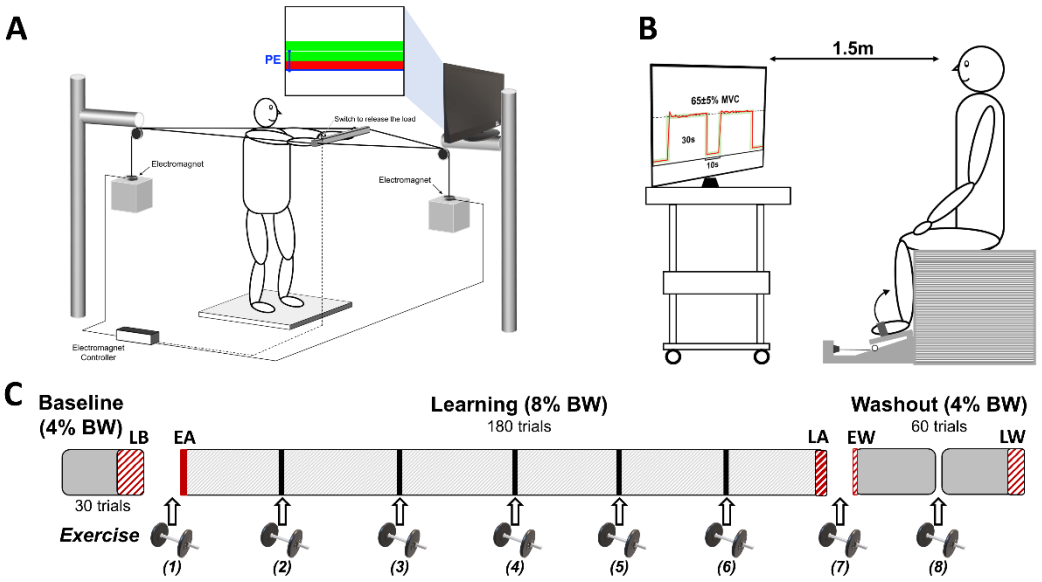

*Figure 4.1 Schematic representation of the experimental setup. **A**. Illustration of the postural task. Grey boxes represent the mechanical load released by the electromagnets through a switch on the handle. The upper box represents a typical feedback of performance error (PE) after the execution of a trial. **B**. Isometric exercise setup illustration. Knee and ankle joint angles were kept ~90° and*

110° throughout the exercise. Visual feedback of the real-time isometric force production was provided by a monitor through a dedicated software by means of a green-shaded area between two horizontal lines, corresponding to the required force target (FAT= 65±5%, CON= 7.5±5% MVC). ***C****. Schematic outline of the experiment: baseline phase consisted in 30 postural trials with loads corresponding to 4% of participant's bodyweight (BW), learning phase consisted of 180 trials with load increased to 8% BW. Trials were divided into 6 blocks of 30 trials and washout phase consisted in 60 trials identical to baseline (2 x 30 trials). After baseline phase, each of the following blocks was preceded by a bout of isometric exercise (represented by a dumbbell in the graph), where the intensity (%MVC) varied between groups only for the first session (Day 1)(see: Localized isometric exercise in the text). Experimental phases used in the analyses to compare variables are highlighted in red: LB= late baseline (last 10 trials of baseline phase), EA= early adaptation (1st trial of learning phase), LA= late adaptation (last 5 trials in the adaptation phase), EW= early washout (1st trial of washout phase), LW= late washout (last 5 trials of washout phase). The two experimental sessions differed only for the exercise intensity (set to 7.5% MVC for both groups in Day2).*

Data analysis

Datasets were preprocessed and analyzed in MATLAB software (R2023a, version 9.14). GRFs and COP signals were preprocessed using a 15 Hz low-pass, 6^{th} order, zero-phase digital Butterworth filter.

Performance and postural variables

Center of pressure (COP) two-dimensional coordinates were computed from GRF and force moments of the force plate. Participant's $COP_{AP\text{-}Target}$ value – computed during calibration trial – was subtracted from COP coordinates in the anteroposterior direction (COP_{AP}).

COP performance error (PE) was computed from COP_{AP} data as the peak, signed value of COP_{AP} over a 1- second window after the release of the load (from 500ms to 1.5 s after *t0*). The same window was used to provide feedback at the end of each trial during the experiment ($COP_{feedback}$) and was defined based on pilot tests. We excluded the first 500 ms from the analysis of PE to facilitate the detection by the algorithm, since in pilot tests data there was a clear anticipatory phase shifting the COP forward within that time window (see Figure 4.2). The trailing 500 ms window of each trial was excluded to avoid slow postural movements not related to the perturbation.

Savings and adaptation rate

We calculated the movement onset of COP_{AP} (COP_{onset}) from its position data as the instant in time when magnitude of COP_{AP} crossed 5% of its maximal value (Cesari et al., 2022). Resulting COP_{onset} were then visually inspected and

confirmed. Values of COP_{onset} are reported respect to *t0* (i.e., negative values represent anticipation of COP movement respect to perturbation).

Individual values of PE and COP_{onset} during the first adaptation block (n = 30 points) were also fitted by a 2-terms exponential function (command: *fit(x,y,'exp2')* in Matlab software) to obtain fitting coefficients and then compared between group and sessions.

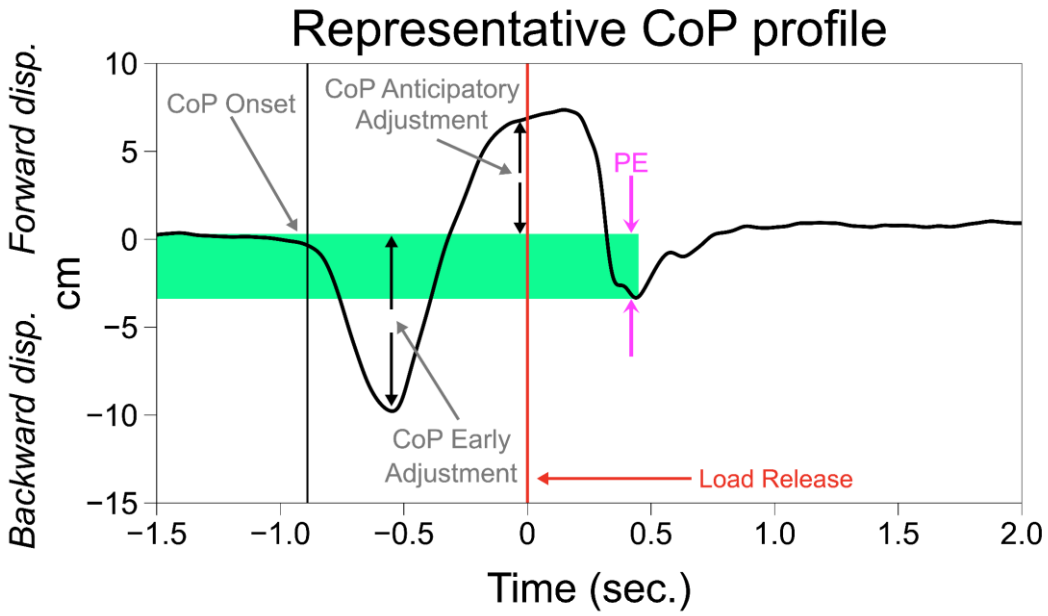

Figure 4.2 Representative profile of Center of pressure coordinates in the anteroposterior direction COP_{AP} during standing perturbation in learning phase. Green shaded area represents the target value of COP, set during the calibration trial ($COP_{AP\text{-}Target}$). Starting from left side, grey lines and arrows display the instant the COP starts moving to prepare for perturbation (vertical line, COP_{onset}), the early adjustment in COP profile (compatible with EPA activity in EMGs) and the COP anticipatory adjustment (compatible with APA activity in EMGs). Magenta-colored line and arrow represents the performance error for the trial. Time 0 (t0) represents the instant of load release.

Statistical analysis

Jamovi statistical software (The jamovi project (2023). jamovi (Version 2.3.28) [Computer Software]. Retrieved from https://www.jamovi.org) was used for all statistical analyses. All data in the text, Tables, and Figures – unless otherwise stated – are presented as mean ± 1 standard deviation (SD). Critical p value was set at an α of 0.05 for all the comparisons. Data distribution (skewness and kurtosis) was assessed, the normality of the data was assessed by the Shapiro–Wilk test and confirmed by the inspection of density and Q–Q plots. When normality assumption

was violated, non-parametric statistical tests were performed (Friedman's test with pairwise Durbin-Conover comparisons) Successively, non-parametric independent samples t-test (Welch-test) was used for pairwise comparisons.

To test the effects of the isometric exercise protocol, group differences in MVC changes from initial (pre-exercise) to final (post-exercise) were assessed using a two-way mixed-design ANOVA (group–time) within each session. To test the effects of fatigue on the adaptation process, a three-way mixed-design ANOVA (*Phase* and *Day* as a repeated measure factors) was used to assess group differences in performance and postural variables across the three experimental *Phases* (three levels: LB, EA, LA) and *Sessions* (two levels: *Day1*, *Day2*). Similarly, to test the effects of fatigue on the washout process, a three-way mixed-design ANOVA (*Phase* and *Session* as a repeated measure factors) was used to assess *Group* (two levels: *Fatigue, Control*) differences in performance and postural variables across three experimental *Phases* (three levels: LB, EW, LW) and sessions (*Day1*, *Day2*). Assumptions of sphericity were confirmed by Mauchly's test and controlled for using the Greenhouse–Geisser adjustment in instances where the test was significant ($\alpha < 0.05$) and relative corrected degrees of freedom (DOF) are reported in results. In the event of a significant interaction or main effect, post hoc comparisons were performed using Holm-Bonferroni correction. Non-parametric independent-sample t-tests (Welch-test) were used to assess pairwise differences if Levene's test revealed unequal variance.

To test for savings, PE fitting coefficients and their 95% C.I. were compared between groups (*Fatigue, Control*) and sessions (*Day1, Day2*). When C.I.s did not overlap, differences were considered significant. For COP_{onset}, we computed the time constant of adaptation (tk), defined as the trials required for the COP_{onset} to drop by 63% (similarly to (Takahashi et al., 2006).

RESULTS

Isometric force

Isometric exercise duration across bouts was on average 4:45 ± 0:53 min:s (number of cycles: 7.1 ± 1.3), with a trend for a reduction across bouts (bout1: 5:58 ± 1:47 min:s, bout2: 5:07 ± 1:52 min:s, bout3: 5:40 ± 2:51 min:s, bout4: 4:43 ± 2:45 min:s,

bout5: 3:50 ± 1:39 min:s, bout6: 4:13 ± 2:55 min:s, bout7: 3:40 ± 1:49 min:s). Maximal voluntary contraction (MVC) isometric force prior to the exercise did not differ between groups (FAT: 250.8 ± 83.7 N, CON: 251.9 ± 91.6 N; p>.05). The fatiguing exercise led to a significant drop in tibialis anterior MVC isometric force for Fatigue group at *Day1*, and no differences in both groups at *Day2* (*Day1:* FAT: -32 ± 4%, CON: 1 ± 3%, p<.001; *Day2*: FAT: -0.8 ± 2.2%, CON: 0.4 ± 2.3%, p>.05). Figure 4.3 shows pre-post exercise difference in isometric force (calculated as the difference from the mean force during 1st cycle to the force during last cycle of each bout) for each session (*Day1, Day2*).

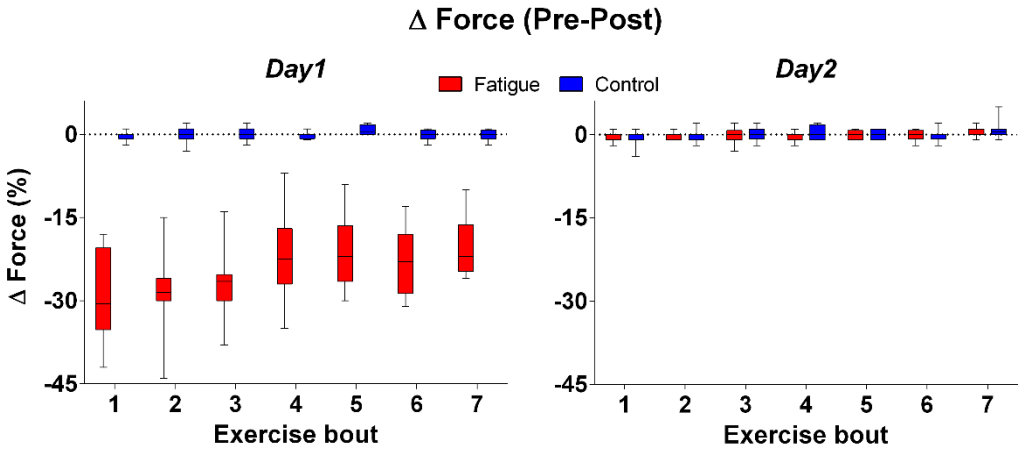

Figure 4.3 Differences in isometric force (expressed as %) from the first to the last exercise cycle within each bout. Data in box-plots represent 5th – 95th percentiles of values and median is marked by the horizontal black line. Left panel shows values for the first experimental session (Day1), right panel shows values for the second session (Day2).

Performance and postural variables

Participants in both groups exhibited consistent adaptation curves in performance error (PE), showing a clear reduction in PE across blocks and also a visible saving effect during Day 2 (Figure 4.4).

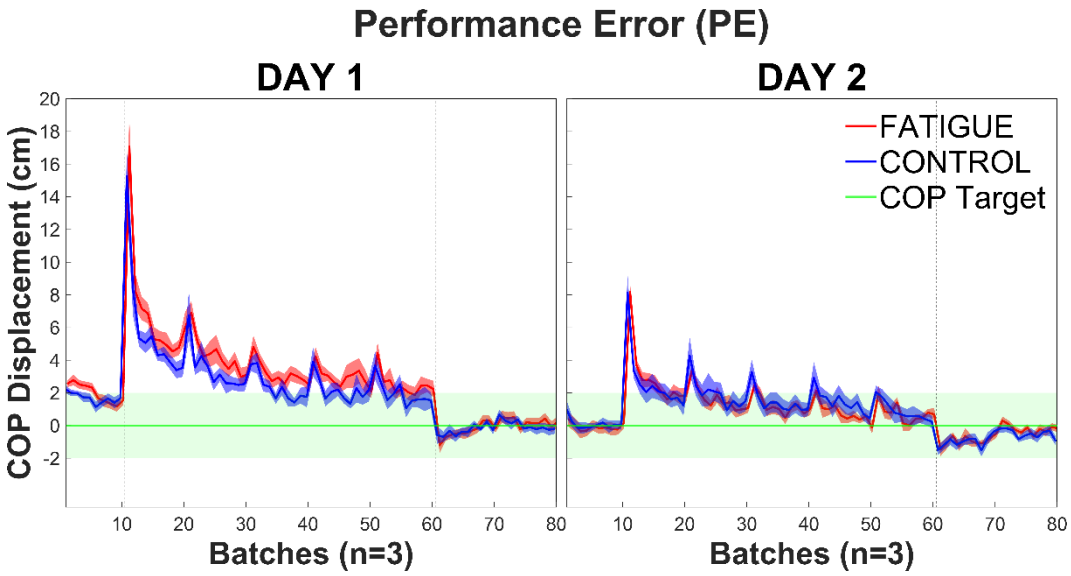

Figure 4.4 Performance error (PE) averaged over batches of n=3 trials across the whole experiment. Blue and red lines with shaded errors represent CON and FAT group average ±1 standard error (SE), respectively. Positive values represent a backward displacement. Vertical thin dashed lines represent changes in experimental phases (baseline – learning – washout). The green solid line represents individual $COP_{AP\text{-}target}$) and its shade represents ±2 cm.

Short-term effects of neuromuscular fatigue on motor adaptation (Day1)

Results for performance error (PE) across all the experimental phases and sessions are illustrated in Figure 4.5. The mixed design ANOVA found significant main effects for factors *Session* ($F_{1,23} = 32.664$, $p < .001$, $\eta^2 = 0.047$) and *Phase* ($F_{2,42} = 232.504$, $p < .001$, $\eta^2 = 0.692$). Significant interactions were also found for *Phase*Day* ($F_{2,42} = 15.166$, $p < .001$, $\eta^2 = 0.046$). Pairwise post-hoc contrasts using Holm correction found significant differences between Phases across sessions ($p < 0.05$, Figure 4.5).

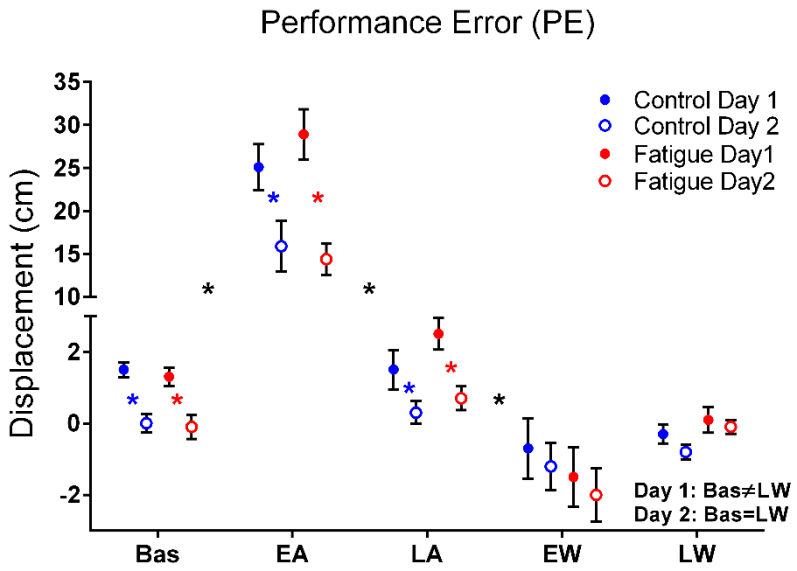

*Figure 4.5 Results for performance error (PE) of COP across the 5 considered experimental phases (Bas – LB, EA, LA, EW, LW). Red circles represent Fatigue group, while blue circles represent Control. Values during Day1 are presented as filled circles, whereas values for Day2 are depicted as empty circles. Circles represent the group mean, while error bars report ± 1 standard error (SE). * significant effects between adjacent phases (p < .05), colored asterisks (*/*) are used to highlight differences between sessions (Day1 vs Day2).*

Results for onset of COP anticipation (COP_{onset}) across all the experimental phases and sessions are illustrated in Figure 4.6. The mixed design ANOVA found significant main effects for factors *Session* ($F_{1,23} = 22.142$, $p < .001$, $\eta^2 = 0.044$) and *Phase* ($F_{2,42} = 22.586$, $p < .001$, $\eta^2 = 0.231$). Significant interactions were also found for *Phase*Day* ($F_{2,42} = 3.47$, $p = .022$, $\eta^2 = 0.012$). Pairwise post-hoc contrasts using Holm correction found significant differences between Phases across sessions ($p < 0.05$, Figure 4.6).

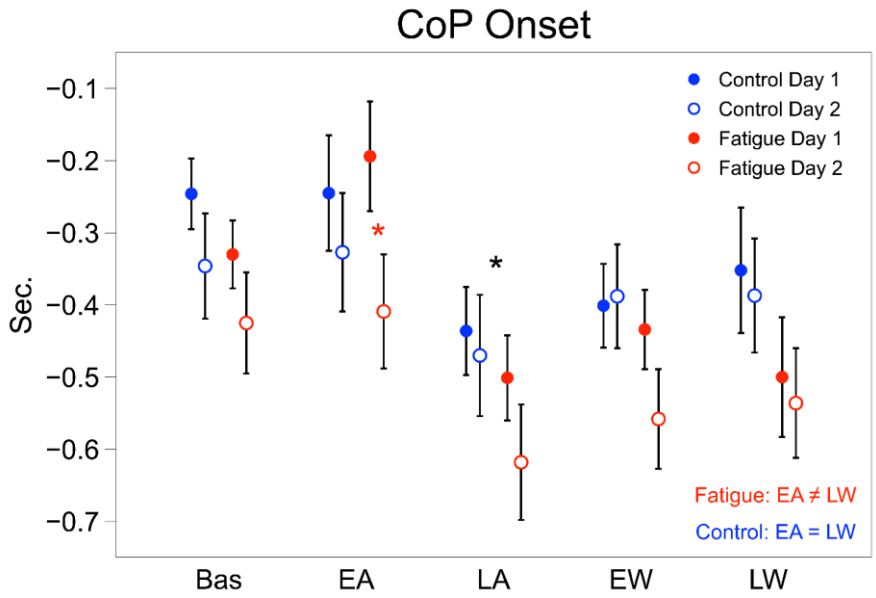

*Figure 4.6 Results for CoP onset across the 5 considered experimental phases (Bas – LB, EA, LA, EW, LW). Red circles represent Fatigue group, while blue circles represent Control. Values during Day1 are presented as filled circles, whereas values for Day2 are depicted as empty circles. Circles represent the group mean, while error bars report ± 1 standard error (SE). * significant effects between adjacent phases (p < .05), colored asterisks (*/*) are used to highlight differences between sessions (Day1 vs Day2).*

Long-term effects/Savings – Day2

Savings in PE and COP_{onset} were assessed by means of a two-term exponential curve-fitting, using the averaged values during the first block (n=30 points) for each group and session separately (Figure 4.7 and Figure 4.8, respectively). Coefficients of determination (R^2) of the exponential fittings were >0.94 for each group and session ($p < .001$). The coefficients, with their 95% confidence of intervals, were then compared and considered to differ when they did not overlap. The second coefficient was significantly lower (more negative – meaning a faster re-learning) during *Day2*, compared to *Day1* in control group (Coefficient "b" in Figure 4.9). A similar difference was seen in COP_{onset} time-constant of decay (tk; Figure 4.8), where tk for Control group, on average was lower (less trials needed to drop by 63%) and further reduced during second exposure (Day2; Figure 4.8 – Right panel). The results are in accordance with the profile of group averaged trials across phases and sessions (Figure 4.10), where a more evident shift in the profile is seen in Control group.

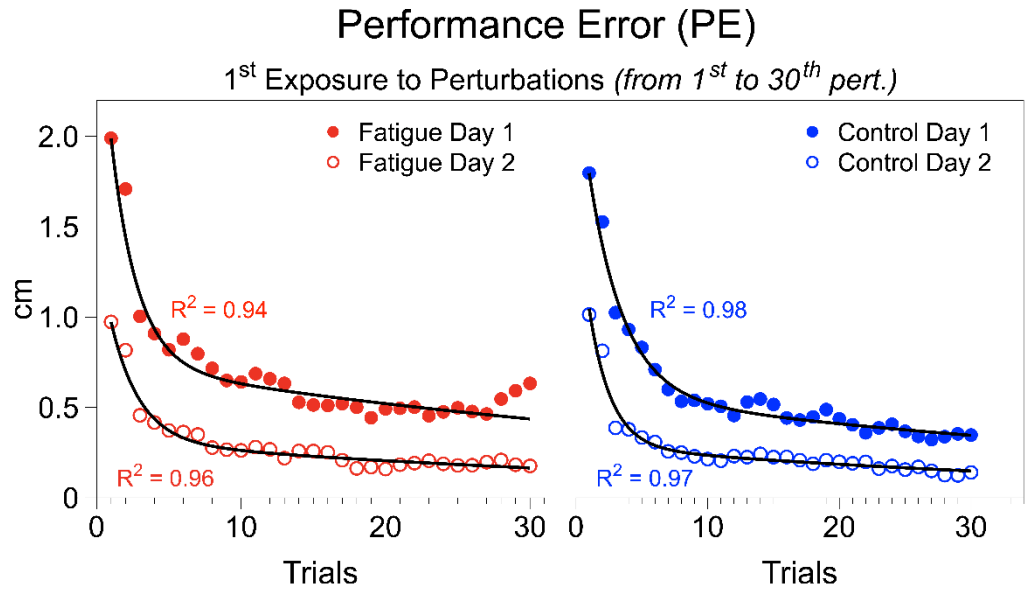

Figure 4.7 Exponential fitting results for PE in each group and session separately. Red circles represent Fatigue group, while blue circles represent Control. Values during Day1 are presented as filled circles, whereas values for Day2 are depicted as empty circles. Circles represent the averaged values trial-wise for each group. Coefficients of determination (R^2) are reported in the graphs ($p < .001$).

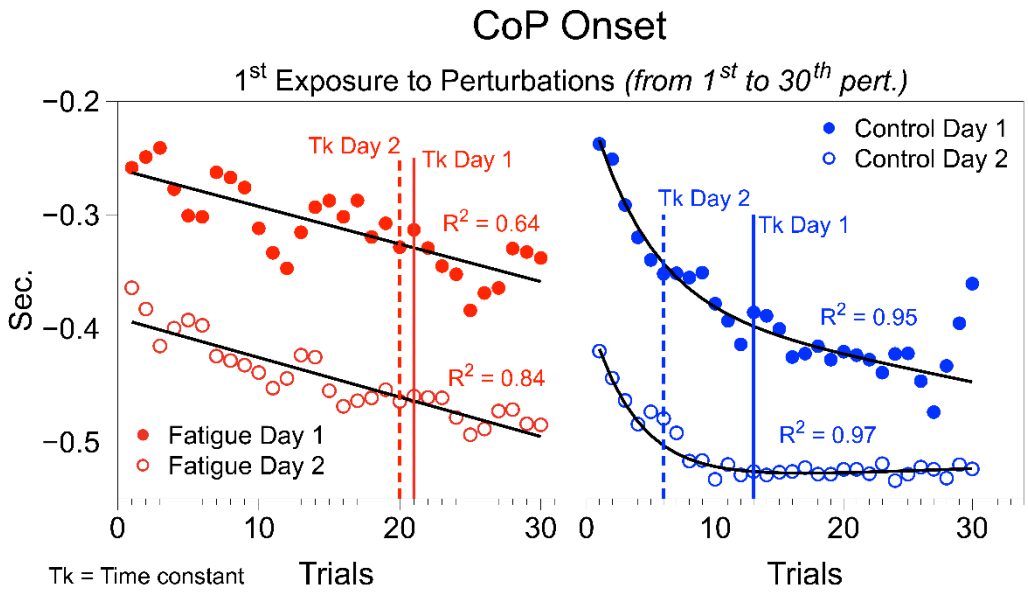

Figure 4.8 Exponential fitting results for COP_{onset} in each group and session separately. Red circles represent Fatigue group, while blue circles represent Control. Values during Day1 are presented as filled circles, whereas values for Day2 are depicted as empty circles. Circles represent the averaged values trial-wise for each group. Coefficients of determination (R^2) are reported in the graphs ($p < .001$). Vertical solid and dashed lines represent the time-constant of decay in COP_{onset} values for Day1(Tk Day 1) and Day2 (Tk Day 2), respectively.

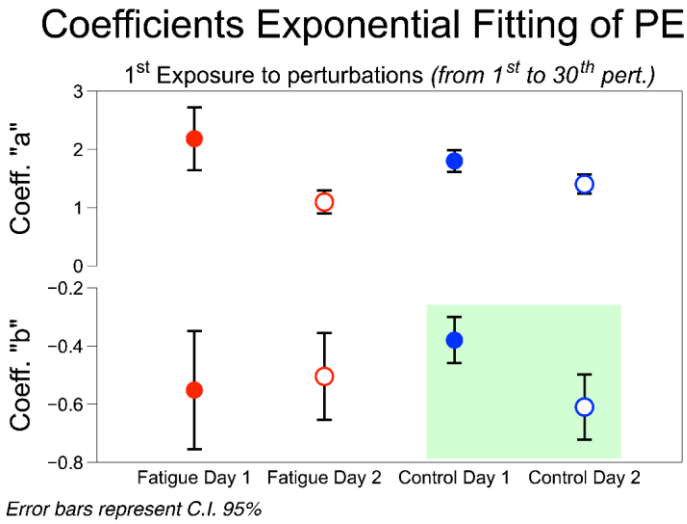

Figure 4.9 Exponential fitting coefficients for PE in each group and session separately. Red circles represent Fatigue group, while blue circles represent Control. Values during Day1 are presented as filled circles, whereas values for Day2 are depicted as empty circles. Highlighted in green-shaded box the difference in Control group for the second fitting coefficient "b".

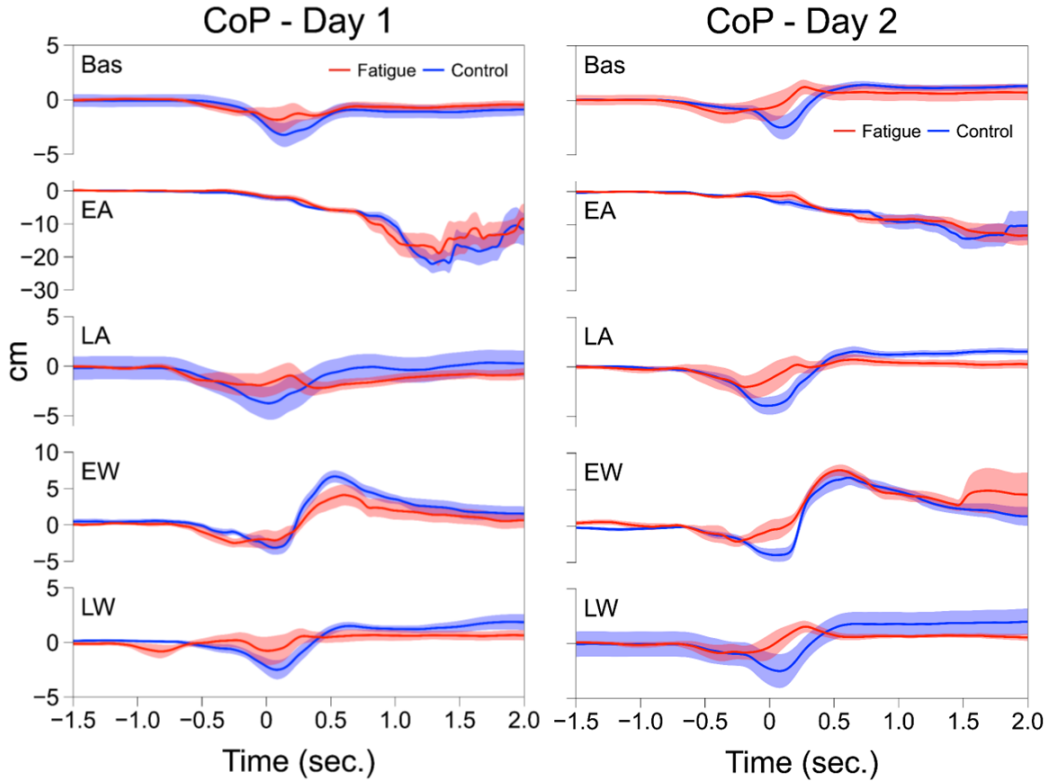

Figure 4.10 Group-averaged profiles of COP_{AP} during each experimental phase in each session. Red solid lines represent Fatigue group average, while blue solid lines represent Control. Left panel: profiles during Day1. Right panel: values during Day2. Negative values represent backward displacement of COP.

DISCUSSION

Overall, the study findings partially confirm our hypotheses. Conversely to what we hypothesized, performance error (PE) followed the same trends in Control and Fatigue groups (Figure 4.4 and Figure 4.5), and we found no significant differences between groups across the experimental phases. Results are in line with a previous study in the field (Takahashi et al., 2006). Even though the same results seem in contrast to previous results using a force-field adaptation paradigm (Study 2), the peculiar nature of the performance variable itself – dynamic control of the COP position – might have reduced group differences. Similarly, a recent study found no effects of neuromuscular fatigue on dynamic maintenance of balance, despite differences in lower limb EMG activation (Marcolin et al., 2022). We interpret these findings as the evidence that the CNS is efficiently able to adapt to a mechanical perturbation and maintain postural stability even in the case of a physiologically perturbed state such as localized NMF, which alters muscle properties, perception of effort and proprioceptive feedback loops (Taylor et al., 2000; Gandevia, 2001). Potentially, this mechanism is driven by a reorganization at the level of the descending motor command from CNS to muscles, as already demonstrated in previous studies (Strang et al., 2009; Singh et al., 2010; Singh and Latash, 2011). We recently observed that NMF affects the adaptation processes by inducing remodulation in EMG activation patterns in both fatigued and non-fatigued postural muscles, to stabilize reaching performance (*Study 2*). Similar results have been reported in other studies in motor learning field (Takahashi et al., 2006; Branscheidt et al., 2019). Recent evidence from Branscheidt et al. suggested that NMF not only negatively affects motor skill learning at the moment they are acquired, but also induced long-lasting detrimental changes (Branscheidt et al., 2019). The main limitation in that study is that the fatigued muscle was also directly involved in the movement execution, making it hard to discern peripherally-mediated from centrally-mediated (Gandevia, 2001) causes of these long-lasting changes. Furthermore, due to the transient nature of the NMF physiological phenomenon, a standardized and cyclical protocol would benefit the replicability of results, trying to control for a "minimal" level of NMF. For this reason, in our study we chose to induce localized fatigue through multiple exercise bouts in

postural muscles in the lower limbs, which are essential for standing postural control.

Considering the other focus of this study, NMF affected savings and adaptation rate during a second re-exposure to the task in a non-fatigued state (*Day2*), confirming our second hypothesis. Both performance error (PE) and COP_{onset} variables demonstrate a clear savings effect (Figure 4.5 and Figure 4.6), in line with similar studies in the field (Huang et al., 2011; Coltman et al., 2019; Krakauer et al., 2019). PE showed a significant reduction of the error between *Day1* and *Day2* at all the stages during adaptation phase (Figure 4.5), and a similar trend was appreciable for COP_{onset} (Figure 4.6). Adaptation rate of PE and COP_{onset}, assessed by comparing and PE fitting coefficients and COP_{onset} slopes during first-exposure blocks (Takahashi et al., 2006) (Figure 4.7 and Figure 4.8), demonstrated a slower adaptation process during *Day2* for Fatigue group. Our results are in accordance with that of a previous study, where NMF caused detrimental effects on long-term recall of motor-skills learning (Branscheidt et al., 2019). We suggest that the inefficient sensorimotor integration when learning in a fatigued condition (Takakusaki et al., 2017) negatively affected the performance retention at the second exposure (*Day2*), through the generation/update of suboptimal internal models (Takahashi et al., 2006; Monjo et al., 2015). Finally, it appears that adapting a movement in a fatigued state affects the following long-term recall of the same performance, even in the absence of neuromuscular fatigue. These findings are in line and confirm previous work by Branscheidt et al. (Branscheidt et al., 2019), this time using a novel, whole-body postural perturbation mechanism. Results have potential implications in the context of skill learning in sports and even in rehabilitation settings, when dealing with specific populations experiencing higher presence of fatigue and/or fatigability (Brunton and Rice, 2012; Brownstein et al., 2022).

CHAPTER 5 – SUMMARY AND FINAL CONCLUSIONS

Highlights

- Central nervous system (CNS) mechanisms seem capable of efficiently compensating for different fatiguing modalities.
- CNS adopts different strategies of agonist-antagonist muscle-pairs activation, depending on the fatiguing modality.
- During motor adaptation, localized neuromuscular fatigue (NMF) seems to modify CNS strategy for counteracting a postural perturbation, possibly by increasing motor exploration in order to attain successful performance.
- Localized NMF in the course of adaptation demonstrated long-term effects on retention and adaptation rate during a second exposure to the task.

Overall discussion and conclusions

Overall, the findings of the three studies suggest that CNS effectively controls and reorganizes motor outputs to counteract NMF. This process works to stabilize salient performance or postural variables during several tasks (Ambike et al., 2016; Madarshahian and Latash, 2021; Nardon et al., 2022). However, this strategy is not always optimal, such as in motor learning. Performing a task when a muscle is fatigued could have detrimental effects on immediate performance (Strang et al., 2009; Paillard, 2012). This is especially true when the parameters of the task are still partially unknown and motor learning processes are ongoing (Herzfeld et al., 2014; Krakauer et al., 2019). It has been suggested that NMF might affect long-term performance by the formation of novel, suboptimal internal model of the task while practicing it in a fatigued state (Takahashi et al., 2006). In our studies we showed that the CNS adopts different strategies depending on the type of fatiguing exercise (Study 1), suggesting that these adaptation processes are centrally mediated. Furthermore, when localized NMF is present, not only adaptation seemed slower and incomplete, but the whole EMG activation patterns of postural and agonist muscle for the task was altered and reorganized (Study 2). The reorganization of muscle activity occurs at the level of individual muscles and is

reflected in agonist-antagonist muscles coupling at joint level, both in fatigued and non-fatigued muscles. Especially, NMF decreased co-activation of muscles and reorganized motor output to other, non-fatigued muscles, in accordance with previous works (Strang et al., 2009; Singh et al., 2010; Singh and Latash, 2011). In terms of long-lasting effects, few studies investigated the role of NMF on savings and retention processes (Takahashi et al., 2006; Branscheidt et al., 2019), with some limitations in the protocols. Our findings support the idea that learning in a fatigued state increased the boundaries of motor exploration and forces the CNS to adopt strategies to stabilize performance or posture, which appeared to be suboptimal when the physiological state was restored, and participants recovered from fatigue. This study is the first, to the best of our knowledge, that tried to address these aspects with a broader point of view and tried to standardize the presence of NMF throughout the protocol. Possible practical implications of these findings encompass sport skills learning, physical rehabilitation from injuries, but also working settings and neuromuscular disorders. In fact, each of the mentioned fields, everyday faces challenges of learning, adapting or re-learning new skills, actions and procedures in potentially fatiguing conditions.

REFERENCES

Adkin AL, Frank JS, Carpenter MG, Peysar GW (2002) Fear of falling modifies anticipatory postural control. Exp Brain Res 143:160–170.

Ahmed AA, Wolpert DM (2009) Transfer of dynamic learning across postures. J Neurophysiol 102:2816–2824.

Amann M, Venturelli M, Ives SJ, McDaniel J, Layec G, Rossman MJ, Richardson RS (2013) Peripheral fatigue limits endurance exercise via a sensory feedback-mediated reduction in spinal motoneuronal output. J Appl Physiol Bethesda Md 1985 115:355–364.

Ambike S, Mattos D, Zatsiorsky VM, Latash ML (2016) Synergies in the space of control variables within the equilibrium-point hypothesis. Neuroscience 315:150–161.

Aruin AS, Forrest WR, Latash ML (1998) Anticipatory postural adjustments in conditions of postural instability. Electroencephalogr Clin Neurophysiol 109:350–359.

Aruin AS, Latash ML (1995) The role of motor action in anticipatory postural adjustments studied with self-induced and externally triggered perturbations. Exp Brain Res 106:291–300.

Bastian AJ (2008) Understanding sensorimotor adaptation and learning for rehabilitation. Curr Opin Neurol 21:628–633.

Belen'kiĭ VE, Gurfinkel' VS, Pal'tsev EI (1967) [Control elements of voluntary movements]. Biofizika 12:135–141.

Bertucco M, Cesari P (2010) Does movement planning follow Fitts' law? Scaling anticipatory postural adjustments with movement speed and accuracy. Neuroscience 171:205–213.

Bertucco M, Nardello F, Magris R, Cesari P, Latash ML (2021) Postural Adjustments during Interactions with an Active Partner. Neuroscience 463:14–29.

Bigland-Ritchie B, Furbush F, Woods JJ (1986) Fatigue of intermittent submaximal voluntary contractions: central and peripheral factors. J Appl Physiol 61:421–429.

Branscheidt M, Kassavetis P, Anaya M, Rogers D, Huang HD, Lindquist MA, Celnik P (2019) Fatigue induces long-lasting detrimental changes in motor-skill learning. eLife 8:e40578.

Bridgeman B (1995) A review of the role of efference copy in sensory and oculomotor control systems. Ann Biomed Eng 23:409–422.

Brownstein CG, Twomey R, Temesi J, Medysky ME, Culos-Reed SN, Millet GY (2022) Mechanisms of Neuromuscular Fatigability in People with Cancer-Related Fatigue. Med Sci Sports Exerc 54:1355–1363.

Brunton LK, Bartlett DJ (2017) Construction and validation of the fatigue impact and severity self-assessment for youth and young adults with cerebral palsy. Dev Neurorehabilitation 20:274–279.

Brunton LK, Rice CL (2012) Fatigue in cerebral palsy: A critical review. Dev Neurorehabilitation 15:54–62.

Carroll TJ, Taylor JL, Gandevia SC (2017) Recovery of central and peripheral neuromuscular fatigue after exercise. J Appl Physiol 122:1068–1076.

Cassady K, Ruitenberg M, Koppelmans V, Reuter-Lorenz P, De Dios Y, Gadd N, Wood S, Riascos Castenada R, Kofman I, Bloomberg J, Mulavara A, Seidler R (2017) Neural predictors of sensorimotor adaptation rate and savings. Hum Brain Mapp 39:1516–1531.

Cesari P, Piscitelli F, Pascucci F, Bertucco M (2022) Postural threat influences the coupling between anticipatory and compensatory postural adjustments in response to an external perturbation. Neuroscience.

Chen B, Lee Y-J, Aruin AS (2015) Anticipatory and compensatory postural adjustments in conditions of body asymmetry induced by holding an object. Exp Brain Res 233:3087–3096.

Chen B, Lee Y-J, Aruin AS (2017) Role of point of application of perturbation in control of vertical posture. Exp Brain Res 235:3449–3457.

Coco M, Di Corrado D, Cirillo F, Iacono C, Perciavalle V, Buscemi A (2021) Effects of General Fatigue Induced by Exhaustive Exercise on Posture and Gait Stability of Healthy Young Men. Behav Sci 11:72.

Coltman SK, Cashaback JGA, Gribble PL (2019) Both fast and slow learning processes contribute to savings following sensorimotor adaptation. J Neurophysiol 121:1575–1583.

Danion P Frederic, Latash P Mark (2010) Motor Control: Theories, Experiments, and Applications. Oxford University Press.

Danna-Dos-Santos A, Slomka K, Zatsiorsky VM, Latash ML (2007) Muscle modes and synergies during voluntary body sway. Exp Brain Res 179:533–550.

Davidson BS, Madigan ML, Nussbaum MA, Wojcik LA (2009) Effects of localized muscle fatigue on recovery from a postural perturbation without stepping. Gait Posture 29:552–557.

Enoka RM, Baudry S, Rudroff T, Farina D, Klass M, Duchateau J (2011) Unraveling the neurophysiology of muscle fatigue. J Electromyogr Kinesiol 21:208–219.

Enoka RM, Duchateau J (2008) Muscle fatigue: what, why and how it influences muscle function: Muscle fatigue. J Physiol 586:11–23.

Feldman AG (1986) Once more on the equilibrium-point hypothesis (lambda model) for motor control. J Mot Behav 18:17–54.

Finsterer J (2012) Biomarkers of peripheral muscle fatigue during exercise. BMC Musculoskelet Disord 13:218.

Gandevia SC (2001) Spinal and supraspinal factors in human muscle fatigue. Physiol Rev 81:1725–1789.

Gribble PA, Hertel J (2004) Effect of lower-extremity muscle fatigue on postural control1. Arch Phys Med Rehabil 85:589–592.

Hermens HJ, Freriks B, Disselhorst-Klug C, Rau G (2000) Development of recommendations for SEMG sensors and sensor placement procedures. J Electromyogr Kinesiol Off J Int Soc Electrophysiol Kinesiol 10:361–374.

Herzfeld DJ, Vaswani PA, Marko MK, Shadmehr R (2014) A Memory of Errors in Sensorimotor Learning. Science 345:1349–1353.

Horak FB, Nashner LM (1986) Central programming of postural movements: adaptation to altered support-surface configurations. J Neurophysiol 55:1369–1381.

Huang VS, Haith A, Mazzoni P, Krakauer JW (2011) Rethinking Motor Learning and Savings in Adaptation Paradigms: Model-Free Memory for Successful Actions Combines with Internal Models. Neuron 70:787–801.

Huberdeau DM, Krakauer JW, Haith AM (2015) Dual-process decomposition in human sensorimotor adaptation. Curr Opin Neurobiol 33:71–77.

Ivanenko Y, Gurfinkel VS (2018) Human Postural Control. Front Neurosci 12.

Jiang P, Chiba R, Takakusaki K, Ota J (2016) Generation of the Human Biped Stance by a Neural Controller Able to Compensate Neurological Time Delay. PLOS ONE 11:e0163212.

Kaewmanee T, Liang H, Aruin AS (2020) Effect of predictability of the magnitude of a perturbation on anticipatory and compensatory postural adjustments. Exp Brain Res 238:2207–2219.

Kanekar N, Santos MJ, Aruin AS (2008) Anticipatory postural control following fatigue of postural and focal muscles. Clin Neurophysiol 119:2304–2313.

Kawato M (1999) Internal models for motor control and trajectory planning. Curr Opin Neurobiol 9:718–727.

Kendall FP (2005) Muscles: Testing and Function with Posture and Pain. Lippincott Williams & Wilkins.

Kennedy A, Guevel A, Sveistrup H (2012) Impact of ankle muscle fatigue and recovery on the anticipatory postural adjustments to externally initiated perturbations in dynamic postural control. Exp Brain Res 223:553–562.

Kim I, Hacker E, Ferrans CE, Horswill C, Park C, Kapella M (2018) Evaluation of fatigability measurement: Integrative review. Geriatr Nur (Lond) 39:39–47.

King B, Fogel S, Albouy G, Doyon J (2013) Neural correlates of the age-related changes in motor sequence learning and motor adaptation in older adults. Front Hum Neurosci 7.

Kitaoka K, Ito R, Araki H, Sei H, Morita Y (2004) Effect of mood state on anticipatory postural adjustments. Neurosci Lett 370:65–68.

Kluger BM, Krupp LB, Enoka RM (2013) Fatigue and fatigability in neurologic illnesses: Proposal for a unified taxonomy. Neurology 80:409–416.

Krakauer JW, Ghez C, Ghilardi MF (2005) Adaptation to visuomotor transformations: consolidation, interference, and forgetting. J Neurosci Off J Soc Neurosci 25:473–478.

Krakauer JW, Hadjiosif AM, Xu J, Wong AL, Haith AM (2019) Motor learning. Compr Physiol 9:613–663.

Krishnan V, Kanekar N, Aruin AS (2012) Anticipatory postural adjustments in individuals with multiple sclerosis. Neurosci Lett 506:256–260.

Laginestra FG, Amann M, Kirmizi E, Giuriato G, Barbi C, Ruzzante F, Pedrinolla A, Martignon C, Tarperi C, Schena F, Venturelli M (2021) Electrically induced quadriceps fatigue in the contralateral leg impairs ipsilateral knee extensors performance. Am J Physiol-Regul Integr Comp Physiol 320:R747–R756.

Latash ML (2018) Muscle coactivation: definitions, mechanisms, and functions. J Neurophysiol 120:88–104.

Lyu H, Fan Y, Hao Z, Wang J (2021) Effect of local and general fatiguing exercises on disturbed and static postural control. J Electromyogr Kinesiol 56:102487.

Lyu H, Fan Y, Hua A, Cao X, Gao Y, Wang J (2022) Effects of unilateral and bilateral lower extremity fatiguing exercises on postural control during quiet stance and self-initiated perturbation. Hum Mov Sci 81:102911.

Madarshahian S, Latash ML (2021) Synergies at the level of motor units in single-finger and multi-finger tasks. Exp Brain Res 239:2905–2923.

Marcolin G, Cogliati M, Cudicio A, Negro F, Tonin R, Orizio C, Paoli A (2022) Neuromuscular Fatigue Affects Calf Muscle Activation Strategies, but Not Dynamic Postural Balance Control in Healthy Young Adults. Front Physiol 13.

Marcora SM, Staiano W, Manning V (2009) Mental fatigue impairs physical performance in humans. J Appl Physiol 106:857–864.

Martignon C, Laginestra FG, Giuriato G, Pedrinolla A, Barbi C, DI Vico IA, Tinazzi M, Schena F, Venturelli M (2022) Evidence that Neuromuscular Fatigue Is not a Dogma in Patients with Parkinson's Disease. Med Sci Sports Exerc 54:247–257.

Martin K, Meeusen R, Thompson KG, Keegan R, Rattray B (2018) Mental Fatigue Impairs Endurance Performance: A Physiological Explanation. Sports Med 48:2041–2051.

Massion J (1992) Movement, posture and equilibrium: Interaction and coordination. Prog Neurobiol 38:35–56.

McGibbon CA, Krebs DE (2004) Discriminating age and disability effects in locomotion: neuromuscular adaptations in musculoskeletal pathology. J Appl Physiol 96:149–160.

Mezaour M, Yiou E, Le Bozec S (2010) Effect of lower limb muscle fatigue on anticipatory postural adjustments associated with bilateral-forward reach in the unipedal dominant and non-dominant stance. Eur J Appl Physiol 110:1187–1197.

Monjo F, Terrier R, Forestier N (2015) Muscle fatigue as an investigative tool in motor control: A review with new insights on internal models and posture-movement coordination. Hum Mov Sci 44:225–233.

Morris SL, Allison GT (2006) Effects of abdominal muscle fatigue on anticipatory postural adjustments associated with arm raising. Gait Posture 24:342–348.

Nagy E, Toth K, Janositz G, Kovacs G, Feher-Kiss A, Angyan L, Horvath G (2004) Postural control in athletes participating in an ironman triathlon. Eur J Appl Physiol 92:407–413.

Nardon M, Pascucci F, Cesari P, Bertucco M, Latash ML (2022) Synergies Stabilizing Vertical Posture in Spaces of Control Variables. Neuroscience 500:79–94.

Nardon M, Ruzzante F, O'Donnell L, Adami A, Dayanidhi S, Bertucco M (2021) Energetics of walking in individuals with cerebral palsy and typical

development, across severity and age: A systematic review and meta-analysis. Gait Posture 90:388–407.

Nardone A, Schieppati M (1988) Postural adjustments associated with voluntary contraction of leg muscles in standing man. Exp Brain Res 69:469–480.

Nardone A, Tarantola J, Giordano A, Schieppati M (1997) Fatigue effects on body balance. Electroencephalogr Clin Neurophysiol 105:309–320.

Paillard T (2012) Effects of general and local fatigue on postural control: A review. Neurosci Biobehav Rev 36:162–176.

Pascucci F, Cesari P, Bertucco M, Latash ML (2023) Postural adjustments to self-triggered perturbations under conditions of changes in body orientation. Exp Brain Res 241:2163–2177.

Perry J, Burnfield JM (2010) Gait Analysis: Normal and Pathological Function. SLACK.

Pienciak-Siewert A, Horan DP, Ahmed AA (2016) Trial-to-trial adaptation in control of arm reaching and standing posture. J Neurophysiol 116:2936–2949.

Pienciak-Siewert A, Horan DP, Ahmed AA (2020) Role of muscle coactivation in adaptation of standing posture during arm reaching. J Neurophysiol 123:529–547.

Piscitelli D, Falaki A, Solnik S, Latash ML (2017) Anticipatory postural adjustments and anticipatory synergy adjustments: Preparing to a postural perturbation with predictable and unpredictable direction. Exp Brain Res 235:713–730.

Ricotta JM, De SD, Nardon M, Benamati A, Latash ML (2023) Effects of fatigue on intramuscle force-stabilizing synergies. J Appl Physiol Bethesda Md 1985 135:1023–1035.

Sadnicka A, Patani B, Saifee TA, Kassavetis P, Pareés I, Korlipara P, Bhatia KP, Rothwell JC, Galea JM, Edwards MJ (2014) Normal Motor Adaptation in Cervical Dystonia: A Fundamental Cerebellar Computation is Intact. The Cerebellum 13:558–567.

Santos MJ, Kanekar N, Aruin AS (2010a) The role of anticipatory postural adjustments in compensatory control of posture: 1. Electromyographic analysis. J Electromyogr Kinesiol 20:388–397.

Santos MJ, Kanekar N, Aruin AS (2010b) The Role of Anticipatory Postural Adjustments in Compensatory Control of Posture: 2. Biomechanical Analysis. J Electromyogr Kinesiol Off J Int Soc Electrophysiol Kinesiol 20:398–405.

Šarabon N, Mekjavić IB, Eiken O, Babič J (2018) The Effect of Bed Rest and Hypoxic Environment on Postural Balance and Trunk Automatic (Re)Actions in Young Healthy Males. Front Physiol 9.

Schmidt RA (1975) A schema theory of discrete motor skill learning. Psychol Rev 82:225–260.

Scott SH, Cluff T, Lowrey CR, Takei T (2015) Feedback control during voluntary motor actions. Curr Opin Neurobiol 33:85–94.

Singh T, Latash ML (2011) Effects of muscle fatigue on multi-muscle synergies. Exp Brain Res 214:335–350.

Singh T, Skm V, Zatsiorsky VM, Latash ML (2010) Fatigue and Motor Redundancy: Adaptive Increase in Finger Force Variance in Multi-Finger Tasks. J Neurophysiol 103:2990–3000.

Sinha O, Madarshahian S, Gómez-Granados A, Paine ML, Kurtzer I, Singh T (2023) Smooth pursuit eye movements contribute to anticipatory force control during mechanical stopping of moving objects. J Neurophysiol 129:1293–1309.

Slijper H, Latash M (2000) The effects of instability and additional hand support on anticipatory postural adjustments in leg, trunk, and arm muscles during standing. Exp Brain Res 135:81–93.

Slijper H, Latash ML (2004) The effects of muscle vibration on anticipatory postural adjustments. Brain Res 1015:57–72.

Smith MA, Ghazizadeh A, Shadmehr R (2006) Interacting adaptive processes with different timescales underlie short-term motor learning. PLoS Biol 4:e179.

Solnik S, DeVita P, Rider P, Long B, Hortobágyi T (2008) Teager-Kaiser operator improves the accuracy of EMG onset detection independent of signal-to-noise ratio. Acta Bioeng Biomech 10:65–68.

Solnik S, Rider P, Steinweg K, Devita P, Hortobágyi T (2010) Teager-Kaiser energy operator signal conditioning improves EMG onset detection. Eur J Appl Physiol 110:489–498.

Strang A, Choi H, Berg W (2008) The effect of exhausting aerobic exercise on the timing of anticipatory postural adjustments. J Sports Med Phys Fitness 48:9.

Strang AJ, Berg WP (2007) Fatigue-induced adaptive changes of anticipatory postural adjustments. Exp Brain Res 178:49–61.

Strang AJ, Berg WP, Hieronymus M (2009) Fatigue-induced early onset of anticipatory postural adjustments in non-fatigued muscles: support for a centrally mediated adaptation. Exp Brain Res 197:245–254.

Takahashi CD, Nemet D, Rose-Gottron CM, Larson JK, Cooper DM, Reinkensmeyer DJ (2003) Neuromotor Noise Limits Motor Performance, But Not Motor Adaptation, in Children. J Neurophysiol 90:703–711.

Takahashi CD, Nemet D, Rose-Gottron CM, Larson JK, Cooper DM, Reinkensmeyer DJ (2006) Effect of muscle fatigue on internal model formation and retention during reaching with the arm. J Appl Physiol 100:695–706.

Takakusaki K, Takahashi M, Obara K, Chiba R (2017) Neural substrates involved in the control of posture. Adv Robot 31:2–23.

Tanaka H, Sejnowski TJ, Krakauer JW (2009) Adaptation to Visuomotor Rotation Through Interaction Between Posterior Parietal and Motor Cortical Areas. J Neurophysiol 102:2921–2932.

Tanaka M, Shigihara Y, Ishii A, Funakura M, Kanai E, Watanabe Y (2012) Effect of mental fatigue on the central nervous system: an electroencephalography study. Behav Brain Funct BBF 8:48.

Taylor JL, Amann M, Duchateau J, Meeusen R, Rice CL (2016) Neural Contributions to Muscle Fatigue: From the Brain to the Muscle and Back Again. Med Sci Sports Exerc 48:2294–2306.

Taylor JL, Butler JE, Gandevia SC (2000) Changes in muscle afferents, motoneurons and motor drive during muscle fatigue. Eur J Appl Physiol 83:106–115.

Theofilidis G, Bogdanis GC, Koutedakis Y, Karatzaferi C (2018) Monitoring Exercise-Induced Muscle Fatigue and Adaptations: Making Sense of Popular or Emerging Indices and Biomarkers. Sports 6:153.

Vuillerme N, Danion F, Forestier N, Nougier V (2002) Postural sway under muscle vibration and muscle fatigue in humans. Neurosci Lett 333:131–135.

Wang J, Sainburg RL (2006) Interlimb transfer of visuomotor rotations depends on handedness. Exp Brain Res 175:223–230.

Weavil JC, Amann M (2019) Neuromuscular fatigue during whole body exercise. Curr Opin Physiol 10:128–136.

Winter DA (2009) Biomechanics and motor control of human movement. John Wiley & Sons.

Wulf G (2012) Motor Schema. In: Encyclopedia of the Sciences of Learning (Seel NM, ed), pp 2350–2352. Boston, MA: Springer US.

Yamagata M, Falaki A, Latash ML (2019) Effects of Voluntary Agonist-Antagonist Coactivation on Stability of Vertical Posture. Motor Control 23:304–326.

Yamagata M, Gruben K, Falaki A, Ochs WL, Latash ML (2021) Biomechanics of Vertical Posture and Control with Referent Joint Configurations. J Mot Behav 53:72–82.

CHAPTER 6 APPENDIX I

Manuscripts authored and co-authored during the PhD program

- Tam E, **Nardon M**, Bertucco M, Capelli C (2023) The mechanisms underpinning the slow component of V˙O2 in humans. Eur J Appl Physiol 2023 Sep 29. doi: 10.1007/s00421-023-05315-z. Epub ahead of print. PMID: 37775591.
- Ricotta JM, De SD, **Nardon M**, Benamati A, Latash ML (2023). Effects of fatigue on intra-muscle force-stabilizing synergies. J Appl Physiol (1985). 2023 Sep 21. doi: 10.1152/japplphysiol.00419.2023. Epub ahead of print. PMID: 37732378.
- Ricotta JM, **Nardon M**, De SD, Jiang J, Graziani W, Latash ML (2023) Motor unit-based synergies in a non-compartmentalized muscle. Exp Brain Res. 2023 May;241(5):1367-1379. doi: 10.1007/s00221-023-06606-9. Epub 2023 Apr 5. PMID: 37017728.
- Bertucco M, **Nardon M**, Mueske N, Sandhu S, Rethlefsen SA, Wren TAL, Sanger TD (2022). The Effects of Prolonged Vibrotactile EMG-Based Biofeedback on Ankle Joint Range of Motion During Gait in Children with Spastic Cerebral Palsy: A Case Series. Physical & Occupational Therapy In Pediatrics 0:1–16.
- **Nardon M**, Pascucci F, Cesari P, Bertucco M, Latash ML (2022). Synergies Stabilizing Vertical Posture in Spaces of Control Variables. Neuroscience 500:79–94.
- **Nardon M**, Venturelli M, Ruzzante F, Longo VD, Bertucco M (2022). Fasting-Mimicking-Diet does not reduce skeletal muscle function in healthy young adults: a randomized control trial. Eur J Appl Physiol 122, 651–661.
- Comment in: **Nardon M**, Venturelli M, Ruzzante F, Longo VD, Bertucco M (2022) Response to: Dealing with menstrual cycle in sport: stop finding excuses to exclude women from research. European Journal of Applied Physiology 122:2491–2492.

- **Nardon M**, Ruzzante F, O'Donnell L, Adami A, Dayanidhi S, Bertucco M (2021) Energetics of walking in individuals with cerebral palsy and typical development, across severity and age: A systematic review and meta-analysis. Gait Posture 90:388–407.

Manuscripts Under revision (as of 10/12/2023)

- Boldo M, Di Marco R, Martini E, **Nardon M**, Bertucco M, Bombieri N. On the reliability of single-camera markerless systems for overground gait monitoring in telemedicine.

Manuscripts in preparation

- **Nardon M**, Piscitelli F, Tam E, Bertucco M. *The effects of generalized and local muscle fatigue on anticipatory and compensatory postural adjustments under an external perturbation*. (finalizing the final draft)
- **Nardon M**, Piscitelli F, Singh T, Bertucco M. *Effects of muscle fatigue on motor adaptation and savings using a novel postural-task paradigm*. (in preparation)
- **Nardon M**, Sinha O, Kpankpa J, Albenze E, Bertucco M, Singh T. *Localized neuromuscular fatigue of postural muscles is efficiently compensated during a force-field motor adaptation task*. (in preparation)
- **Nardon M**, Martini L, Ruzzante F, Venturelli M, Bertucco M. *Central and peripheral components of neuromuscular fatigue in individuals with cerebral palsy and typically developing peers*. (in preparation)